

Spring 6-30-1970

## Theoretical and experimental evaluation of cardiac state utilizing indicator dilution methods for nonuniform ventricular mixing

Stanley Myron Welland  
*New Jersey Institute of Technology*

Follow this and additional works at: <https://digitalcommons.njit.edu/dissertations>



Part of the [Mechanical Engineering Commons](#)

---

### Recommended Citation

Welland, Stanley Myron, "Theoretical and experimental evaluation of cardiac state utilizing indicator dilution methods for nonuniform ventricular mixing" (1970). *Dissertations*. 1346.  
<https://digitalcommons.njit.edu/dissertations/1346>

This Dissertation is brought to you for free and open access by the Electronic Theses and Dissertations at Digital Commons @ NJIT. It has been accepted for inclusion in Dissertations by an authorized administrator of Digital Commons @ NJIT. For more information, please contact [digitalcommons@njit.edu](mailto:digitalcommons@njit.edu).

## **Copyright Warning & Restrictions**

The copyright law of the United States (Title 17, United States Code) governs the making of photocopies or other reproductions of copyrighted material.

Under certain conditions specified in the law, libraries and archives are authorized to furnish a photocopy or other reproduction. One of these specified conditions is that the photocopy or reproduction is not to be “used for any purpose other than private study, scholarship, or research.” If a user makes a request for, or later uses, a photocopy or reproduction for purposes in excess of “fair use” that user may be liable for copyright infringement,

This institution reserves the right to refuse to accept a copying order if, in its judgment, fulfillment of the order would involve violation of copyright law.

**Please Note: The author retains the copyright while the New Jersey Institute of Technology reserves the right to distribute this thesis or dissertation**

Printing note: If you do not wish to print this page, then select “Pages from: first page # to: last page #” on the print dialog screen

The Van Houten library has removed some of the personal information and all signatures from the approval page and biographical sketches of theses and dissertations in order to protect the identity of NJIT graduates and faculty.

71-907

WELLAND, Stanley Myron, 1943-  
THEORETICAL AND EXPERIMENTAL EVALUATION OF  
CARDIAC STATE UTILIZING INDICATOR DILUTION  
METHODS FOR NONUNIFORM VENTRICULAR MIXING.

Newark College of Engineering, D.Eng.Sc., 1970  
Engineering, biomedical

University Microfilms, A XEROX Company, Ann Arbor, Michigan

THEORETICAL AND EXPERIMENTAL EVALUATION OF CARDIAC STATE  
UTILIZING INDICATOR DILUTION METHODS FOR NONUNIFORM  
VENTRICULAR MIXING

BY  
STANLEY M. WELLAND

A DISSERTATION  
PRESENTED IN PARTIAL FULFILLMENT OF  
THE REQUIREMENTS FOR THE DEGREE  
OF  
DOCTOR OF ENGINEERING SCIENCE  
AT  
NEWARK COLLEGE OF ENGINEERING

This dissertation is to be used only with due regard to the rights of the author. Bibliographical references may be noted, but passages must not be copied without permission of the College and without credit being given in subsequent written or published work.

Newark, New Jersey  
1970

ABSTRACT

This research is directed toward the development and application of a new approach to the evaluation of cardiac work to diagnose cardiac state. A procedure has been developed for calculating the work performed on the fluid by the left ventricle during the heartbeat. The procedure involves the continuous direct measurement of ventricular fluid mixture temperature during and following the controlled injection, through a catheter, of a known volume of cold saline into the left ventricle. The measured mixture temperatures are used to calculate continuous ventricular volumes during the systolic and diastolic functions of the heartbeat. Plotting measured ventricular pressure versus the volume of the ventricle results in the work diagram for the left ventricle.

The method described above to evaluate cardiac work is based upon the assumption of instantaneous and uniform mixing of the injected saline and the ventricular fluid. This assumption is typically made in studies which employ indicator dilution methods to measure cardiac output and ventricular end-volumes. The effect of ventricular non-mixing of indicators as a source of error in ventricular volume calculations and cardiac output measurement was studied. From references and the author's original invitro and invivo experimental work a description of indicator mixing in the left ventricle and of its effects on indicator dilution studies is given.

A theoretical deterministic analysis of nonuniform ventricular mixing is presented to derive expressions for stroke volume as a function of indicator concentration measured at the aorta. It was found that a purely deterministic analysis when supplemented with a probabilistic analysis results in an analysis of nonuniform ventricular mixing. A mathematical model is developed which explains the shape of indicator concentration curves and allows for the evaluation of ventricular mixing and cardiac state.

A derivation of the classical Stewart-Hamilton relationship for the calculation of cardiac output from dye indicator studies is presented. With this derivation conclusions are formulated which show the validity of the Stewart-Hamilton equation for the case of nonuniform ventricular mixing of the indicator and the limitations of this relationship in the presence of certain heart defects.

The deterministic and probabilistic analyses are applied to the thermodilution technique to derive expressions relating ventricular volume and ejection fraction to measured fluid temperatures for the case of nonuniform mixing of the injected cold saline. An originally designed "Thermocatheter", which employs a single catheter to inject and measure invivo ventricular fluid temperatures, was used to evaluate cardiac state applying the mathematical analyses presented.

Experimental studies performed in a heart model, mongrel dogs, and in human subjects are presented in verification of the analytical approaches used.



APPROVAL OF DISSERTATION  
THEORETICAL AND EXPERIMENTAL EVALUATION OF CARDIAC STATE  
UTILIZING INDICATOR DILUTION METHODS FOR NONUNIFORM  
VENTRICULAR MIXING

BY

STANLEY M. WELLAND

FOR

DEPARTMENT OF MECHANICAL ENGINEERING  
NEWARK COLLEGE OF ENGINEERING

BY

FACULTY COMMITTEE

APPROVED: \_\_\_\_\_ Chairman

\_\_\_\_\_  
\_\_\_\_\_  
\_\_\_\_\_  
\_\_\_\_\_

NEWARK, NEW JERSEY

JUNE, 1970

### ACKNOWLEDGEMENTS

The author wishes to express his sincere appreciation to his research advisor, Professor Martin J. Levy, for his guidance and suggestions throughout the author's graduate education. He also extends his gratitude to Dr. Russell W. Brancato and Professor Robert M. Jacobs for their assistance in this research. The author thanks the Saint Michael Hospital and the Newark College of Engineering Foundation for Graduate Study for without their support this research project would not possible.

TABLE OF CONTENTS

	PAGE
Abstract.....	1
Approval Page.....	iv
Acknowledgements.....	v
Table of Contents.....	vi
List of Figures.....	x
Symbols.....	xv
1. Introduction	
1.1 Structure of the Heart.....	1
1.2 History of Indicator Dilution Techniques for Measuring Left Ventricular Volume and Cardiac Output.....	2
1.3 The Left Ventricle as a Mixing Chamber.....	5
1.4 Evaluation of Cardiac Output from Indicator Dilution Curves.....	8
1.5 Derivation of the Thermodilution Equations for Uniform Ventricular Mixing.....	9
2. Theoretical Analysis of Ventricular Mixing	
2.1 Mathematical Model of the Left Ventricle.....	11
2.2 Deterministic Analysis of Nonuniform Ventricular Mixing.....	13
2.3 Probabilistic Analysis of Nonuniform Ventricular Mixing.....	15
2.4 Residence Time Distributions.....	17

2.5	Multichamber Probabilistic Analysis of Ventricular Mixing.....	20
2.6	Application of Multichamber Probabilistic Model.....	21
2.7	The Effect of Injection Site Upon the Shape of Dye Indicator Dilution Curves.....	27
3.	Application of the Theoretical Analysis of Ventricular Mixing and the Experimental Indicator Dilution Methods to Evaluate Cardiac State	
3.1	Deterministic Analysis for Nonuniform Ventricular Mixing Applied to the Thermodilution Technique	30
3.2	Application of the Generalized Thermodilution Equation to Derive an Expression for the Ejection Fraction of the jth Volume Element.....	32
3.3	Relationship between Ejection Fraction and Probability Density Function.....	34
3.4	Application of the Probabilistic Analysis of Nonuniform Ventricular Mixing to the Thermo- dilution Technique.....	36
4.	Experimental Results	
4.1	Invitro Apparatus.....	37
4.2	Invivo Apparatus.....	37
4.3	Invitro and Invivo Mixing Studies.....	38
4.4	Invivo Thermodilution Procedure.....	40
4.5	Invivo Thermodilution Study.....	45

4.6	Invivo Thermodilution Study of Abnormal Ventricular Function.....	50
4.7	Thermocatheter.....	51
4.8	Invivo Thermodilution Study in the Dog Employ- ing the Thermocatheter.....	52
4.9	Invivo Thermodilution Study in Man Employing the Thermocatheter.....	53
4.10	Results of Experimental Thermodilution Studies	54
5.	Conclusions.....	60
6.	Recommendations.....	64
7.	Figures.....	66
A.	Appendix.....	118
A.1	Derivation of the Stewart-Hamilton Relationship	118
A.2	Use of Stewart-Hamilton Equations in the presence of Valvular Insufficiency or Regurgitation...	120
B.	Appendix.....	122
B.1	Derivation of the Generalized Thermodilution Equation.....	122
B.2	Derivation of the Fundamental Thermodilution Equations.....	125
C.	Appendix.....	129
C.1	Theory of Thermal Tracers in Multicompartment Systems.....	129
C.2	Three Compartment System.....	130
C.3	Derivation of Equations for Instantaneous Ventricular Volumes during the Heartbeat.....	132
C.4	Theoretical Thermodilution Study.....	134

D.	Appendix.....	141
	D.1 Derivation of Probability Density Function for N Volume Chamber Model	141
E.	Appendix.....	143
	E.1 Temperature Correction for Warming of Injected Fluid in Catheter during Injection Process.....	143
	E.2 Experimental Evaluation of $\bar{h}_c$ .....	144
	E.3 Analytical Considerations.....	145
	REFERENCES.....	148
	VITA.....	154

LIST OF FIGURES

- Figure 1 Diagram of the Human Heart
- Figure 2 Classic Stewart-Hamilton Indicator Dilution Curve
- Figure 3 Dye Concentration versus Time Obtained by Discontinuous Sampling Technique After Instantaneous Injection of Dye
- Figure 4 Ideal Thermodilution Curve With Thermistor In Aorta
- Figure 5 Experimental Green Dye Study in Man Obtained by the Injection of 5 mgm of Green Dye into the Pulmonary Artery and the Fluid Dye Concentration Measured in the Aorta
- Figure 6 Steady Flow System
- Figure 7 Theoretical Concentration Based on the Theory of Instantaneous Uniform Mixing for a Steady Flow System
- Figure 8 The Left Ventricle Assumed to be a Cyclical Steady Flow System
- Figure 9 Theoretical Concentration Based on the Theory of Instantaneous Uniform Mixing
- Figure 10 Experimental Concentration versus Time Plot for a Normal Left Ventricle following the Instantaneous Injection of a Bolus of Dye Employing an Ideal Apparatus with no Response Lag and a Real Apparatus with a Response Lag greater than zero
- Figure 11 Multichamber Probabilistic Model
- Figure 12 Plot of Equation (2-24) for  $Q = 5$  liters/minute and  $V = 200 \text{ cm}^3$  for Various Values of  $N$

Figure 13 Experimental Density Function  $f(t)$  for the Experimental Green Dye Curve in Figure 5 and the Theoretical Density Function for  $N = 1$

Figure 14 Green Dye Study for a Subject with an Enlarged Heart

Figure 15 Green Dye Study of a Subject with an Aortic Stenosis

Figure 16 Green Dye Study of a Subject with a Slight Aortic Insufficiency

Figure 17 Experimental Density Functions for a Normal Heart, Enlarged Heart and a Heart with an Aortic Stenosis

Figure 18 Experimental Density Functions for a Normal Heart, a Heart with Aortic Insufficiency and a Heart with Mitral Insufficiency

Figure 19 Theoretical and Experimental Density Functions for a Normal Heart, Enlarged Heart and a Heart with an Aortic Stenosis

Figure 20 Fluid Dye Concentration versus Time for Green Dye Studies Employing Various Injection Sites

Figure 21 Fluid Dye Concentration versus Time Measured from the First Appearance of Dye in the Carotid Artery for the Green Dye Studies Employing an Injection of Dye in the Right Auricle, Pulmonary Artery and the Pulmonary Vein

Figure 22 Multichamber Model for the Normal Heart Shown in Figure 17

Figure 23 Density Function versus Time for the Models obtained by adding 1, 2, and 4 Mixing Chambers to the Model in Figure 22



- Figure 24 Experimental Apparatus
- Figure 25 System Response
- Figure 26 Simultaneous Green Dye and Thermodilution Study in a Dog
- Figure 27 Simultaneous Green Dye and Thermodilution Study in a Dog During Cardiac Infarction
- Figure 28 Schematic Diagram of the Patient to Equipment Relationship
- Figure 29 The Proper Catheter Configuration in the Left Ventricle
- Figure 30 Thermodilution Study in Man in which the Injection Process produced PVC'S thus confusing the Temperature-Time Trace
- Figure 31 Catheters in the Left Ventricle during the Injection Process
- Figure 32 Catheters in the Left Ventricle after the Injection Process
- Figure 33 Thermodilution Study in Man Utilizing the Brancato Technique
- Figure 34 Calculated Ventricular Volume versus Time for the Thermodilution Study in Figure 33
- Figure 35 Work Diagram for the Left Ventricle
- Figure 36 Thermodilution Study in Man Utilizing the Brancato Technique
- Figure 37 Calculated Ventricular Volume versus Time for the Thermodilution Study in Figure 36
- Figure 38 Left Ventricular Work Diagram for the Thermodilution Study in Figure 36

- Figure 39 Thermodilution Study in Man Utilizing the Brancato Technique
- Figure 40 Calculated Left Ventricular Volume versus Time for the Thermodilution Study in Figure 39, Heartbeat C
- Figure 41 Left Ventricular Work Diagram for the Thermodilution Study in Figure 39
- Figure 42 Volume versus Time Plots for Heartbeats D, C and E in Figure 39
- Figure 43 Thermodilution Study for a Subject with Aortic Insufficiency
- Figure 44 Thermocatheter Design
- Figure 45 Thermodilution Study in a Dog Utilizing the Thermocatheter and a Bolus Injection of Cold Saline
- Figure 46 Thermodilution Study for a Subject with Aortic Insufficiency Utilizing the Thermocatheter
- Figure 47 Nondimensionalized Left Ventricular Volume Plots from the Results of the Thermodilution Studies Employing the Brancato Technique and the Thermocatheter
- Figure 48 Ventricular Stroke Work versus Ventricular End-Diastolic Volume
- Figure 49 Ventricular Stroke Work versus Ventricular End-Diastolic Pressure
- Figure 50 Ventricular End-Diastolic Pressure versus Ventricular End-Diastolic Volume

Figure 51 Left Ventricular Pressure versus Left Ventricular  
Volume from the Results of the Thermodilution Studies  
in Man Employing the Brancato Technique and the  
Thermocatheter

Figure 52 Left Ventricular Pressure versus Volume Plots  
From Individual Patients with Different Varieties  
of Heart Disease

SYMBOLS

A	lumen surface area of catheter, $\text{cm}^2$
$b_{ij}$	transport or exchange rate from the $i$ th compartment to $j$ th compartment, gm/sec
C	indicator concentration
$C_p$	specific heat at constant pressure, $\text{B}/\text{lb}_m \text{ } ^\circ\text{F}$
$C_v$	specific heat at constant volume, $\text{B}/\text{lb}_m \text{ } ^\circ\text{F}$
c	indicator concentration per unit mass
E	total energy, sum of potential, kinetic and internal energy
EDV	end-diastolic volume, $\text{cm}^3$
ESV	end-systolic volume, $\text{cm}^3$
$F(t)$	cumulative density function
$f(t)$	probabilistic density function, 1/sec
$g_{ij}$	fraction at the end of systole of the $j$ th volume element that has contributed to the stroke volume
H	enthalpy, $\rho C_p T V$ , B
h	specific enthalpy, $u + P/\rho$ , $\text{B}/\text{lb}_m$
$h_c$	local convective heat-transfer coefficient, $\text{B}/\text{hr ft}^2 \text{ } ^\circ\text{F}$
$\bar{h}_c$	average convective heat-transfer coefficient, $\text{B}/\text{hr ft}^2 \text{ } ^\circ\text{F}$
I	total quantity of indicator injected
k	ratio of indicator concentration from consecutive beats
M	mass, gm
N	number of mixing chambers or volume elements
P	pressure, mmHg
$\bar{P}$	mean pressure, mmHg

$Q$	mean volumetric flow rate, $\text{cm}^3/\text{sec}$ or $\text{l}/\text{min}$
$\dot{q}$	rate of heat transfer, $\text{B}/\text{hr}$
$q_{ij}$	fraction of indicator in the $j$ th volume element during the $i$ th heartbeat
$SV$	stroke volume, $\text{cm}^3$
$T$	fluid temperature, $^{\circ}\text{F}$
$T_B$	base line fluid temperature, $^{\circ}\text{F}$
$T_b$	body temperature, $^{\circ}\text{F}$
$T_{\text{wall}}$	lumen surface temperature of catheter, $^{\circ}\text{F}$
$\Delta T_{\text{max}}$	maximum ventricular fluid temperature change due to cold saline injection
$\Delta T_n$	temperature change of fluid at the end of the systolic function of heartbeat $n$ . $n = 2, 3, \dots$
$t$	time, $\text{sec}$
$\bar{t}$	abscissal value of the centroid of the indicator dilution curve, $\text{sec}$
$U$	internal energy, $\ominus C_v T V$ , $\text{B}$
$U_i$	initial internal energy, $\ominus C_v T_o V_o$ , $\text{B}$
$u$	specific internal energy, $\text{B}/\text{lb}_m$
$V$	volume, $\text{cm}^3$
$v$	velocity of fluid, $\text{cm}/\text{sec}$
$v_b$	velocity of control volume boundary, $\text{cm}/\text{sec}$
$v_{ij}$	fraction which the $j$ th volume contributes to the flow during the $i$ th systole
$W$	total work done on system, sum of shaft and viscous work, $\text{B}$
$\dot{W}_{\text{shear}}$	rate of shear work, $\text{B}/\text{hr}$

## Subscripts

cv	control volume
ed	end-diastolic
es	end-systolic
f	final condition
inj	injected fluid
n	number of heartbeat cycle, cycle consists of a diastolic and systolic function
o	initial condition
s	stored
sv	stroke volume
v	ventricle

## Greek Symbols

$\alpha, \eta$	dummy variables
$\delta_{ij}$	kronecker delta
$\theta$	time of indicator injection
$\rho$	fluid density, mass per unit volume, gm/cm <sup>3</sup>
$\sigma$	normal stress on an element of fluid
$\tau$	shear stress
$\lambda$	volume flow rate through system divided by volume of system, 1/sec

## 1. INTRODUCTION

### 1.1 Structure of the Heart

The heart is a two-pump, four-chamber structure which circulates blood through the pulmonary and systemic vascular beds. A blood particle travels through a closed circuit which may be described as follows. From the right atrium through the tricuspid valve into the right ventricle, out the pulmonary artery into and out of the lungs into the left atrium, out through the mitral valve into the left ventricle and out the aortic valve through the systemic circulation back to the right atrium. Figure 1 is a diagram of the human heart which indicates the path of a blood particle as described above. The right and left ventricles are the pumps which are often referred to as the right and left heart.

Each heart actually contains two compartments, the atrium and the ventricle. The atrium serves as a temporary storage reservoir and assists, by contraction, the last stages of ventricular filling. The ventricles are surrounded by muscle tissue which provides the pumping power of the ventricle. The muscle tissue of the left heart is greater than that of the right heart since it sends the blood through the systemic circuit which offers greater resistance than the pulmonary circuit. Thus, the left heart does more work than the right heart, about five times as much. It is therefore

of particular importance to be able to determine the volume, output and work of the left ventricle in order to detect disease.

The normal circulation of the human heart is between five and six liters per minute, for an adult. Since the two hearts are in series the average ventricular outputs of the hearts must be equal. In addition, since the frequencies of contraction are identical the average output per beat is also the same.

The heart is neither a constant volume nor a constant rate pump. The output varies from one individual to another. In the same individual the output depends on physiological conditions. The indicator dilution method offers one of the means whereby some of the parameters of the heart and circulation such as cardiac output may be estimated.

The indicator dilution technique consists of injecting an injectate or dye at some site proximal to the region under study and taking samples at a distal site. A mathematical analysis of the output concentration as a function of time yields information about the parameters of the heart and circulation.

## 1.2 History of Indicator Dilution Techniques for Measuring Left Ventricular Volume and Cardiac Output

The indicator dilution principle has been used to study the circulation since the classic works of Stewart<sup>(1)</sup> in 1894.



The classic Stewart-Hamilton indicator dilution curve, as shown in Figure 2, for measuring cardiac output was obtained by means of arterial sampling following the injection of an indicator into the right side of the circulation. This originally involved the collection of samples of arterial blood over a long period of time. Today, this curve is obtained by using long catheters with slow flow rates through a continuously recording densitometer. Investigators have tried to calculate left and right ventricular volumes by analysis of such indicator dilution curves.

The mathematical basis for ventricular volume calculations was derived by Hamilton et al<sup>(2)</sup> in 1932. In 1951, Newman et al<sup>(3)</sup> refined Hamilton's result and derived theoretical equations for calculating the end-volumes of the ventricle from dye dilution curves. Bing et al<sup>(4)</sup> in 1951 made the first attempt to measure right ventricular volumes in man by injecting a dye solution, T-1824, into the right ventricle and sampling from the pulmonary artery through a long catheter. But due to mixing within the catheter a distortion in the indicator curve made ventricular volume calculations difficult. In 1954, Holt<sup>(5)</sup> overcame this problem by employing a discontinuous sampling technique and obtained the first step function dye concentration curve as shown in Figure 3. In this technique a catheter was passed retrograde into the left ventricle and one or two milliliters of sodium chloride solution was injected instantaneously. The electric conduc-

tivity of the aortic blood near the aortic valve was determined continuously by means of a catheter-tipped electric conductivity cell. With the improvement of catheter and densitometer design ventricular volume measurements by means of continuous recording densitometer curves were first reported in 1960 by Swan and Beck.<sup>(6)</sup>

Folse and Braunwald,<sup>(7)</sup> in 1962, described a method utilizing a radioisotope as the indicator to determine the fraction of left ventricular end-diastolic volume that is ejected during each cardiac cycle. Radioiodinated Diodrast was rapidly injected into the left ventricle and the fraction of isotope discharged from this chamber per beat was determined with a shielded scintillation probe placed on the chest wall over the left ventricle. The mathematical basis for the stroke volume calculation was the same as that for other indicator dilution techniques.

In 1954 Fegler<sup>(8)</sup> developed the thermal dilution technique for measuring cardiac output. In this technique several milliliters of cold saline were injected instantaneously into the left ventricle and the temperature of the aortic blood was measured continuously by a thermocouple. Holt,<sup>(9)</sup> in 1956, derived the fundamental equations for the thermal dilution technique which are given by,

$$EDV = V_{inj} ( T_B - T_{inj} ) / \Delta T_{max} \quad (1-1)$$

and

$$EDV = SV / ( 1 - k ) \quad (1-2)$$

Figure 4 shows the meaning of the symbols in the above equations. Fegler and Holt were followed by many investigators (10-23) who used bead tipped thermistors to measure aortic blood temperature in man and animals. All their calculations employed the same two equations given above. In 1968 this author published new equations for the calculation of continuous ventricular volumes from measured ventricular fluid mixture temperatures (24) which differed from the earlier Holt equations which allow for the calculation of ventricular end-volumes only.

The history presented of indicator dilution techniques discussed the four types of indicator used; dye solutions which use a long catheter and a continuously recording densitometer, chloride solutions which employ catheter-tipped electric conductivity cells, radioactive solutions which require external scanning devices and finally cold saline for which thermal probes are used to measure aortic or ventricular fluid mixture temperatures. It appears that prior to 1968 all indicator dilution studies involved end-volume calculations based on the theory of instantaneous and uniform mixing.

### 1.3 The Left Ventricle as a Mixing Chamber

There are four general possible models which may be used

to study the injection and mixing of indicators during diastole in the left ventricle. They are:

Case 1 Instantaneous injection, instantaneous uniform mixing at the end of diastole (instantaneous temperature change of the ventricle fluid)

Case 2 Injection of indicator as a known function of time, instantaneous mixing (temperature change is some function of time)

Case 3 Instantaneous injection, nonuniform mixing

Case 4 Injection as a known function of time, nonuniform mixing.

Mathematically an instantaneous injection during diastole is described by a delta function on a plot of volume injected versus time. Uniform mixing implies that there are no temperature or dye concentration gradients within the ventricular volume. Past investigators have employed various models in addition to uniform mixing to evaluate ventricular mixing. In an investigation made by Levinson and Frank<sup>(25)</sup> the measurement of the end-diastolic volume was made in a heart model and a dog. It was their conclusion that instantaneous uniform mixing occurs in the ventricle between the injected dye solution and the end-diastolic volume. Irisawa, Wilson and Rushmer<sup>(26)</sup> also evaluated ventricular mixing in a model by injecting saline into the chamber and measuring the fluid conductivity in two different locations of the model. They concluded that uniform mixing is a rare phenomenon and not a safe assumption.

It is this author's opinion that the test model used by Levinson and Frank was too small to study the effects of mixing. They also introduced forced agitation which enhanced the mixing to an unrealistic degree. All mixing in the model used by Irisawa, Wilson and Rushmer was due to diffusion only which is not the case in the living ventricle where mixing is mainly due to forced convection caused by the ventricular wall agitation.

The thermal mixing of an injected volume of cold saline depends on mechanical mixing (forced convection) and direct transfer of heat from warm blood to cold blood (conduction). Mechanical mixing is fundamentally dependent on the extent to which the entering stroke volume mixes with the end-systolic volume which is true for all indicator methods. Conduction is the transfer of kinetic energy from one molecule of blood to another. Conduction occurs faster than the diffusion of a large ion such as a particle of dye; therefore equilibration of temperature should occur faster than the mixing of dye particles within the ventricular volume by diffusion. But even so, the forced convection of the entering injected fluid, thermal or dye indicator, and the motion of the ventricular walls are mainly responsible for ventricular mixing. Hence, the mixing phenomenon may be studied experimentally employing thermal probes or densitometers. In vivo studies are presented later which show simultaneous thermal and dye indicator mixing in

the ventricle of a dog.

#### 1.4 Evaluation of Cardiac Output from Indicator Dilution Curves

The dye indicator dilution technique for the estimation of left heart output involves injecting a known quantity of indicator in the pulmonary artery or in the left heart and measuring the fluid dye concentration at the aorta. Figure 5 is an experimental green dye curve obtained by injecting 5 mgm of green dye instantaneously into the pulmonary artery and measuring the fluid dye concentration at the aorta with a continuously recording densitometer. A completely deterministic analysis attempting to explain the shape of this curve would be very difficult since it would require a mathematical description of the dye flow through the labyrinth of the lungs, mixing in the pulmonary artery, pulmonary vein, left atrium and left ventricle, and the recirculation of dye which occurs before the green dye is completely washed from the left ventricle.

The cardiologist employs the dye dilution curve to calculate the cardiac output of the heart with the aid of the Stewart-Hamilton equation given by,

$$Q = I_{inj} / \int_0^{\infty} C(t) dt \quad (1-3)$$

Appendix A contains a derivation of this equation which shows the limitations of the Stewart-Hamilton equation in the presence of certain heart defects such as mitral and aortic regurgitation and insufficiency. The Stewart-Hamilton relationship is shown

to be valid even if the fluid dye concentration of the ventricular fluid in the left ventricle is nonuniform if one defines the cardiac output calculated by equation (1-3) as the mean cardiac output of the heart.

### 1.5 Derivation of the Thermodilution Equations for Uniform Ventricular Mixing

Section 1.2 briefly described the thermodilution technique developed by Fegler which involved the placing of a thermal probe just above the aortic valve and the injection of a small amount of cold saline into the left ventricle during the diastolic function of the heartbeat. The temperatures measured by the thermal probe and the basic thermodilution equations were used to calculate the end-volumes of the ventricle.

The thermodilution equations derived by Holt were developed using physical arguments and did not consider all of the assumptions inherent in the thermodilution technique. Appendix B contains a derivation of the thermodilution equations based upon the general thermodynamic energy equation and the conservation of mass equation for the conditions described by case 1 on page 6. A generalized thermodilution equation is presented which was employed to derive equations for continuous ventricular volumes and is presented in the author's Master of Science Thesis, reference (24).

In reference (24) the continuous ventricular volume during systole was related to measured pressure differentials across

the aortic valve. Simultaneous measurement of ventricular and aortic pressures are made using catheters and pressure transducers. Since the pressure differential across the valve is on the order of magnitude of 0 to 5 mmHg, except in the presence of aortic stenosis, there is a large error due to transmission length and viscous damping within the catheter. Hence, it was desired to relate ventricular volume during systole to measured fluid temperatures. The equations for continuous ventricular volume during systole and diastole are derived in appendix C where the theory of thermal tracers in multicompartment systems is introduced.

By treating the left atrium, ventricle and aorta as a three compartment system, thermodilution equations for continuous compartmental volumes in the presence of cardiac defects are derived. Thus far no other investigator has published any work, to the author's knowledge, which considered the possibility of measuring continuous ventricular volumes utilizing any indicator dilution technique. Likewise no work has been published which presented equations to quantitatively evaluate valvular incompetence, <sup>(27,28,29,30,31,32)</sup> to the author's knowledge.



## 2. THEORETICAL ANALYSIS OF VENTRICULAR MIXING

### 2.1 Mathematical Model of the Left Ventricle

Consider the steady flow system in Figure 6.  $Q$  is the volumetric rate of inflow and outflow. At some time  $t = \theta_1$  an instantaneous injection of a bolus of dye indicator is made into the volume near the inlet. The sampling catheter pulls a small sample of the system's contents continuously so that the fluid outlet concentration  $C(t)$  of the system can be measured. The concentration based on an instantaneous mixing model is given by,

$$C(t) = C(0) \exp \left( (-Q/V) (t - \theta_1) \right) \quad (2-1)$$

where

$$C(0) = I_{inj}/V \text{ and } t \geq \theta_1 \quad (2-2)$$

$I_{inj}$  is the total amount of dye injected, measured in grams, and  $V$  is the steady state volume of the system therefore the concentration  $C(t)$  is in grams of dye per ml. Equation (2-1) is plotted in Figure 7.

Since the heartbeat consists of a diastolic and systolic function the left ventricle is not a steady flow system but the heartbeat can be broken up as shown in Figure 8. The theoretical concentration  $C(t)$  as a function of time based on the theory of instantaneous uniform mixing following an instantaneous injection of dye at time  $t = 0$  is shown in Figure 9. The dashed line connects the values of  $C(t)$  at

the beginning of systole and is given by,

$$C(t) = C(0) \exp \left( (\ln k) \left( (t - \theta_1) / 2\theta_1 \right) \right) \quad (2-3)$$

where

$$C(0) = I_{inj} / V_{ed}, \quad k = C_{n+1} / C_n \quad \text{and} \quad t \geq \theta_1 \quad (2-4)$$

Equations (2-1) and (2-3) are equivalent if the steady state volume of the system  $V$  equals the end-diastolic volume  $V_{ed}$  and

$$\left( (\ln k) / 2\theta_1 \right) = -Q / V_{ed} \quad (2-5)$$

Hence, the left ventricle which is a cyclical steady flow system may be treated as a steady flow system with a mean cardiac output  $Q$  which is given by equation (2-5). To show an application of equation (2-5) consider the average values,  $k = 0.6$ ,  $V_{ed} = 150.0 \text{ cm}^3$  and  $2\theta_1 = 1.0$  second which yields a mean cardiac output of  $Q = 4.5$  liters per minute.

A plot of  $C(t)$  versus time for a normal left ventricle following the instantaneous injection of a bolus of dye employing an ideal apparatus with no response time lag is shown in Figure 10. A similar plot is also shown in Figure 10 for a study employing an experimental apparatus with a response lag greater than zero. It is noted that the latter system cannot follow the step changes in the system. The difference between the theoretical and experimental concentration curves is due to the response time lag of the apparatus employed to measure  $C(t)$ , the internal mixing of the fluid

within the catheter, and to the nonuniformity of the dye mixing within the ventricle following the injection. Hence, from Figures 9 and 10 it is concluded that the single chamber uniform mixing model is not a valid model to describe the mixing phenomena of an injected bolus of dye indicator with the ventricular fluid.

## 2.2 Deterministic Analysis of Nonuniform Ventricular Mixing (Case 3, Page 6)

As a bolus of indicator is injected instantaneously, at the beginning of the diastolic function of the  $i$ th heartbeat, into the ventricle its dispersion rate and profile determine the concentration of the indicator as a function of time measured at the aorta. Originally confined to a small spatial volume, random influences exerted by the surrounding fluid particles cause the spatial volume occupied by the indicator particles to increase. The fluid contents of the ventricle are not uniformly mixed at the end of diastole and the  $i$ th end-diastolic volume  $EDV_i$  is imagined to be divided into  $N$  equal but arbitrarily small volumes each of uniform concentration.

The fraction of indicator present in the  $j$ th volume at some time  $t$  during the  $i$ th heartbeat is defined as  $q_{1j}(t)$  and must satisfy,

$$\sum_{j=1}^N q_{1j}(t) = 1.0, \quad 1.0 \geq q_{1j} \geq 0 \quad (2-6)$$

at the end of the  $i$ th diastole and,

$$I_{inj} \sum_{j=1}^N q_{1j}(t) = I(t) \quad (2-7)$$

during the  $i$ th systole where the injection of indicator occurs at the beginning of the  $i$ th diastole.

The fraction which the  $j$ th volume contributes to the flow during the  $i$ th systole at time  $t$  is defined as  $v_{1j}(t)$  such that,

$$1.0 \geq v_{1j}(t) \geq 0 \quad (2-8)$$

The flow rate at time  $t$  during the  $i$ th systole is denoted by  $Q_1(t)$  and is given by,

$$Q_1(t) = (EDV_1/N) \sum_{j=1}^N v_{1j}(t) \quad (2-9)$$

Integrating over the entire systolic function yields,

$$SV_1 = \int_{t_1}^{t_2} Q_1(t) dt, \quad t_2 \geq t \geq t_1 \quad (2-10)$$

or

$$SV_1 = (EDV_1/N) \int_{t_1}^{t_2} \sum_{j=1}^N v_{1j}(t) dt \quad (2-11)$$

Since  $I_{inj}$  is the quantity of indicator in the ventricle prior to the  $i$ th systole, the quantity of indicator in the ventricle during the  $i+1$  diastole is given by,

$$I_{i+1} = I_{inj} - I_{inj} \int_{t_1}^{t_2} \sum_{j=1}^N q_{1j}(t) v_{1j}(t) dt \quad (2-12)$$

Hence, the concentration of the fluid leaving the ventricle during the  $i$ th systole is given by,

$$C_1(t) = I_{inj} \sum_{j=1}^N q_{1j}(t) v_{1j}(t) / Q_1(t) \quad (2-13)$$

This is the concentration that would be measured by a probe above the aortic valve assuming  $C_1$  to be uniform at any particular cross section of the aorta.

Neither  $q_{1j}$  nor  $v_{1j}$  need be uniform but are functions of position and time. They are defined to indicate that in general the ventricle fluid is not well mixed and the fluid ejected at any time is probably not derived from all parts of the ventricle in equal proportions since the fluid close to the valve will tend to be ejected early in systole while apical contents will be ejected later in systole, if at all. If  $v_{1j}$  and  $q_{1j}$  were known for each  $j$ th volume and for time  $t$  from  $t_1$  to  $t_2$  one could calculate the stroke volume of the  $i$ th systole and the concentration  $C_1(t)$ .

However  $v_{1j}$  is not known and is not easily measured. It will be treated as a random variable and given probabilistic values.  $q_{1j}$  can also be treated as a random variable but its values may be verified experimentally by placing a probe within the ventricular fluid. Because of the randomness of the mixing of indicator particles it seems that a purely deterministic point of view must be supplemented with a probabilistic analysis.

### 2.3 Probabilistic Analysis of Nonuniform Ventricular Mixing

Consider an experiment or observation  $E$  which could

conceivably be reproduced a large number of times under conditions judged to be identical in all relevant respects. In many cases it will be found that the outcome of the experiment or observation cannot be predicted accurately, but shows uncontrollable fluctuations from one performance to the next. These fluctuations are regarded as random fluctuations of a random experiment or random observation. This is the case for ventricular mixing of a dye or other indicator in the ventricular fluid volume of different hearts, where the observation of  $E$  is the degree of uniform mixing.

Any variable system subject to random influences constitutes a stochastic process. The concern is with the state and variation of the variable system at any particular instant of time which is described by numerical values of certain observable quantities. Consider the situation where the state of a system is sufficiently described by means of two independent quantities,  $v(t)$  and  $q(t)$ . The numerical values of  $v(t)$  and  $q(t)$  at a fixed time  $t$  will then not be uniquely determined as in the case of a deterministic system, but will depend on the random influences that have been acting on the system up to that instant. Hence, a mathematical model of the mixing process in the ventricle consists of the quantities  $v(t)$  and  $q(t)$  regarded as random variables defined on some probability space  $P$ .

A generalization is obtained by considering the case when several quantities given by,  $v_1(t)$ ,  $v_2(t)$ , .....  $v_n(t)$  and  $q_1(t)$ ,  $q_2(t)$ , .....  $q_n(t)$ , are required for a complete description of the state of the system. These quantities may be regarded as the components of a random vector  $\bar{v}(t)$  and  $\bar{q}(t)$  respectively.  $\bar{v}(t)$  and  $\bar{q}(t)$  are both continuous functions of time which may be written in subscript notation as  $v_{1j}(t)$  and  $q_{1j}(t)$  where  $j$  represents the  $j$ th compartment and  $i$  the  $i$ th heartbeat.

Since  $v_{1j}(t)$  and  $q_{1j}(t)$  are continuous functions of time they are classified as continuous random variables and a density function may be defined for each.

#### 2.4 Residence Time Distributions

The rate of dispersion of an indicator depends on the inertia and viscosity of the particles as well as the magnitude of the agitating forces. In this section the fundamentals of probability are employed to describe the dispersion of an indicator.

Consider the system shown in Figure 6. At time  $t = \theta_1$  there is an injection of a bolus of dye which disperses throughout the volume as previously described. Although each dye particle's motion within the volume is definable in statistical terms no attempt will be made to do this. But since each dye particle in the outflow of the system possesses a previous history the fraction of particles

possessing a residence time  $t$  or less is defined by the cumulative distribution function  $F(t)$ . The fraction of particles whose residence time exceeds  $t$  is given by  $F^*(t)$ . At time  $t = \theta_1$ ,  $F(t) = 0.0$  and in general,

$$F^*(t) = 1.0 - F(t) \quad (2-14)$$

Hence,  $F(t)$  is an increasing function of  $t$  which tends asymptotically toward 1.0 as  $t$  tends toward infinity and  $F^*(t)$  is a decreasing function which equals 1.0 at the time of the instantaneous injection of dye.

From the theory of probability,

$$F(t) = P [T \leq t], \text{ for } -\infty \leq t \leq \infty \quad (2-15)$$

where  $T$  is a random variable defined as the residence time. Equation (2-15) simply states that the probability of a single dye particle staying in the system for a time  $t$  or less is equal to the fraction of particles within the system whose residence time does not exceed  $t$ .

From the cumulative distribution function a probability density function  $f(t)$  is defined,

$$f(t) = dF(t)/dt \quad (2-16)$$

which can be written as,

$$f(t) dt = dF(t) \quad (2-17)$$



$f(t) dt$  is the probability of a single dye particle having a residence time between  $t$  and  $t + dt$ . A density function  $f(t)$  for the continuous random variable  $T$  must possess the following properties;

$$f(t) \geq 0 \quad (2-18)$$

$$\int_{-\infty}^{\infty} f(t) dt = 1.0 \quad (2-19)$$

$$\int_{\theta_1}^t f(\alpha) d\alpha = P[\theta_1 \leq T \leq t] = F(t) - F(\theta_1) \quad (2-20)$$

The density function for the system in Figure 6 is given by,

$$f(t) = C(t) / \int_{\theta_1}^{\infty} C(t) dt \quad (2-21)$$

which satisfies equations (2-18), (2-19) and (2-20).

From equations (1-3) and (2-21) the dye concentration at the outlet of the system in Figure 6 following the instantaneous injection of dye is proportional to the density function  $f(t)$  and is given by,

$$C(t) = I_{inj} f(t) / Q \quad (2-22)$$

It follows from equations (2-1) and (2-22) that,

$$f(t) = (Q/V) \exp((-Q/V)(t - \theta_1)), \text{ where } t \geq \theta_1 \quad (2-23)$$

where  $V$  is the volume of the system. The  $f(t)$  given by equation (2-23) is the density function for a single mixing chamber with an instantaneous injection of dye which mixes uniformly and instantaneously with the contents of the

system.

## 2.5 Multichamber Probabilistic Analysis of Ventricular Mixing

Consider the possibility of dividing the system volume into  $N$  equal but arbitrarily small volumes like that in section 2.2. Hence, each volume represents a perfectly mixed region where dye particles may escape to any other volume element and finally reach the outlet. The number of elements necessary to describe the experimental concentration versus time plot, taken at the outlet, is a measure of the nonuniformity of mixing within the system.

Assume that an  $N$  volume chamber may be represented by  $N$  elements in series with the same density function given by equation (2-23), where  $V$  is the system volume and  $Q$  the volumetric flow rate through the system. Figure 11 shows the assumed mathematical model of the ventricle whose density function is given by,

$$f(t) = \frac{(N Q/V)^N}{(N-1)!} (t - \theta_1)^{N-1.0} \exp(-N Q(t - \theta_1)/V) \quad (2-24)$$

for  $t \geq \theta_1$ . Equation (2-24) is derived in appendix D. The term  $f(t) dt$  where  $f(t)$  is given by equation (2-23) represents the probability of a dye particle escaping a volume element which has a residence time between  $t$  and  $t + dt$ . The process of escaping from any particular chamber is not influenced by what has happened in any other compartment. When a dye particle finally leaves the ventricle it has escaped from  $N$  volume

elements which are considered to be  $N$  successes. This is a special case of a Markov chain. Therefore  $f(t) dt$  where  $f(t)$  is given by equation (2-24) represents the probability of finding a single dye particle at the outlet of the system with a residence time between  $t$  and  $t + dt$ .

Figure 12 is a plot of equation (2-24) for  $Q = 5$  liters per minute and  $V = 200 \text{ cm}^3$  for various values of  $N$ . For  $N = 1$  equation (2-24) yields the density function for a single chamber mixing model. The following section utilizes equations (2-5) and (2-24) to explain the shape of experimental green dye curves like that shown in Figure 5.

## 2.6 Application of Multichamber Probabilistic Model

Figure 5 is an experimental green dye curve obtained by injecting 5.0 mgm of green dye instantaneously into the pulmonary artery and measuring the fluid dye concentration at the aorta. It was previously concluded that a deterministic analysis attempting to explain the shape of this curve would be very difficult since it would require a mathematical description of the dye flow through the lungs, mixing in the pulmonary vein, left atrium, and ventricle and the recirculation of dye. The multichamber probabilistic model developed in section 2.5 explains the shape of the experimental green dye curve obtained by the injection of green dye directly into the left ventricle or by the injection of green dye into the pulmonary artery. Hence, the concentration versus time

curves measured at the aorta for the two different sites of indicator injection differ mainly because of the degree of ventricular non-mixing of the injected indicator. This was shown experimentally by Pearce et al.<sup>(34)</sup>

The experimental work of Pearce, McKeever, Dow and Newman consisted of obtaining repeated curves from the same subject when injecting dye consecutively into the right auricle, pulmonary artery, pulmonary vein and the aorta and when sampling at the carotid artery, or from the left auricle. They concluded that the central circulation behaves as do serial volumes. The lungs, which are the largest volume in the series, acts like a single volume from which dye is washed out in an exponential fashion.

It should be stated that the experimental green dye curve is smooth even though the ventricle is cyclical in function because the experimental apparatus employed had a time constant on the order of 0.1 seconds and because of the effect of mixing within the catheter, which would also smooth the measured  $C(t)$  trace. The theoretical green dye curve is smooth because the left ventricle is treated as a steady flow system as described in section 2.1. It is not the aim of the author to exactly duplicate the experimental curve but to **explain** its shape as it relates to ventricular function and mixing.

Equation (2-22) was used to calculate the experimental density function  $f(t)$  from the experimental green dye curve

in Figure 5 which is plotted in Figure 13. Equation (1-3) was employed to calculate the mean cardiac output and equation (2-23) was applied to find the theoretical density function for  $N = .1$  which is also plotted in Figure 13.

Figure 13 shows that a single chamber mixing model is not a satisfactory approximation to the actual mixing of the green dye injected into the pulmonary artery with the ventricular fluid.

Figures 14, 15, and 16 are experimental green dye curves for different cardiac defects. Figure 14 is the green dye curve for an enlarged left ventricle, confirmed by cine-angiography, with a high cardiac output. Figure 15 is the green dye curve for a subject with an aortic stenosis, confirmed by simultaneous pressure measurement proximal and distal to the aortic valve, with a low cardiac output. Figure 16 is the green dye curve for a subject with a slight aortic insufficiency for which the cardiac output was computed by the Fick technique. For the green dye curve in Figures 5, 14 and 15 an experimental frequency plot was constructed in the same manner as described above and plotted in Figure 17.

The use of a density function as defined by equation (2-22) to detect cardiac defects is presented in Figure 17. The pronounced differences between the abnormal density functions and the normal density function may be noted. There seems to be a relation between the maximum or peak

value of  $f(t)$  and the cardiac output. It is also noted that the peak  $f(t)$  shifts to the right on the time scale as the cardiac output decreases. With sufficient data it appears that one could draw the boundaries of a region outside of which all density functions could be considered abnormal.

Figure 18 is a plot of experimental density functions for a normal heart, a case of aortic insufficiency and a case of mitral insufficiency. Density functions for hearts with valvular incompetence differ from those of normal hearts but show no clear relation between variables. The density function for the mitral insufficiency differs dramatically from the normal density function whereas the aortic insufficiency differs slightly. It was found that the degree of difference from normal depends greatly on the degree of insufficiency. Theoretically a density function cannot be defined for the case of mitral insufficiency since the value of  $\int_0^{\infty} f(t) dt > 1.0$ . Hence, it is possible to relate the degree of insufficiency to the value of the integral.

Equation (2-24) was derived from a simplified mathematical model which relates the mixing of indicators in the ventricle and in the central circulation to the mixing in uniform chambers connected in series. Although this model was developed from a physical standpoint there is no reason to expect it to exactly duplicate experimental results. If it was the aim of this author a more complicated model would have been

developed by the addition of chambers in parallel and series in an attempt to curve fit the theoretical  $f(t)$  to the experimental  $f(t)$ . However, it is shown below that equation (2-24) can be employed to explain the experimental density function in terms of ventricular function related to the number of chambers required to approximate the experimental density function.

For an experimental study consisting of an injection of a bolus of dye indicator into the left ventricle and the measurement of the fluid dye concentration at the aorta, equation (2-22) can be used to plot the experimental density function. Equation (2-5) can be employed to calculate  $V$  and equation (2-24) employed to find the theoretical density function for various values of  $N$ . Thus, the required number of chambers to approximate the experimental density function can be evaluated and the ventricular function diagnosed. A large  $N$  is an indicator of poor ventricular mixing and therefore poor ventricular function or low cardiac output. Experimental verification of the relationship between poor mixing and poor function is presented in chapter 4. From Figures 10 and 12 and other indicator studies, the mixing of an injected bolus of dye in a normal left ventricle can be represented by a series of approximately 3 to 5 uniformly mixed chambers.

For an experimental study consisting of an injection of a bolus of dye indicator into the right heart or the pulmonary

artery and the measurement of the fluid dye concentration at the aorta, equation (2-22) can be used to plot the experimental density function. Equation (2-24) can be employed to find the theoretical density function for various values of N where V is the central fluid volume given by, <sup>(35)</sup>

$$\text{C.V.} = Q \int_0^{\infty} t C(t) dt / \int_0^{\infty} C(t) dt = Q \bar{t} \quad (2-25)$$

$\bar{t}$  is the abscissal value of the centroid of the indicator dilution curve. Equations (2-24) and (2-25) were used to find the theoretical density function for the subjects in Figure 17. The value of N selected gave the best agreement between the experimental and theoretical density function plots. The theoretical density functions for each case are plotted in Figure 19 as well as the experimental density functions.

It was concluded that the mathematical model shown in Figure 11 is a valid approximation for the mixing of an injected bolus of dye indicator into the right heart or pulmonary artery from the time of appearance of dye in the aorta to the time of recirculation. Equation (2-24) can be easily modified to take into account the delay time by the addition of an expression for the density function from time  $t = \theta_1$  to  $t = t_a$ ,

$$\begin{aligned} f(t) &= 0, & \theta_1 \leq t < t_a \\ f(t) &= (2-24), & t_a \leq t \leq \infty \end{aligned} \quad (2-26)$$



where  $t_a$  is the appearance time of dye in the aorta. Equation (2-26) satisfies equations (2-18), (2-19) and (2-20).

Recirculation is a mathematical problem in itself. An analysis of the recirculation of dye involves convolution integrals for which no simple modification of the model in Figure 11 was found. However, an original mathematical model of the mixing of an injected bolus of dye has been developed which explains quantitatively the experimental density function in terms of ventricular performance related to the number of mixing chambers required to approximate it.

## 2.7 The Effect of Injection Site Upon the Shape of Dye Indicator Dilution Curves

In the previous sections a multichamber probabilistic model was employed to explain the shape of experimental green dye curves obtained by the injection of dye indicator directly into the left ventricle and by the injection of dye indicator into the pulmonary artery. The fluid dye concentration was measured in the aorta for both injection sites. The green dye curve obtained by the injection of dye into the pulmonary artery may be distorted by the mixing of the indicator in the lungs. Hence, a subject could be diagnosed as having a cardiac defect when in fact the abnormal shape of the green dye curve was due to a respiratory disorder. The green dye curve obtained by the injection of indicator into the left ventricle is not influenced by the mixing effectiveness of

the lungs.

Figure 20 is a reproduction of the work of Pearce et al, discussed on page 22, where the fluid dye concentration  $C(t)$  is plotted as a function of time for green dye studies employing various injection sites. The fluid dye concentration was measured in the carotid artery. Figure 21 is a plot of fluid dye concentration as a function of time measured from the first appearance of dye in the carotid artery for the green dye studies employing an injection of dye in the right auricle, pulmonary artery and the pulmonary vein of a dog. The difference in the green dye curves obtained by the injection of dye indicator in the pulmonary artery and the pulmonary vein is due to the mixing of dye in the lungs. This effect of injection site upon the shape of indicator dilution curves can be explained by the multichamber model.

Figure 17 shows an experimental density function for a normal heart obtained by the injection of dye indicator into the pulmonary artery and measured in the aorta. The multichamber model which explains the shape of this plot of density function versus time is shown in Figure 22. The shape of the green dye curve which would be obtained by an injection of dye in the pulmonary vein and measured in the aorta can be predicted by subtracting a single mixing chamber from the model in Figure 22 and applying equation (2-22). The green dye curve which would be obtained by an injection of green

dye in the pulmonary artery and measured in the aorta for a subject with a normal heart and a lung disorder can be predicted by the addition of mixing chambers to the model in Figure 22. Figure 23 is a plot of density function  $f(t)$  versus time for the models obtained by adding 1, 2, and 4 chambers to the model in Figure 22. It is noted that the density function obtained by adding 4 chambers appears similar in shape to that of an aortic stenosis in Figure 17. It was concluded that the shape of the green dye curve and the mathematical multichamber model can be used to diagnose cardiac state but the investigator must consider the calculated value of cardiac output  $Q$  and the central circulation fluid volume  $C.V.$  when employing the pulmonary artery as the green dye injection site.

It is usually undesirable to inject an indicator in the pulmonary vein, except in animals. However, it is possible to diagnose the blood flow through the lungs by obtaining green dye curves following the injection of dye into the pulmonary artery and the pulmonary vein. In the case of normal blood flow through the lungs the mathematical models that explain the shape of the green dye curves should differ by no more than two mixing chambers. If the models differ by more than two mixing chambers then pulmonary malfunction should be suspected. Congestion of the lungs is a possible cause of abnormal blood flow.

3. APPLICATION OF THE THEORETICAL ANALYSIS OF VENTRICULAR MIXING AND THE EXPERIMENTAL INDICATOR DILUTION METHODS TO EVALUATE CARDIAC STATE

3.1 Deterministic Analysis for Nonuniform Ventricular Mixing Applied to the Thermodilution Technique

Consider a thermal dilution study in which 5 to 10 cm<sup>3</sup> of cold saline is injected into the left ventricle during the *i*th diastole. The injection process is completed before the end of the *i*th diastolic function and the injectate has mixed in a nonuniform manner with the ventricular fluid at the end of diastole. The injection and mixing described above is given as case 4 on page 6. Dividing the end-diastolic volume of the *i*th heartbeat EDV<sub>*i*</sub> into *N* equal but arbitrarily small volumes of uniform temperature yields,

$$V_{ij} = EDV_i / N \quad (3-1)$$

where  $V_{ij}$  is the volume of the *j*th small volume element at the end of the *i*th diastole.

During the *i*th systole the stroke volume is given by,

$$SV_i = \sum_{j=1}^N g_{ij} V_{ij} \quad (3-2)$$

where  $g_{ij}$  is the fraction at the end of systole of each volume element that has contributed to the stroke volume. From equations (3-1) and (3-2),

$$SV_i = (EDV_i / N) \sum_{j=1}^N g_{ij} \quad (3-3)$$

The fundamental relationship between the  $EDV_i$  and  $SV_i$  is given by,

$$SV_i = EDV_i - ESV_i \quad (3-4)$$

for the  $i$ th heartbeat. Defining  $k$  as,

$$k = ESV_i / EDV_i \quad (3-5)$$

it follows that,

$$SV_i / EDV_i = 1 - k \quad (3-6)$$

From equations (3-3) and (3-6),

$$(1/N) \sum_{j=1}^N g_{ij} = 1 - k \quad (3-7)$$

(24)

It has been shown, utilizing the theory of instantaneous and uniform mixing,

$$k = \Delta T_{n+1} / \Delta T_n \quad (3-8)$$

Thus, from equations (3-6) and (3-8),

$$SV_i / EDV_i = 1 - \Delta T_{n+1} / \Delta T_n \quad (3-9)$$

But the above equation is only valid for uniform mixing and cannot be applied in this analysis without introducing errors in the calculation of ventricular volumes.

$k$  is an important parameter of ventricular function since it is defined as the ratio of the residual volume to

the total volume of the ventricle.  $(1 - k)$  is called the ejection fraction and represents the stroke volume divided by the end-diastolic volume. Consider the case where,  $g_{1j} = g_{1s}$  for all values of  $j$  and  $s$  such that  $0 < j \leq N$  and  $0 \leq s \leq N$  then it follows that,

$$k = 1 - g_{1j} \quad (3-10)$$

This would be the case if each small volume element ejected the same fraction of its volume during systole. This case is not very probable since the fluid ejected is not derived from all parts of the ventricle in equal proportions. The fluid close to the aortic valve will tend to be ejected completely while the apical contents only slightly, if at all. Hence, an equation relating  $g_{1j}$  to measured fluid temperatures for the case of nonuniform ventricular mixing is desired.

### 3.2 Application of the Generalized Thermodilution Equation to Derive an Expression for the Ejection Fraction of the $j$ th Volume Element

The generalized thermodilution equation is given by,

$$\sum_{\substack{\text{mass} \\ \text{entering}}} H - \sum_{\substack{\text{mass} \\ \text{leaving}}} H = U_{s,\text{final}} - U_{s,\text{initial}} \quad (3-11)$$

where  $H = T V C_p \rho$  and  $U = T V C_v \rho$ . Equation (3-11) is derived in appendix B. For the  $i+1$  diastole, the diastolic function following the injection of cold saline during the

ith diastole, equation (3-11) becomes,

$$\sum_{\substack{\text{mass} \\ \text{entering}}} H = U_{s,\text{final}} - U_{s,\text{initial}} \quad (3-12)$$

Equation (3-12) may be written as,

$$T_{sv} V_{sv} C_p e + \sum_{j=1}^N T_{1j} V_{1j} (1-g_{1j}) C_v e = \sum_{j=1}^N T_{i+1,j} V_{i+1,j} C_v e \quad (3-13)$$

and from a mass balance,

$$V_{sv} + \sum_{j=1}^N V_{1j} (1-g_{1j}) = \sum_{j=1}^N V_{i+1,j} \quad (3-14)$$

$$\text{Since } \sum_{j=1}^N V_{i+1,j} = \text{EDV}_{i+1} \text{ and } V_{1j} = \text{EDV}_1 / N \quad (3-15)$$

equation (3-14) becomes,

$$V_{sv} + (\text{EDV}_1 / N) \sum_{j=1}^N (1-g_{1j}) = \text{EDV}_{i+1} \quad (3-16)$$

Assuming  $\text{EDV}_1 = \text{EDV}_{i+1}$ ,

$$V_{sv} / \text{EDV}_1 = 1 - (1/N) \sum_{j=1}^N (1-g_{1j}) \quad (3-17)$$

which can be shown to be equivalent to equation (3-7).

For an incompressible fluid  $C_v = C_p$ , therefore equation (3-13) becomes,

$$T_{sv} V_{sv} = (\text{EDV} / N) \sum_{j=1}^N (T_{i+1,j} - T_{1j} (1-g_{1j})) \quad (3-18)$$

Substituting equation (3-17) into equation (3-18) yields,

$$T_{sv} (N - \sum_{j=1}^N (1-g_{1j})) = \sum_{j=1}^N (T_{i+1,j} - T_{1j} (1-g_{1j})) \quad (3-19)$$

which may be rearranged to give,

$$\sum_{j=1}^N (T_{sv} - T_{sv} (1-g_{ij})) = \sum_{j=1}^N (T_{i+1,j} - T_{ij} (1-g_{ij})) \quad (3-20)$$

It follows from equation (3-20) that,

$$\sum_{j=1}^N (g_{ij} (T_{sv} - T_{ij}) - T_{i+1,j} + T_{ij}) = 0 \quad (3-21)$$

Equation (3-21) represents a sum of terms which equals zero. For each  $j$ th volume,  $T_{i+1,j} \neq T_{ij}$ , therefore

$$g_{ij} = \frac{T_{i+1,j} - T_{ij}}{T_{sv} - T_{ij}} \quad (3-22)$$

for each volume element. Hence, in the case of nonuniform ventricular mixing equation (3-22) allows for the calculation of the fraction of each ventricular volume element that has contributed to the stroke volume. This expression can be used to evaluate the performance of sections of the ventricle wall which may be defective due to the presence of a lesion.

### 3.3 Relationship Between Ejection Fraction and Probability Density Function

In the preceding section an expression for the fraction of each volume element that has contributed to the stroke volume  $g_{ij}$  was found to be a function of measured temperatures as given by equation (3-22). The relationship between  $g_{ij}$  and the fraction of the  $j$ th volume element contributing to the flow during the  $i$ th systole at time  $t$ , defined as  $v_{ij}(t)$ ,



is given by,

$$g_{ij} = \int_{t_1}^{t_2} v_{ij}(t) dt \quad (3-23)$$

The relationship between the probability density function  $f(t)$  and  $v_{ij}(t)$  is given by,

$$f(t) = \sum_{j=1}^N q_{ij}(t) v_{ij}(t) \quad (3-24)$$

Multiplying both sides of the above equation by  $dt$  and integrating over the  $i$ th systole yields,

$$\int_{t_1}^{t_2} f(t) dt = \int_{t_1}^{t_2} \sum_{j=1}^N q_{ij}(t) v_{ij}(t) dt \quad (3-25)$$

or

$$F(t_2) - F(t_1) = \int_{t_1}^{t_2} \sum_{j=1}^N q_{ij}(t) v_{ij}(t) dt \quad (3-26)$$

Equations (3-23) and (3-25) can be used to obtain the relationship between  $q_{ij}$  and  $f(t)$ . Hence, the probabilistic analysis of nonuniform ventricular mixing presented in section 2.3 can be applied to the thermodilution technique. Equation (3-25) can theoretically be used to calculate  $F(t)$  from time  $t$  equal 0 to time  $t$  equal  $t$ ,

$$F(t) = \int_0^t f(t) dt = \sum_i \int \sum_{\text{systole}} q_{ij}(t) v_{ij}(t) dt \quad (3-27)$$

since  $F(0) = 0$ . Equation (3-27) however is difficult to apply since it requires the knowledge of  $q_{ij}$  for all values of  $j$  and  $i$ .

### 3.4 Application of the Probabilistic Analysis of Nonuniform Ventricular Mixing to the Thermodilution Technique

From the discussion in chapter 2 the probability density function for the thermal indicator is,

$$f(t) = T(t) / \int_0^{\infty} T(t) dt \quad (3-28)$$

(36)

Fegler derived the relationship between cardiac output Q and the measured aortic fluid temperatures for the thermodilution technique discussed on page 4,

$$Q = V_{inj} (T_B - T_{inj}) / \int_0^{\infty} T(t) dt \quad (3-29)$$

From equations (3-28) and (3-29),

$$f(t) = Q T(t) / V_{inj} (T_B - T_{inj}) \quad (3-30)$$

Equation (3-30) allows for the calculation of the density function from the temperature versus time trace of an experimental thermodilution study.

By plotting many normal thermodilution studies on a f(t) versus time plot abnormal studies may be diagnosed with a minimum of calculation. This was not done in this paper since this requires a large number of thermodilution studies utilizing the bolus injection technique. The experimental thermodilution studies presented in this paper employ a new technique which uses a continuous injection over multiple heartbeats.

#### 4. EXPERIMENTAL RESULTS

##### 4.1 Invitro Apparatus

A mechanical model of the left ventricle was designed and built in conjunction with Harvard Apparatus Company, Millis, Massachusetts to study the mixing of indicators in the ventricular fluid. The model had an end-diastolic volume of  $100 \text{ cm}^3$  and a variable stroke volume ranging from 0 to  $40 \text{ cm}^3$ . The stroke rate was variable ranging from 5 to 100 strokes per minute with an adjustable phase ratio between systole and diastole from 25% to 75% of the total cycle thus making it possible to simulate the normal cardiac cycle. A complete description of the invitro apparatus employed to study indicator mixing appears in reference (24) and is shown in Figure 24. The invitro studies are discussed in section 4.3.

##### 4.2 Invivo Apparatus

A fast response temperature probe was designed and built in conjunction with High Temperature Instruments Corporation, Philadelphia, Pennsylvania. This thermocouple probe consisted of chromel and alumel elements fully enclosed in a stainless steel sheath with an unexposed junction. The probe had a maximum diameter of 0.020 inches tapered to 0.014 inches and flattened to 0.010 inches at the tip. The thermal probe was proven safe, by invitro testing in the heart model described above, for clinical studies using human subjects. The time constant of the probe was found to be 0.008 seconds.

It was found that for a temperature probe to follow temperature changes during a heartbeat its time constant should be less than  $1/5$  the time interval of the systolic function. <sup>(37)</sup> For a heart rate of 70 beats per minute in which the diastolic and systolic periods are of equal length, the time constant of the probe must be less than 0.08 seconds to follow temperature changes during the heartbeat. In order to follow temperature changes during the systolic and diastolic periods it was found that a probe with a time constant of less than 0.02 seconds was required. Figure 25 is the response trace of the thermal probe manufactured by High Temperature Instruments Corporation to a step temperature change. This trace was taken in the Catheterization Laboratory while a catheterization was in progress, on the same equipment used for the invivo investigations. Hence, it was concluded from the above that continuous fluid temperature changes may be measured in the ventricle and aorta during the systolic and diastolic functions.

The thermocouple signal was amplified by a high gain, low noise, direct current amplifier manufactured by Ellis Associates, Pelham, New York and further amplified and recorded on a monitoring oscillograph manufactured by Electronics for Medicine, White Plains, New York.

#### 4.3 Invitro and Invivo Mixing Studies

A major concern of investigators today is the assumption of instantaneous and uniform mixing of indicators with the

ventricular fluid. In section 1.3 a macroscopic description of mixing was presented in which it was concluded that ventricular mixing of indicators is mainly due to forced convection. In order to extend the mixing studies of other investigators who employed mechanical models, the heart model discussed in section 4.1 was used to study the mixing of thermal indicators. These mixing studies are discussed in detail in references (24) and (38). The experimental mixing studies of thermal indicators were performed at various heart rates and stroke volumes. It was concluded that instantaneous and uniform mixing of the injected thermal indicator with the ventricular fluid can be assumed with a maximum error of 15% in the theoretically calculated continuous ventricular volume.

The mixing of thermal indicators was also studied in the dog's heart. In order to compare thermal and dye indicator mixing a bolus of  $3 \text{ cm}^3$  of cold green dye was injected into the left ventricle during the diastolic function. Figure 26 is a mixing study in which the ventricular fluid temperature was measured in the ventricle and the ventricular fluid dye concentration was measured at the aorta. It was found that the relative mixing of both indicators with the ventricular fluid is about the same in the normal dog's heart.

By the injection of Lycopodium seeds into the coronary artery an infarction was produced in the dog's heart which

reduces the cardiac output and the mixing effectiveness of the left ventricle. Figure 27 is a simultaneous green dye and thermodilution study following the bolus injection of  $3 \text{ cm}^3$  of cold green dye into the left ventricle. The left ventricular fluid mixture temperature was measured in the ventricle and the ventricular fluid dye concentration was measured at the aorta. This study was performed while the dog was having a cardiac infarction. In the failing heart the mixing of dye and thermal indicators becomes dependent on diffusion and conduction respectively, since the forced convection of the heart walls and the incoming stroke volume is reduced substantially. From the mixing studies performed invivo in the dog it was concluded that the mixing of indicators injected as a bolus into the left ventricle is related to ventricular performance and cardiac state.

The dye injected into the right heart mixes with the central fluid volume in the right heart, pulmonary artery, the lungs, the pulmonary vein and the left atrium before it enters the left ventricle. Except in the case of poor left ventricular filling the fluid dye concentration can be safely assumed uniform by the end of each diastolic function.

#### 4.4 Invivo Thermodilution Procedure

Section 1.2 briefly described the thermodilution technique developed by Fegler which involved the placing of a thermal probe just above the aortic valve and the injection

of a small amount of cold saline into the left ventricle during the diastolic function of the heartbeat. The thermodilution equations derived by Holt for the calculation of ventricular end-volumes from measured temperatures were introduced. In this chapter a new thermodilution technique is presented which utilizes a continuous injection of cold saline over three or four heartbeats and equations which allow for the calculation of continuous left ventricular volume. Two procedures will be discussed. One employs two catheters and the other only one specially designed catheter called a "Thermocatheter".

The two catheter invivo thermodilution procedure employed at Saint Michael Medical Center was developed in conjunction with Dr. R. Brancato, Chief of Cardiac Catheterization. This procedure, called the "Brancato Technique", consisted of first introducing a Number 5 French Sones catheter into the right brachial artery and directing it into the left ventricle. A second catheter, a Number 6 French Percutaneous catheter, was then introduced percutaneously into the right femoral artery and directed to either the left ventricle or the ascending aorta depending on which was to be studied first. Usually the left ventricle was studied before the aorta. The percutaneous catheter served as a guide for the thermal probe

which was passed through it until it projected from the tip of the catheter approximately  $3/16$  of an inch in the ventricular fluid. This projected length was desired since it allowed the probe to act as an infinite pin and conduction along the probe tip was negligible.

The positioning of the two catheters in the left ventricle was accomplished by means of an X-ray monitoring system using standard cineangiographic equipment. Figure 28 is a schematic diagram of the in vivo patient to equipment relationship. The proper catheter configuration in the left ventricle is shown in Figure 29, which is a cine-X-ray frame showing the location of the two catheters in the left ventricle. The injecting catheter is distal to the thermocouple.

After the catheters were positioned and the thermal probe was measuring ventricular fluid temperature, an injection of between 30 and 40  $\text{cm}^3$  of cold saline at a temperature of between 40 and 60  $^{\circ}\text{F}$  was made over a period of 3 to 4 heartbeats by a continuous and constant injection device with a low injection pressure. This type of injection of cold saline has three major advantages over the classical instantaneous bolus injection:

- 1) An instantaneous injection usually involves the injection of between 5 and 8  $\text{cm}^3$  of saline during a single diastolic function. This injection requires a high injection pressure and a programmed injector utilizing the EKG signal. The



catheter dead space must also be taken into account since the start of the injection will only tend to empty the contents of the catheter which are at body temperature.

The high injectate velocity resulting from the high injection pressure tends to produce ventricular wall irritation producing extra systolic functions called premature ventricular contractions or pvc's. The presence of pvc's confuses the interpretation of the data and discomforts the patient. An injection over 3 or 4 heartbeats with a low injection pressure was found to produce the least ventricular irritation.

2) The continuous injection of cold saline enhances the ventricular mixing, thus reducing the error incurred by assuming that the ventricular fluid temperature gradient at any time during the heartbeat is zero. The experimental mixing studies discussed in section 4.3 indicated that a maximum error of 15% in calculated ventricular volumes is incurred by assuming that instantaneous and uniform mixing of the bolus of injected cold saline with the ventricular fluid occurs. Therefore it has been assumed that the calculated continuous ventricular volumes are within  $\pm 15\%$  of the actual volumes.

3) The continuous injection allows the investigator to inject during any time of the heartbeat and is assured of calculable data from at least two heartbeats. The first heartbeat during the continuous injection is usually not analyzed since

it is when the catheter dead space is cleared.

Figure 30 shows the effect of the extra systoles on the thermodilution study. Figures 31 and 32 show the catheters in the left ventricle during the continuous injection over multiple heartbeats and the catheters after the injection process is completed. Note that the catheters return to their respective positions at the end of the injection. Usually two or more runs were made with both catheters in the left ventricle and the ventricular fluid temperature was recorded during the injection process and during the warming process as the ventricular fluid returned to body temperature.

The thermocouple was then pulled back into the catheter and the catheter was then placed in the aorta just above the aortic valve. The thermocouple was then pushed forward in the catheter so that it was exposed in the aortic fluid in the same manner as in the ventricle fluid. An injection of cold saline as described above was then performed and the aortic fluid temperature was recorded throughout the cooling and warming periods. This procedure was also performed at least twice to insure repeatability.

With the catheters in the above position, one in the ventricle and the other in the aorta, simultaneous pressures were recorded utilizing a Statham transducer connected to each catheter end. The data recorded in addition to the temperature tracings was, the volume of saline injected,

temperature of saline in injector syringe, temperature of saline reaching the ventricle, injection pressure and the amplitude gain settings on the monitoring oscillograph. The temperature of saline reaching the ventricle is calculated by adding the temperature increase across the catheter, which is determined experimentally, to the temperature of saline in the injector syringe. Appendix E explains the experimental procedure for the temperature correction for the warming of the injected fluid in the catheter during the injection process.

#### 4.5 Invivo Thermodilution Studies in Man

Figure 33 is a thermodilution study of a coronary patient with good left ventricular function. Trace (a) is a measured temperature versus time plot for the left ventricle during and following the constant injection over multiple heartbeats of  $40 \text{ cm}^3$  of cold saline at a temperature of  $50^\circ\text{F}$ . A low injection pressure, 250 psi, was used to inject the saline in 3.8 seconds over 5 heartbeats. During the injection process the heart rhythm and the electrocardiogram remained unchanged. From trace (a) it is obvious that the thermal probe was too close to the aortic valve flow. Hence, with each systolic function the thermocouple would record a temperature change in the left ventricle as the unmixed ventricular fluid passed by the probe on its way out the aorta. This unmixed fluid is close to the aortic valve outside of the mixed region of

the ventricular fluid and is ejected at the start of systolic flow. If the probe were placed properly within the well mixed fluid region no temperature change would be recorded during systole after the injection of the saline.

Trace (b) in Figure 33 is an aortic thermodilution study obtained with the same injection process described above. Trace (c) is a simultaneously recorded ventricular and aortic pressure trace which allows for the verification of the onset of systolic and diastolic flows indicated by the thermodilution study. From trace (c) and the electrocardiogram the four functions which make up the heartbeat are characterized as the ejection process, isovolumetric relaxation, filling process and the isovolumetric contraction. These functions are labeled I, II, III, and IV respectively on trace (c). The points a, b, c, and d refer to the onset of each particular function and refer to the opening and closing of the aortic and mitral valves. Traces (a), (b) and (c) can be compared by relating the points a, b, c, and d of each trace to the other.

Usually the measured temperature versus time plot for the left ventricle is used to calculate the continuous ventricular volume during the diastolic and systolic functions of the heartbeat with equations (C-23) and (C-27). The aortic temperature trace is usually employed to calculate the end-volumes of the left ventricle with equations (B-34), (B-35) and (B-36). However, in this study the thermal probe was

placed too close to the aortic valve during the ventricular thermodilution study, trace (a). Hence, this trace was only used to calculate the continuous volume of the left ventricle during the diastolic function with equation (C-27). It was assumed that the measured aortic fluid temperature was equal to the temperature of the fluid in the ventricle during the systolic function and during the continuous injection of cold saline. Equation (C-23) and trace (b) were used to calculate the continuous volume of the ventricle during the systolic function of the heartbeat. The measured aortic fluid temperature during the diastolic function can be employed to study the mixing in the aorta. No calculation of aortic mixing was made in this research utilizing measured aortic temperature during diastole.

Figure 34 is the calculated ventricular volume versus time plot for the thermodilution study described above. The points a, b, c, and d on the volume plot refer to the opening and closing of the aortic and mitral valves as described on Figure 33. Figure 35 is the measured ventricular pressure versus the calculated ventricular volume plot, called the work diagram, for the left ventricle. From Figures 34 and 35 the left ventricular function can be diagnosed as normal.

Figure 36 is a thermodilution study of a normal left ventricle in which the thermal probe was placed within the

well mixed region. Trace (a) is the measured ventricular fluid temperature during and following the injection of  $40 \text{ cm}^3$  of saline at a temperature of  $45^\circ \text{F}$  over 5 heartbeats. During the injection process there were two extra systolic functions followed by two abnormal heartbeats. Hence, there was only a single beat during the injection process which could be employed to calculate the continuous ventricular volume. The portion of the ventricular temperature trace labeled by the points a, b, c, and d was used with equations (C-23) and (C-27) to calculate the continuous volume of the left ventricle during the diastolic and systolic functions. The points a, b, c, and d are defined on Figure 33.

Figures 37 and 38 are the volume and work diagrams constructed from the calculated ventricular volumes and the measured ventricular pressures. Trace (b) in Figure 36 is a trace of the ventricle and aortic pressures obtained by pulling the catheter across the aortic valve and recording the measured pressures. This type of pressure trace is known as a pull back pressure.

The calculated end-volumes in this thermodilution study were verified by the Fick and green dye techniques. The cardiac output calculated by the thermodilution, Fick and green dye techniques were 5.47, 5.5 and 4.95 liters per minute, respectively. Hence, from this and similar studies it was concluded that the fraction of unmixed ventricular fluid is

negligible in the normal left ventricle.

Figure 39 is a thermodilution study in which  $40 \text{ cm}^3$  of saline at a temperature of  $45^\circ \text{F}$  was injected into the left ventricle with an injection pressure of 250 psi over 5 heartbeats. Trace (a) in Figure 39 is the trace of the left ventricular fluid temperature during and after the injection process. The heartbeat was unaffected by the injection process. The continuous ventricular volume was calculated using equations (C-23) and (C-27) and the temperature trace for heartbeat C in Figure 39. Figures C-3 and C-4 are the computer solutions for the calculation of the ventricular volume during the heartbeat C.

Trace (b) in Figure 39 is the simultaneous ventricular and aortic pressures. Figure 40 is the volume diagram and Figure 41 is the work diagram for this subject's left ventricle which was diagnosed as normal with good left ventricular function.

The last three heartbeats during the injection process were analyzed in order to show the repeatability of this new thermodilution technique. From the temperature versus time traces of heartbeats C, D, and E in Figure 39 the volume versus time plot was constructed for each heartbeat and is shown in Figure 42. The maximum difference in the calculated volumes for the three heartbeats was 14.3% which

is consistent within the limits of accuracy discussed on page 39.

#### 4.6 Invivo Thermodilution Study of Abnormal Ventricular Function

Figure 43 is a thermodilution study of a patient with advanced aortic regurgitation confirmed by cineangiography. Trace (a) is the aortic fluid mixture temperature versus time during and following the injection of 30 cm<sup>3</sup> of saline at a temperature of 47 °F. Trace (b) is the ventricular fluid temperature. No calculation of ventricular volume could be made from either of these traces using equations (C-23) or (C-27) since they were derived in appendix C for ventricles without valvular incompetence. In appendix C equations are presented which could be solved simultaneously to obtain a measure of the insufficiency. But even without calculations the temperature trace shows that the patient had an enlarged ventricle and regurgitant flow from the aorta to the ventricle during diastole.

By comparing Figure 43 to Figures 33, 36 and 39, the thermodilution studies previously discussed, the differences between a thermodilution study of a normal left ventricle and one with valvular incompetence are recognized. Note from traces (a) and (b) in Figure 43 the large number of beats required to expell the cold saline. The calculated value of k was found to be 0.80 which is outside of the normal range of .55 to .65. In trace (b) the regurgitant flow is measured



by the thermal probe in the left ventricle at the end of diastole. Trace (c) is the simultaneous pressures measured in the ventricle and aorta. The exaggerated aortic pressure trace is an indicator of aortic incompetence.

#### 4.7 The Thermocatheter

The Brancato technique originally developed in order to estimate continuous left ventricular volume and work employs two catheters, one for the injection of cold saline and the other for the continuous measurement of ventricular fluid mixture temperature. For patients with aortic stenosis it is usually very difficult to pass two catheters across the aortic valve. For patients with a small left ventricle, which is usually the case in the presence of mitral stenosis, it is very difficult to establish the proper catheter configuration as described on page 42. The thermocatheter is the author's original design of a device which allows for the injection of saline into the left ventricle and the continuous direct measurement of the ventricular fluid mixture temperature employing a single catheter.

The first design of the thermocatheter consisted of a ventriculography catheter in which a hole had been made at the tip. When the thermocouple was passed through the catheter it occluded the front hole and extended beyond the tip of the catheter a distance of  $\frac{3}{16}$  of an inch. This design fulfilled its purpose but it did not handle as well as desired.

A disadvantage was that it employed a Ventriculography catheter which is used in retrograde catheterization of the left ventricle. It was more desirable to employ a percutaneous catheterization.

During a thermocatheter study in a mongrel dog intended to evaluate the safety of the design it was discovered that the probe can easily find its way through one of the side holes instead of the distal hole. In this position the probe produced a hematoma and the tip of the probe could have easily been broken. Hence, this design was not employed in human studies.

The second thermocatheter design, shown in Figure 44, employs a Percutaneous catheter and an occluder which is cold soldered on the thermal probe. The distal hole is occluded and prevents any cold saline from washing directly on the thermocouple tip which extends from the catheter tip a distance of  $3/16$  of an inch into the ventricular fluid. This design was found to be safe for human studies and easy to use. No premeasurement of the thermocouple length is required since the investigator can see the occluder on the X-ray screen.

#### 4.8 Invivo Thermodilution Study in the Dog Employing the Thermocatheter

The thermodilution studies in the dog differ from those in man since a much smaller volume of cold saline is required to drop the ventricular fluid temperature. Hence, a bolus

injection of 2 or 3 cm<sup>3</sup> made instantaneously into the left ventricle was found to be the best technique. As previously discussed the dead space in the catheter must be corrected for in the case of a bolus injection. This was done by allowing the fluid in the catheter to reach the body temperature of the dog and neglecting the temperature rise across the catheter.

Figure 45 is a thermodilution study which employed a bolus injection of 2 cm<sup>3</sup> of cold saline at 2 °C. Equations (1-1) and (C-21) were used to construct the volume versus time and work diagram for the dog's left ventricle during diastole. The results of this and other thermodilution studies employing the Thermocatheter compared favorably with the results of the green dye studies which only allow for the calculation of end-volumes and cardiac output.

#### 4.9 Invivo Thermodilution Study in Man Employing the Thermocatheter

The procedure used at Saint Michael Medical Center employing the Thermocatheter was to introduce a Number 7 French Percutaneous catheter into the right femoral artery and direct it into the left ventricle. This catheter is then used as a guide for the thermocouple with the occluder which is passed through the catheter until the occluder is felt seating in the distal hole. After the thermal probe is in place 15 to 30 cm<sup>3</sup> is injected over 3 or 4 heartbeats. The measured fluid temperatures are related to ventricular

volumes in the same manner as the studies which involve the use of two catheters.

Figure 46 is a thermodilution study employing the thermocatheter. This patient had valvular incompetence and only a single catheter could be placed in the ventricle safely. Trace (a) is the ventricular fluid temperature during and after the continuous injection, over multiple heartbeats, of cold saline. Note during the cooling and warming periods the indication of regurgitant flow. This is an example of how the thermocatheter can be employed to diagnose ventricular function.

#### 4.10 Results of Experimental Thermodilution Studies

A total of twenty-six thermodilution studies were performed *invivo* in man at Saint Michael Medical Center employing both the Brancato Technique and the Thermocatheter. Eleven of the thermodilution studies were exploratory in nature, in which the thermodilution technique was developed. Table I, on page 55, is a tabulation of the exploratory thermodilution studies which outlines the purpose and results of each of these studies. The procedure which evolved from the exploratory thermodilution studies was discussed on page 40.

Table II, on page 56, is a table of calculations for the diagnostic thermodilution studies in man. The calculated mean value of  $k$ , EDV, ESV and  $Q$  are 0.596, 148 cm<sup>3</sup>, 80.7 cm<sup>3</sup> and 5.7 l/min respectively. These mean values verify those

TABLE I

TABLE OF EXPLORATORY THERMODILUTION STUDIES IN MAN  
PARTIAL ANALYSIS

RUN	PURPOSE AND RESULTS	CALCULATED k
BRANCATO TECHNIQUE		
1	Experimentation to determine the best rate of injection and volume of injection and their effect on the patient. Best results were obtained with an injected volume greater than 20 cm <sup>3</sup> injected continuously over 3 or more beats.	.75
2	Experimentation to determine the best injection pressure. Injection pressure above 350 psia tends to produce arrhythmia. With a #6 French catheter a 350 psia injection pressure corresponds to an injection velocity of 1484 cm/sec.	.68
3	Improper catheter configuration in the left ventricle. Thermocouple catheter too close to injection catheter. Thermocouple catheter should be placed distal to injection catheter.	.57
4	Injected fluid temperature too low. Caused inversion of T wave on EKG signal. Best injected fluid temperature is above 45 °F regardless of amount injected.	
5	Thermocouple catheter too close to aortic fluid flow. Thermocouple must be in well mixed ventricular fluid volume.	.625
6	High injection pressure (350 psia) produced arrhythmia and extra systolic function.	.63
7	Patient with sensitive ventricular wall. Even with low injection pressure of 250 psia produced pvc's throughout injection process. Shown in Figure 30.	
8	Improper catheter configuration.	.60
THERMOCATHETER		
9	Patient with aortic insufficiency determined by temperature rise during systolic function.	.80
10	Thermocouple not placed properly in catheter, distal hole not occluded.	.70
11	Thermal probe too close to mitral valve. Velocity effects appear on temperature versus time trace indicating opening and closing of mitral valve.	

TABLE II

## TABLE OF CALCULATIONS FOR INVIVO THERMODILUTION STUDIES IN MAN

CASE	1	2	3	4	5	6	7	8	9	10	11	12	13	14	15
TECHNIQUE	B	B	B	B	TC	TC	B	B	B	B	B	B	B	TC	TC
DIAGNOSIS BY CINE	N	N	N	AR	AR	PF	N	N	N	N	N	N	N	N	N
DIAGNOSIS BY THERMODILUTION	N	N	N	AR	AR	PF	N	N	N	N	N	N	N*	N	N*
HEARTBEATS PER MINUTE	75	86	86	70	68	80	80	75	76	79	92	100	107	80	100
AVERAGE k	.635	.58	.55	.80	.82	.70	.70	.57	.50	.612	.557	.584	.67	.60	.62
CALCULATED EDV	173	143	138	-	-	160	138	183	140	90.5	-	186	131	120	185
CALCULATED ESV	110	80	62	-	-	112	97	104	70	54.5	-	77.5	87.8	48	115
CALCULATED Q	4.73	5.42	6.5	-	-	3.85	3.28	5.9	5.3	3.15	-	10.85	4.6	5.75	7.0
$\dot{V}_{inj}$	11.4	11.4	11.4	11.4	11.4	11.4	11.4	11.4	11.4	12.3	11.4	11.4	11.4	11.4	12.3
$T_{inj}$	50	45	45	47	50	46	45	65	50	50	50	50	50	50	50
INJECTOR PRESSURE	250	250	250	250	250	250	250	250	250	300	250	250	250	250	300
Q CALCULATED BY FICK	-	5.5	-	-	-	-	-	-	5.1	-	-	-	-	-	-
Q CALCULATED BY GREEN DYE	4.9	4.95	-	-	-	-	-	-	4.7	-	-	-	-	-	-
WORK BY $\bar{P}_v \cdot SV$ , ergs $\times 10^{-7}$	.685	.858	.858	-	-	.543	.490	1.1	.793	.580	-	.960	.342	.90	-
WORK BY $\int P_v dv$ , ergs $\times 10^{-7}$	.640	.814	.860	-	-	.600	.600	1.08	.88	.620	-	1.10	.430	1.10	-

B - Brancato Technique, TC - Thermocatheter, AR - aortic regurgitation, PF - poor ventricle function  
 \* - high cardiac output

published by other investigators utilizing various techniques. Figure 47 is a nondimensionalized left ventricular volume plot for the thermodilution studies outlined in Table II and diagnosed as normal. From this plot the band or range of normalcy can be constructed.

The physiologist uses an approximate formula <sup>(39)</sup> to determine the work done by the left ventricle during the heartbeat,

$$\text{Work} = \bar{P}_v \cdot SV \quad (4-1)$$

where  $\bar{P}_v$  is the mean ventricular pressure during systole. Table II shows the work found by equation (4-1) and the work calculated by measuring the area within the pressure versus volume loop which is equivalent to,

$$\text{Work} = \int_{\text{loop}} P_v \, dV \quad (4-2)$$

Hence, it is concluded that the approximate formula given by equation (4-1) is quite accurate.

Figure 48 is a plot of ventricular stroke work versus ventricular end-diastolic volume for the thermodilution studies presented in this paper. It is concluded from this plot that ventricular stroke work is not singularly dependent on the end-diastolic volume. This is the expected result since the ventricular work is a function of ventricle pressure and stroke volume.

Figure 49 is a plot of ventricular stroke work versus

ventricular end-diastolic pressure. The relationship between stroke work and end-diastolic pressure of the ventricle is clearly shown. This plot indicates the normal range of ventricular stroke work and end-diastolic pressure. The abnormal range is characterized by an increase in end-diastolic pressure for a small or no increase in stroke work;  $dP/dW$  is less than 0.06 and ventricular stroke work is greater than  $1.2 \times 10^7$  ergs.

Figure 50 is a plot of ventricular end-diastolic pressure versus ventricular end-diastolic volume. The relationship between end-diastolic pressure and end-diastolic volume shown is for the range of normal hearts. In the range for abnormal hearts there is a large increase in end-diastolic pressure for a small increase in end-diastolic volume.

Figure 51 is a plot of left ventricular pressure versus left ventricular volume for the thermodilution studies outlined in Table II and diagnosed as normal. From this figure one could estimate the range and area of a pressure versus volume loop for a normal left ventricle. The dashed line loop is the estimated mean pressure versus volume curve for a normal left ventricle. The range and area of the work diagrams for the normal left ventricles compares favorably with the work of Dodge.<sup>(40)</sup> Dodge constructed the volume versus time plot for the left ventricle by the biplane cineangiographic technique. These biplane techniques involve the injection of large quantities of radio-opaque material



and large doses of x-rays thus making it undesirable as a clinical tool.

Figure 52 shows the pressure versus volume plots published by Dodge. Superimposed on his results is a work diagram of a normal left ventricle computed from the results of a thermodilution study, case 8, utilizing the continuous injection of cold saline over multiple heartbeats. This figure clearly indicates how the work diagram can be used to evaluate cardiac state.

## 5. CONCLUSIONS

The major conclusions of the research presented in this paper are the techniques developed for the evaluation of cardiac state utilizing dye and thermal indicators. The green dye curve obtained by the injection of green dye into the pulmonary artery and the measurement of the fluid dye concentration in the aorta was employed to evaluate cardiac state. This was accomplished via a mathematical analysis which related the fluid dye concentration to a probabilistic density function. The density function was shown to be an indicator of cardiac state.

A mathematical model was developed from the physical characteristics of the central circulation which explains the shape of the green dye curve in terms of the number of mixing chambers  $N$  in series which make up the model. A large  $N$  was shown to be an indicator of poor cardiac function. It was concluded that the mathematical model and the green dye curve can be employed to diagnose cardiac state as long as the investigator utilizes a bolus injection of green dye into the pulmonary artery and measures the fluid dye concentration in the aorta. The effect of dye mixing in the lungs on the shape of the green dye curve was studied and it was concluded that the values of cardiac output and central fluid volume must also be considered when making a diagnosis of cardiac state utilizing the mathematical model.

The green dye curve obtained by the injection of green dye into the left ventricle and the measurement of the fluid dye concentration at the aorta was employed to study the mixing effectiveness of the left ventricle. By employing the multichamber model it was found that the mixing of a dye indicator injected as a bolus into a normal left ventricle can be represented by two perfectly mixed chambers in series. An abnormally functioning heart can be represented by calculating the cardiac output and ventricular end-diastolic volume and plotting the density function for different values of  $N$ . In cardiac failure or enlarged heart  $N > 2$ .

Two experimental techniques were developed for calculating the work performed on the fluid by the left ventricle during the heartbeat. Both techniques involve the continuous direct measurement of ventricular fluid mixture temperature during and following the controlled injection, through a catheter, of a known volume of cold saline into the left ventricle. The techniques differ in the number of catheters required. The Brancato technique employs two catheters placed in the proper configuration in the left ventricle. The Thermo-catheter, developed in this research, employs a single catheter to inject and measure the ventricular fluid mixture temperature. Equations (B-34), (B-35) and (B-36) were employed to calculate ventricular end-volumes from the ventricular fluid temperatures measured in the aorta. Equations (C-23) and

(C-27) were used to calculate the continuous ventricular volume during the heartbeat from the ventricular fluid temperature measured in the left ventricle. The work diagram for the left ventricle was constructed by plotting the measured ventricular pressure versus the calculated volume of the ventricle for a heartbeat. The work diagram was employed to diagnose cardiac state.

A total of twenty-six thermodilution studies were performed invivo in man employing both the Brancato Technique and the Thermocatheter. The calculated mean values of  $k$ , EDV, ESV and  $Q$  were 0.596, 148  $\text{cm}^3$ , 80.7  $\text{cm}^3$  and 5.7 l/min respectively. The approximate formula used by physiologists to calculate the stroke work of the left ventricle, given by equation (4-1), was experimentally verified in this research. By plotting the ventricular stroke work versus ventricular end-diastolic volume for the thermodilution studies presented it was concluded that the stroke work is not singularly dependent on the end-diastolic volume.

The relationship between ventricular stroke work and end-diastolic pressure for the range of normal hearts is shown in Figure 49. The relationship between the end-diastolic pressure and the end-diastolic volume for the range of normal hearts is shown in Figure 50. Figure 51 is a plot of left ventricular pressure versus left ventricular volume for the thermodilution studies in normal hearts. From this figure

the range and area of a pressure versus volume loop for a normal left ventricle was estimated and appears as a dashed line loop in the figure.

## 6. RECOMMENDATIONS

In this paper the author has presented many possible areas of investigation. By employing the green dye curve, obtained by the injection of dye in the pulmonary artery and the measurement of the fluid dye concentration at the aorta, and the integral of the density function  $\int_0^{\infty} f(t) dt$  the relationship between the value of the integral and the degree of valvular insufficiency can be evaluated. For a heart with a normally functioning aortic and mitral valve the value of the integral should equal 1.0. In the presence of an insufficiency the value of the integral will be greater than 1.0. In order to establish the relationship between the value of the integral  $\int_0^{\infty} f(t) dt$  and the degree of insufficiency many green dye studies must be performed in hearts with valvular defects.

Equations (C-13), (C-14) and (C-15) may be employed to evaluate abnormal flows between the chambers of the left heart utilizing the Brancato Thermodilution Technique. The investigation would involve simultaneous temperature measurements in the chambers being studied and the simultaneous solution of the above equations.

Section 3.4 presents an application of the probabilistic analysis of nonuniform ventricular mixing to the thermodilution technique. By plotting many normal thermodilution

studies on a  $f(t)$  versus time plot, the range of normalcy can be established from which abnormal studies may be diagnosed with a minimum of calculation. This was not done in this research since this requires a large number of thermodilution studies utilizing the bolus injection technique.

In the case of nonuniform ventricular mixing of the injected saline with the ventricular fluid equation (3-22) allows for the calculation of the fraction of each ventricular volume element that has contributed to the stroke volume. This expression can be used to evaluate the performance of sections of the ventricle wall which may be defective due to the presence of a lesion.

It is the author's opinion that many more thermodilution studies employing the Brancato Technique and the Thermo-catheter should be performed on subjects with different cardiac defects in order to establish the thermodilution technique as a clinical tool.

Diagram of the Human Heart

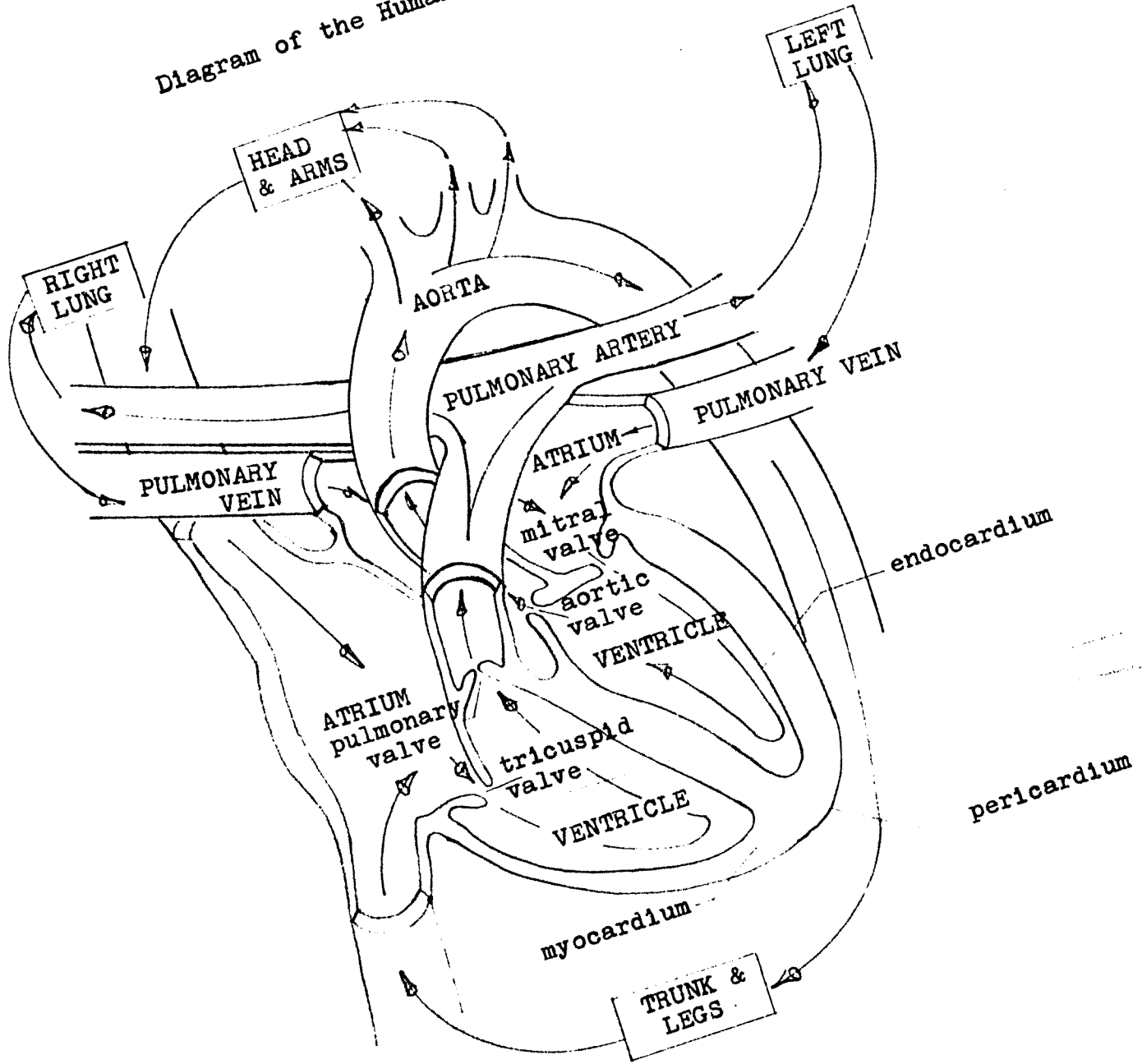


FIGURE 1



## Classic Stewart-Hamilton Indicator Dilution Curve

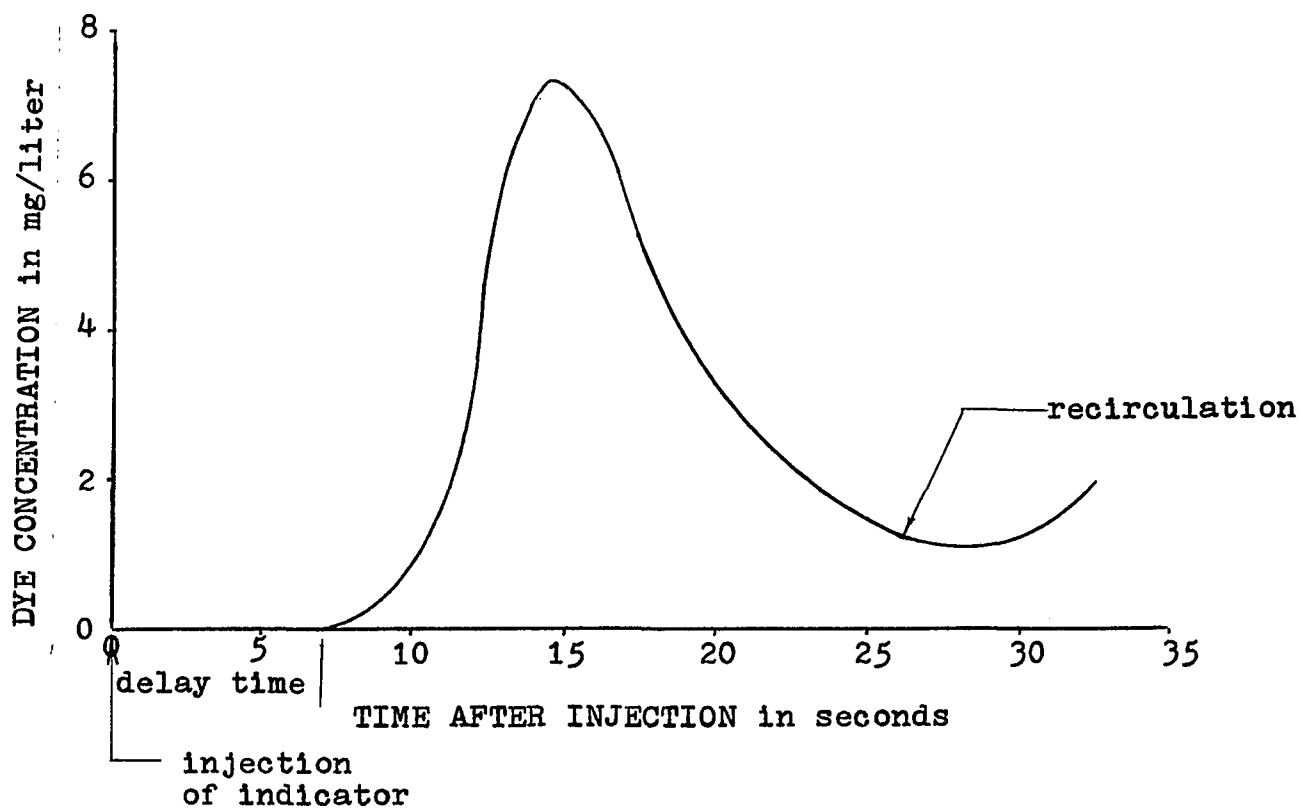


FIGURE 2

Dye Concentration versus Time Obtained by Discontinuous Sampling Technique After Instantaneous Injection of Dye

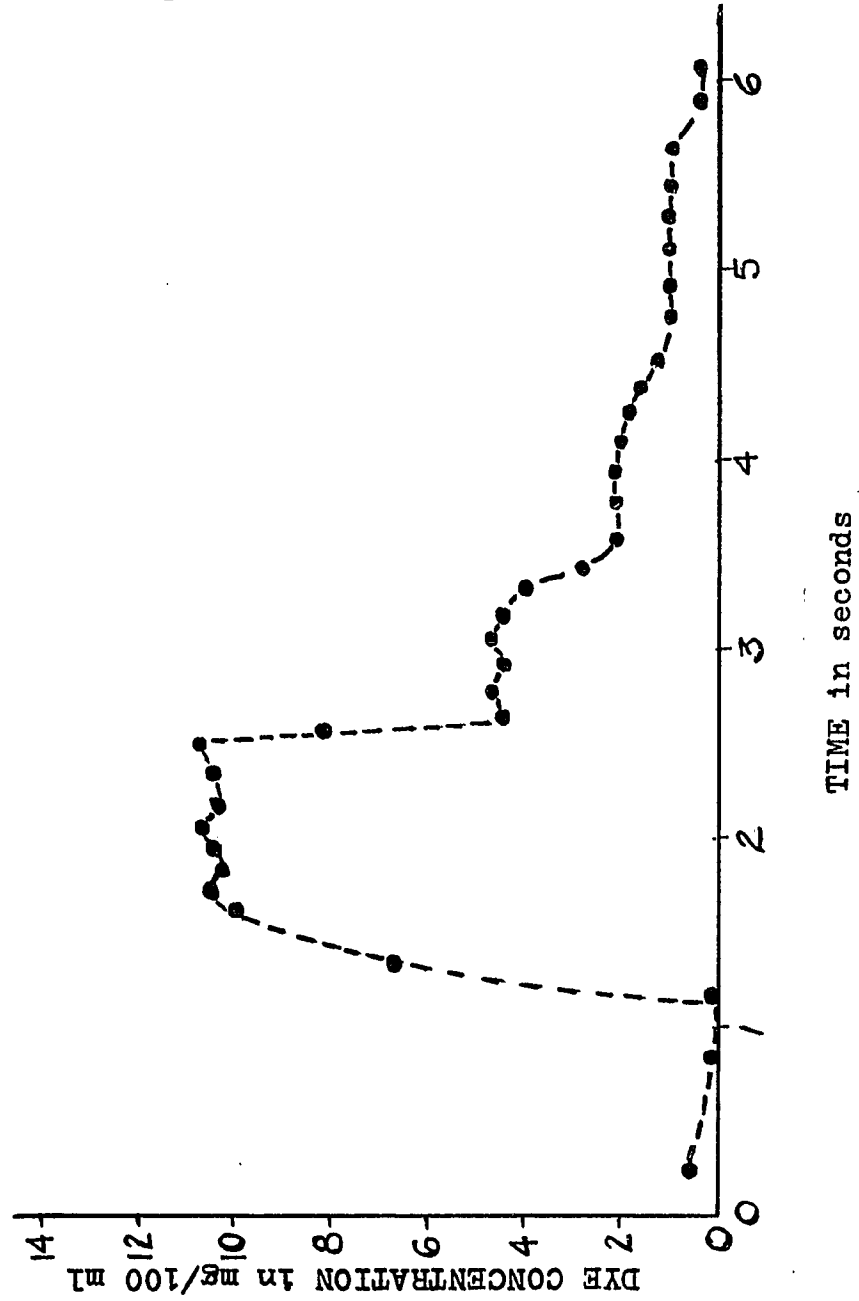


FIGURE 3

## Ideal Thermodilution Curve With Thermistor In Aorta

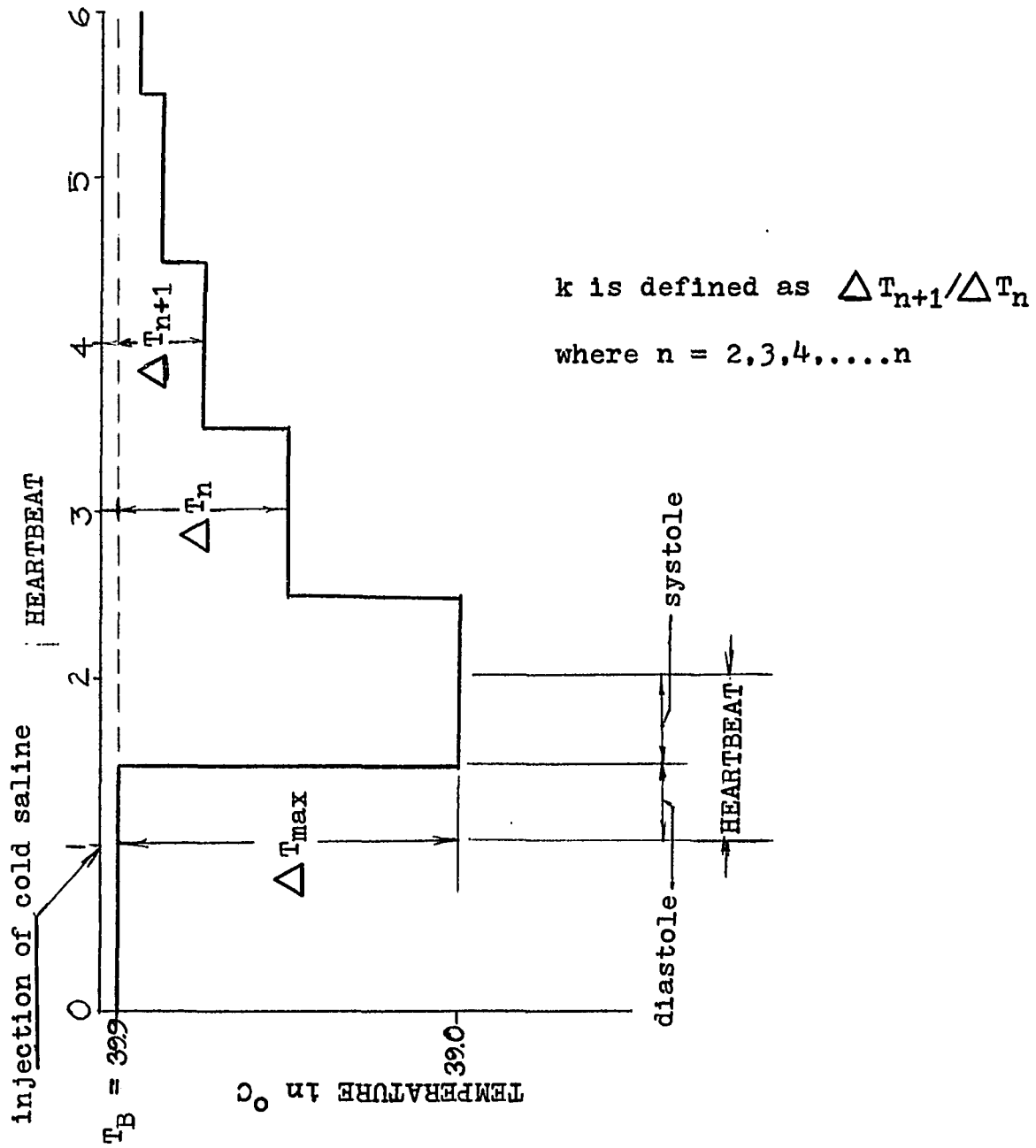


FIGURE 4

Experimental Green Dye Study in Man  
Obtained by the Injection of 5 mgm  
of Green Dye into the Pulmonary Artery  
and the Fluid Dye Concentration Measured  
in the Aorta

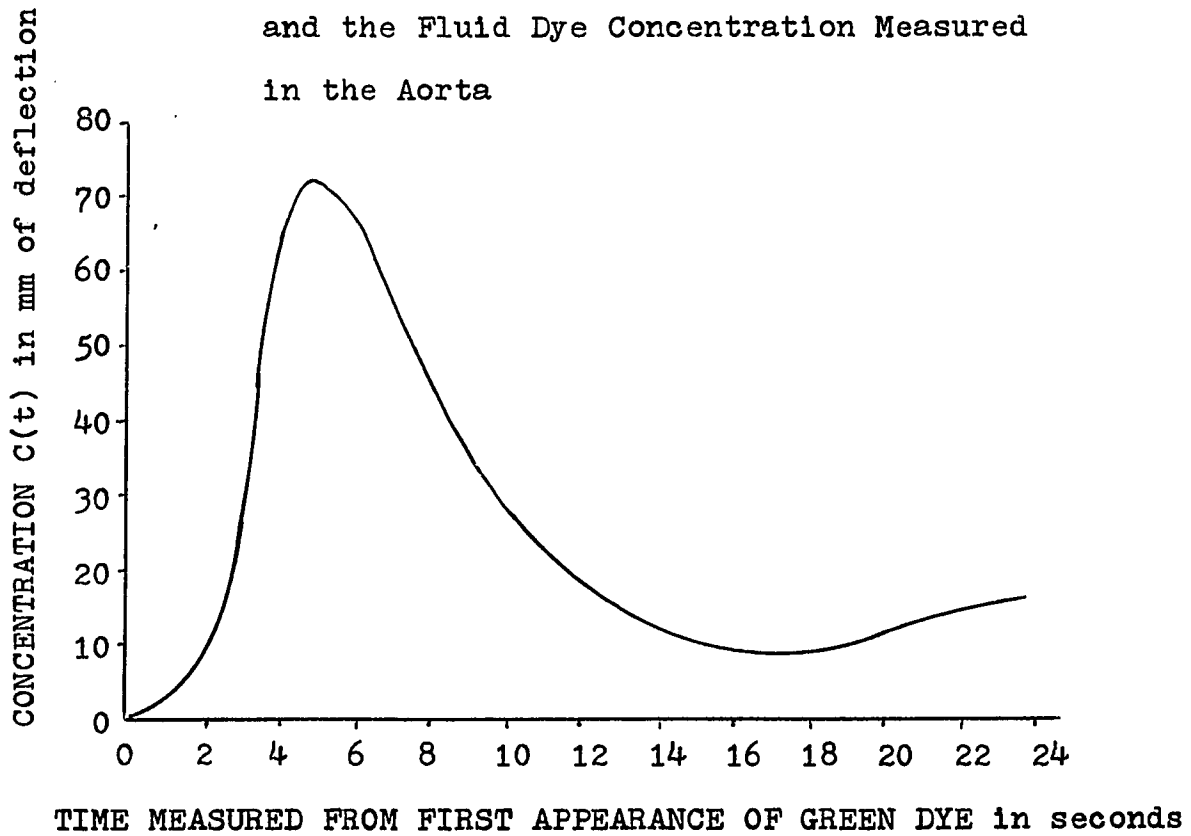


FIGURE 5

## Steady Flow System

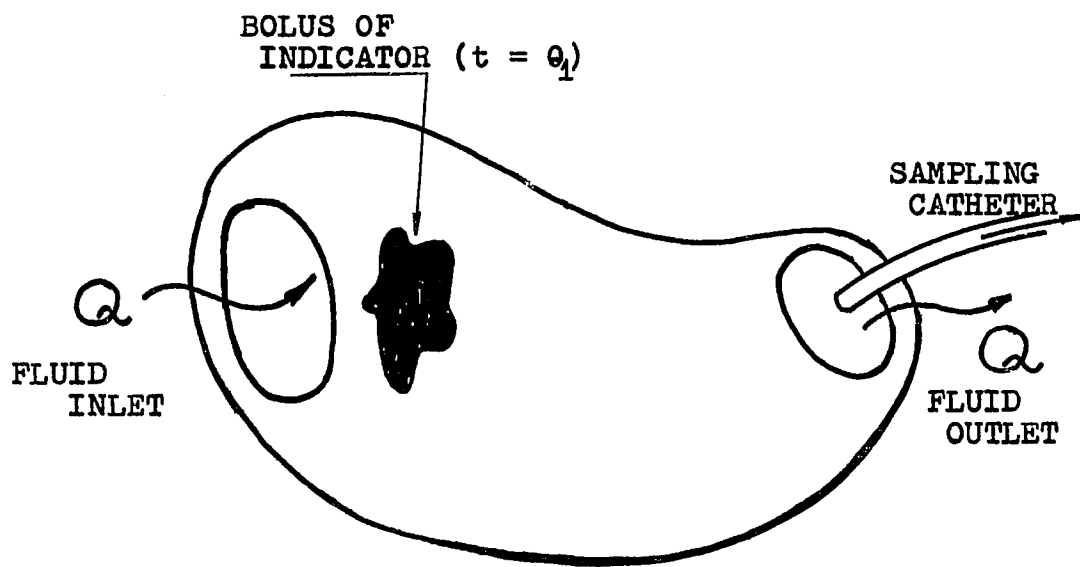


FIGURE 6

Theoretical Concentration Based on the Theory of  
Instantaneous Uniform Mixing for a Steady Flow System

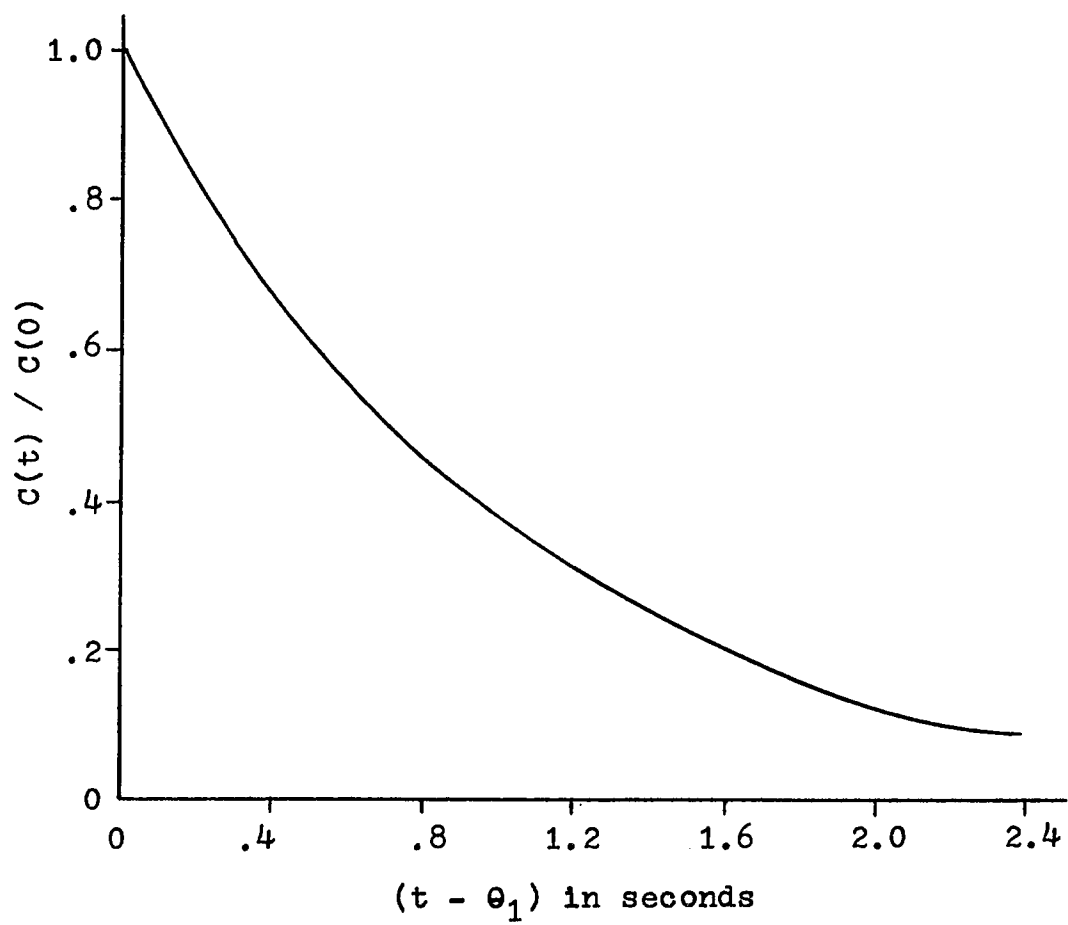
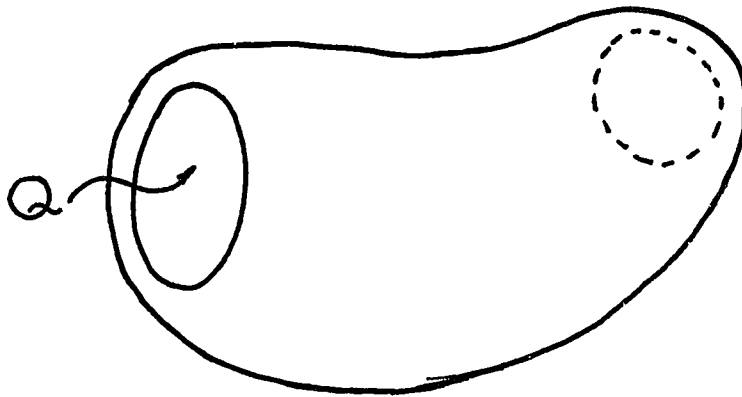


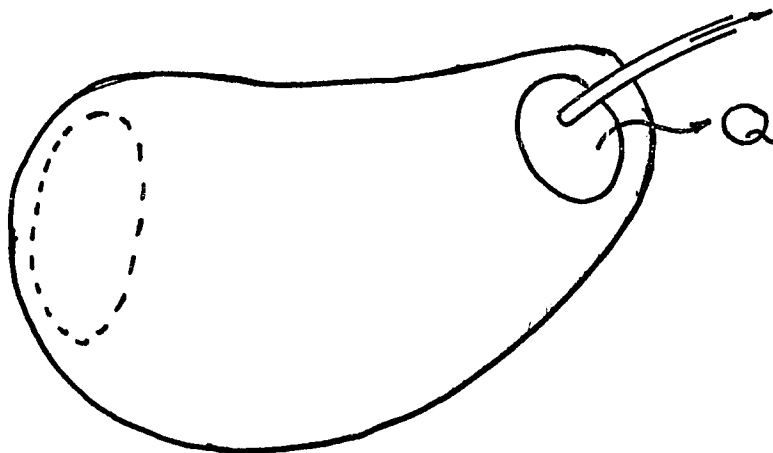
FIGURE 7

The Left Ventricle Assumed to be a Cyclical Steady  
Flow System



FILLING

DIASTOLIC FUNCTION



EMPTYING

SYSTOLIC FUNCTION

FIGURE 8

Theoretical Concentration Based on the Theory  
of Instantaneous Uniform Mixing

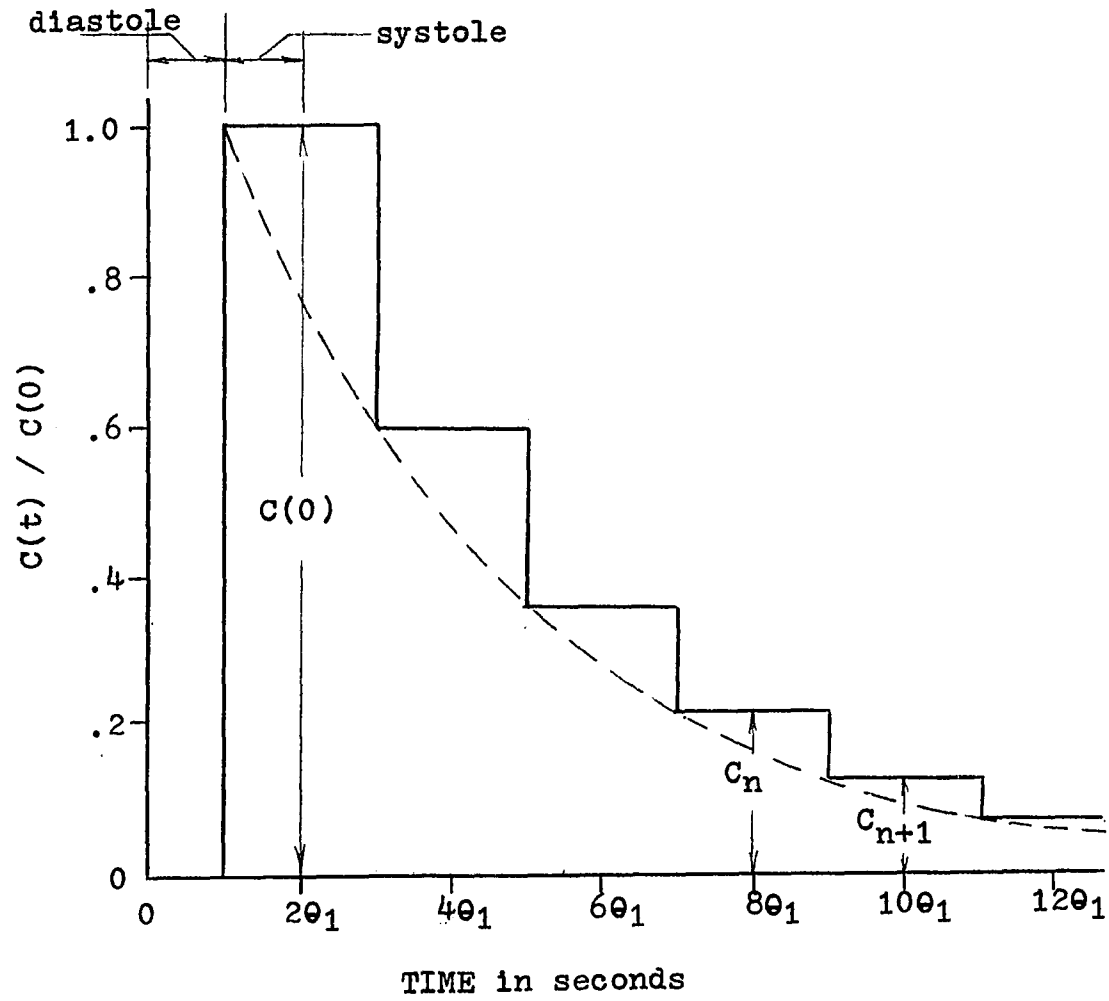


FIGURE 9.



Experimental Concentration versus Time Plot for a Normal Left Ventricle following the Instantaneous Injection of a Bolus of Dye Employing an Ideal Apparatus with no Response Lag and a Real Apparatus

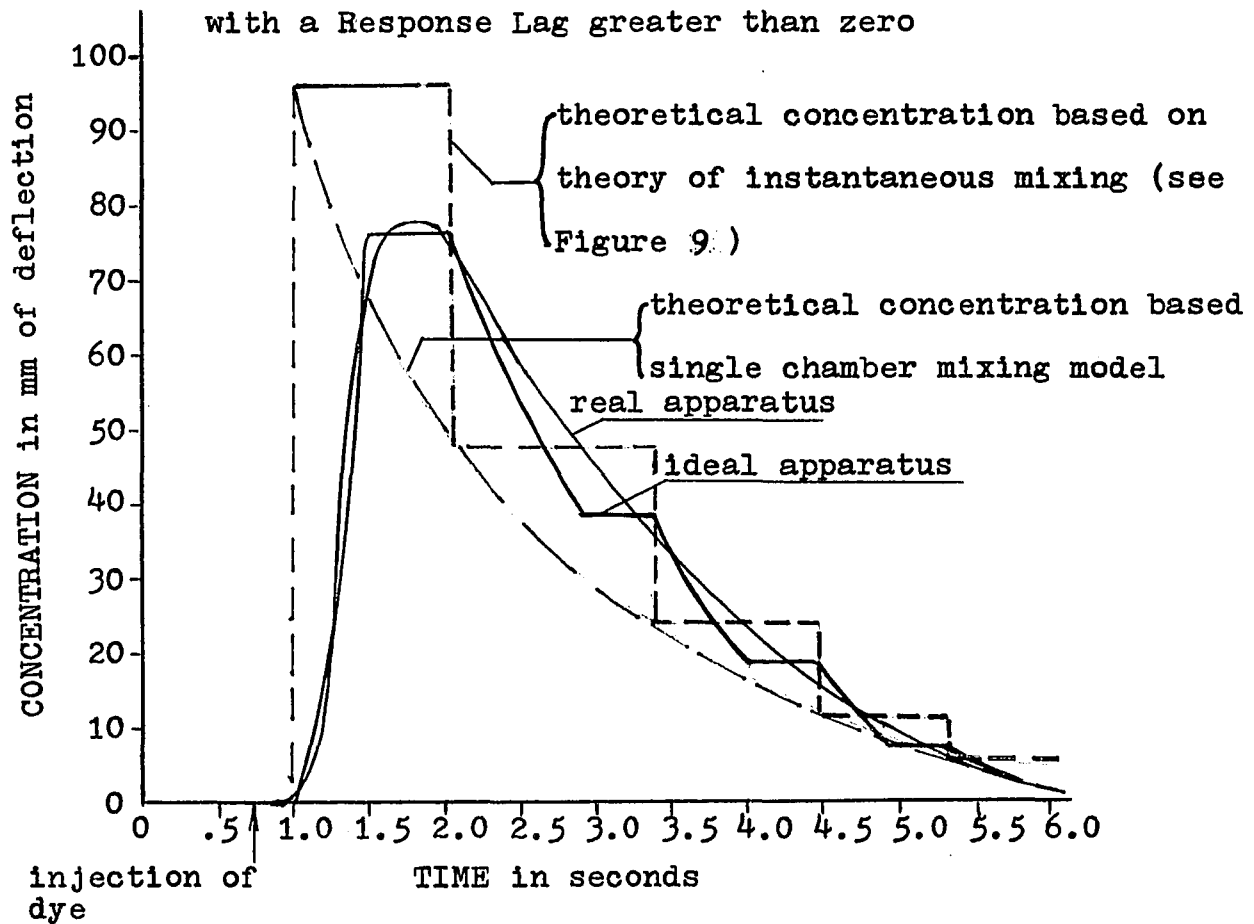
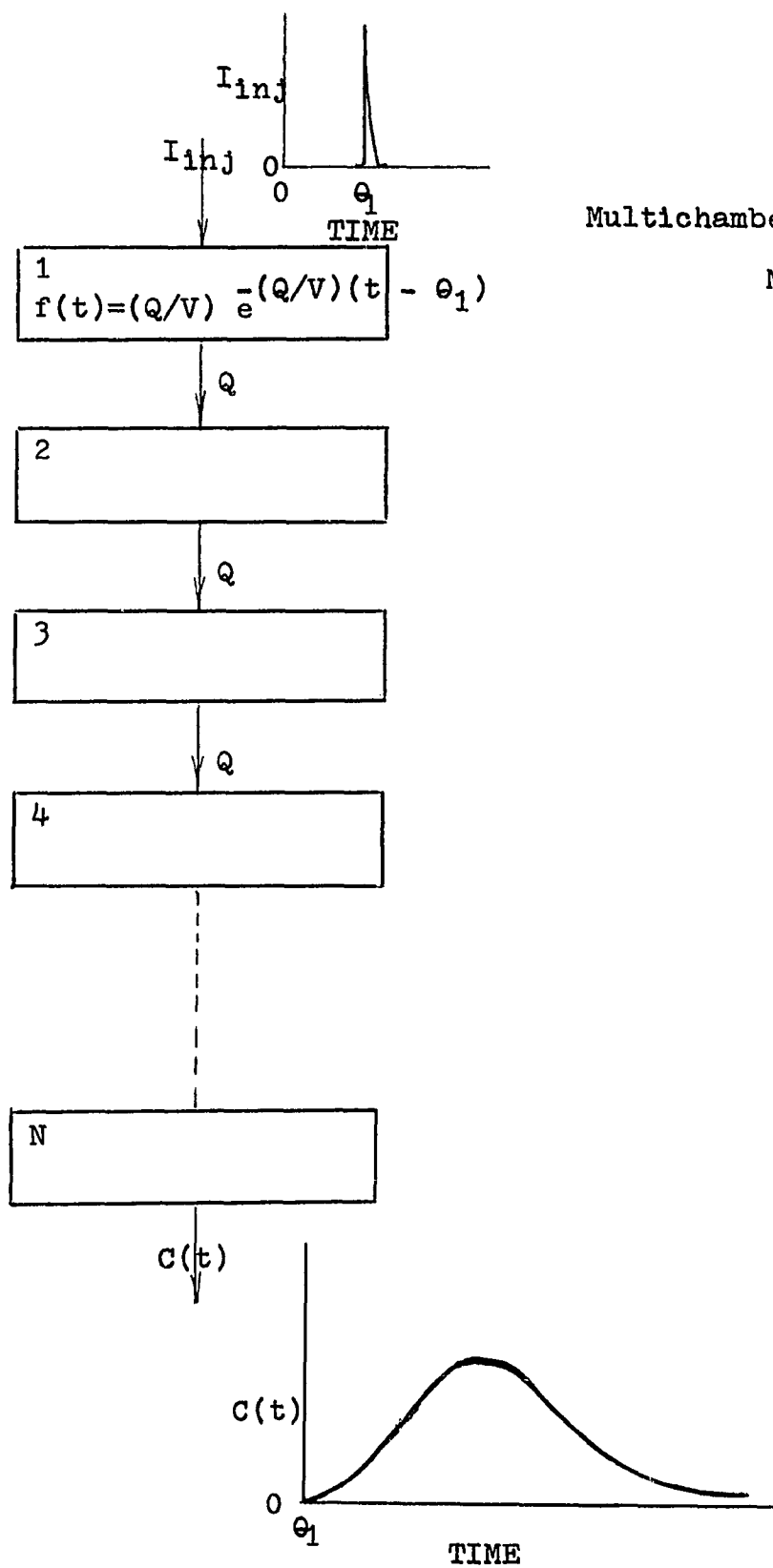


FIGURE 10



Multichamber Probabilistic Model

FIGURE 11

Plot of Equation (2-24) for  $Q = 5$  liters/minute and  $V = 200 \text{ cm}^3$  for Various Values of  $N$

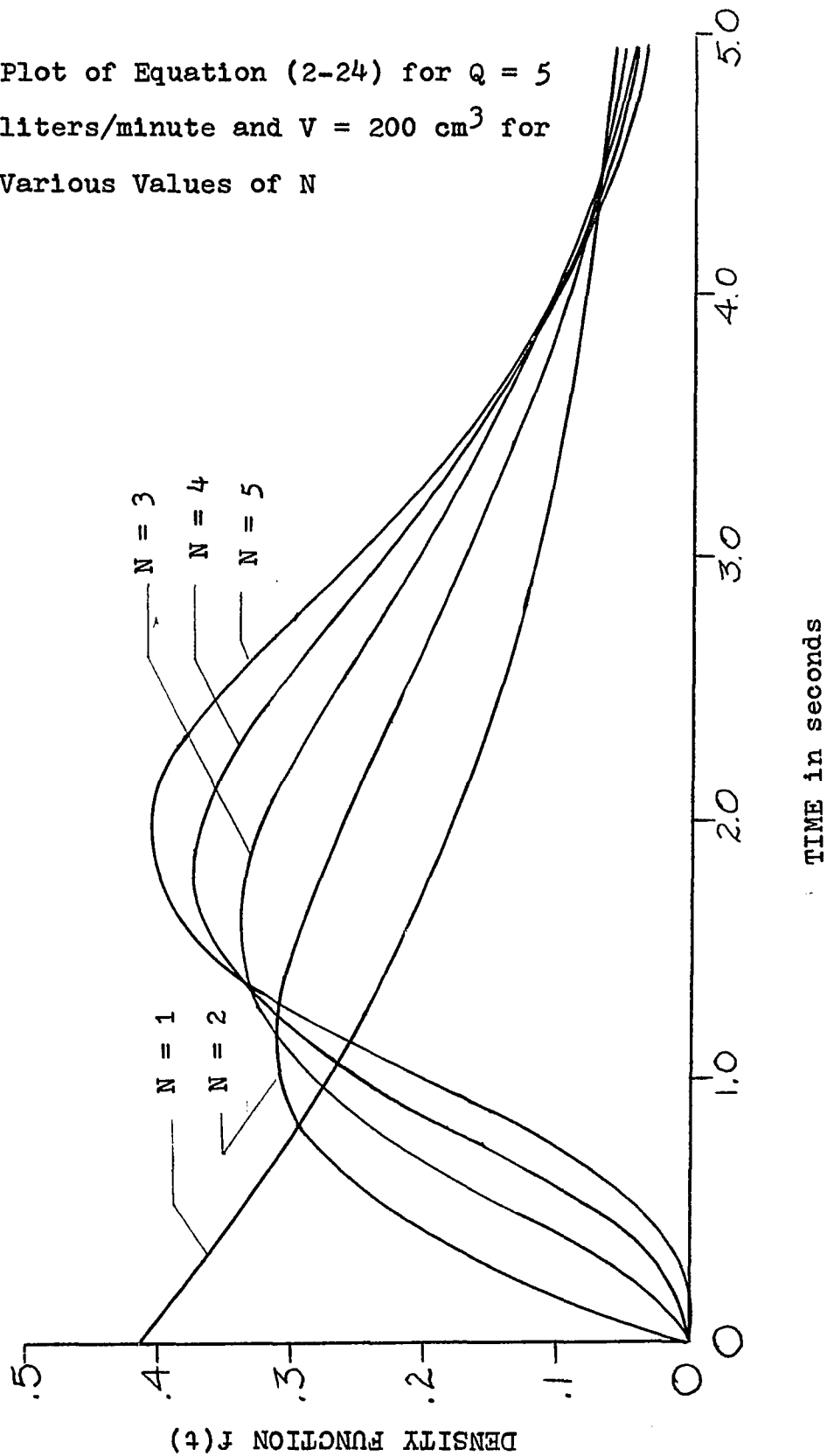


FIGURE 12

Experimental Density Function  $f(t)$  for the Experimental  
Green Dye Curve in Figure 5 and the Theoretical Density  
Function for  $N = 1$

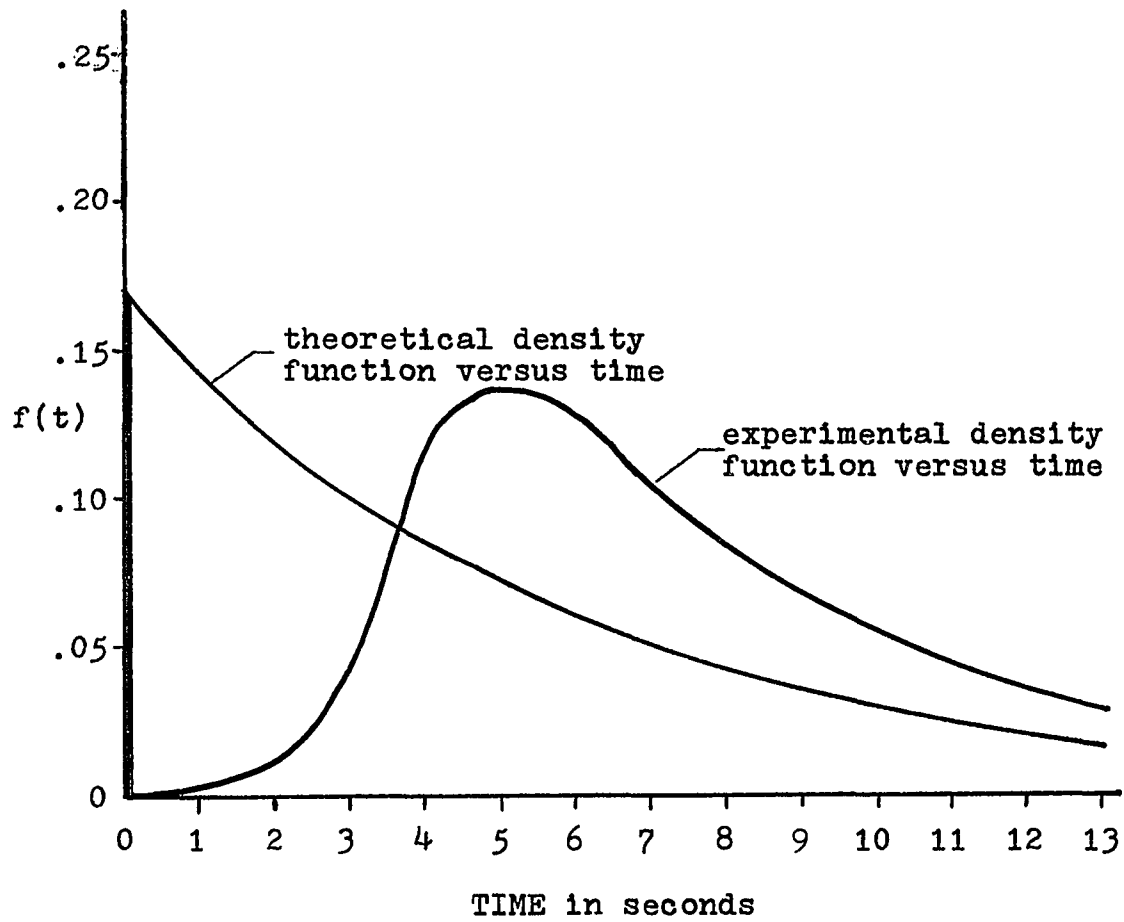


FIGURE 13

## Green Dye Study for a Subject with an Enlarged Heart

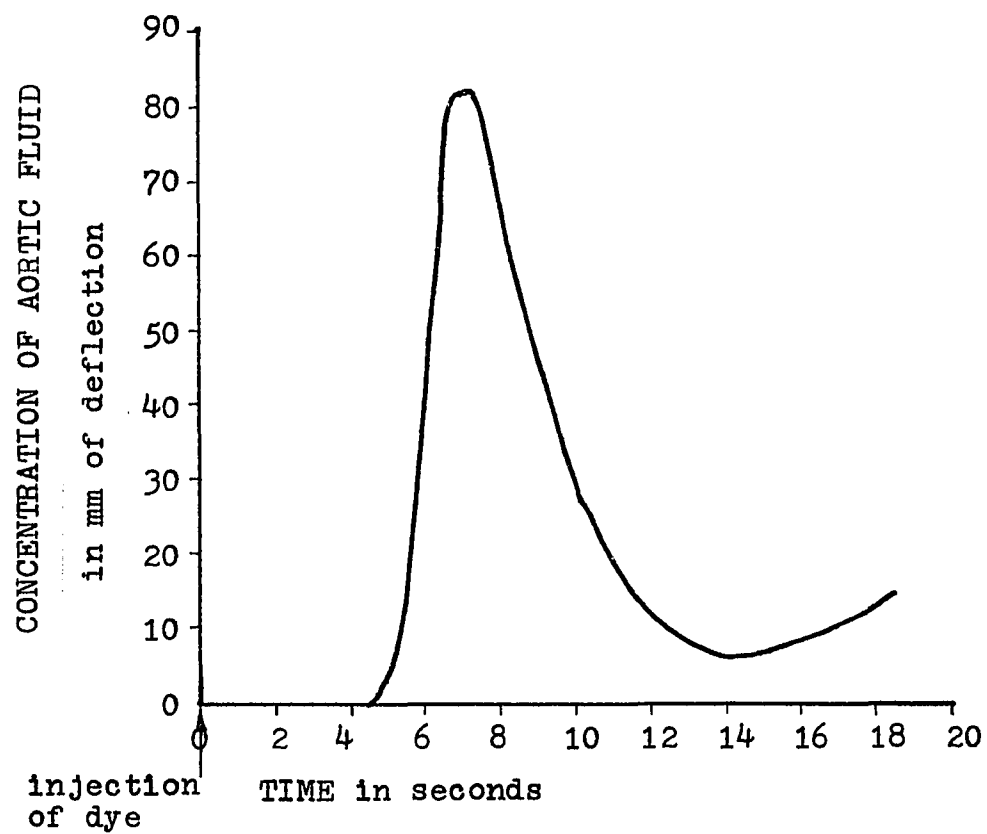


FIGURE 14

Green Dye Study of a Subject with an Aortic Stenosis

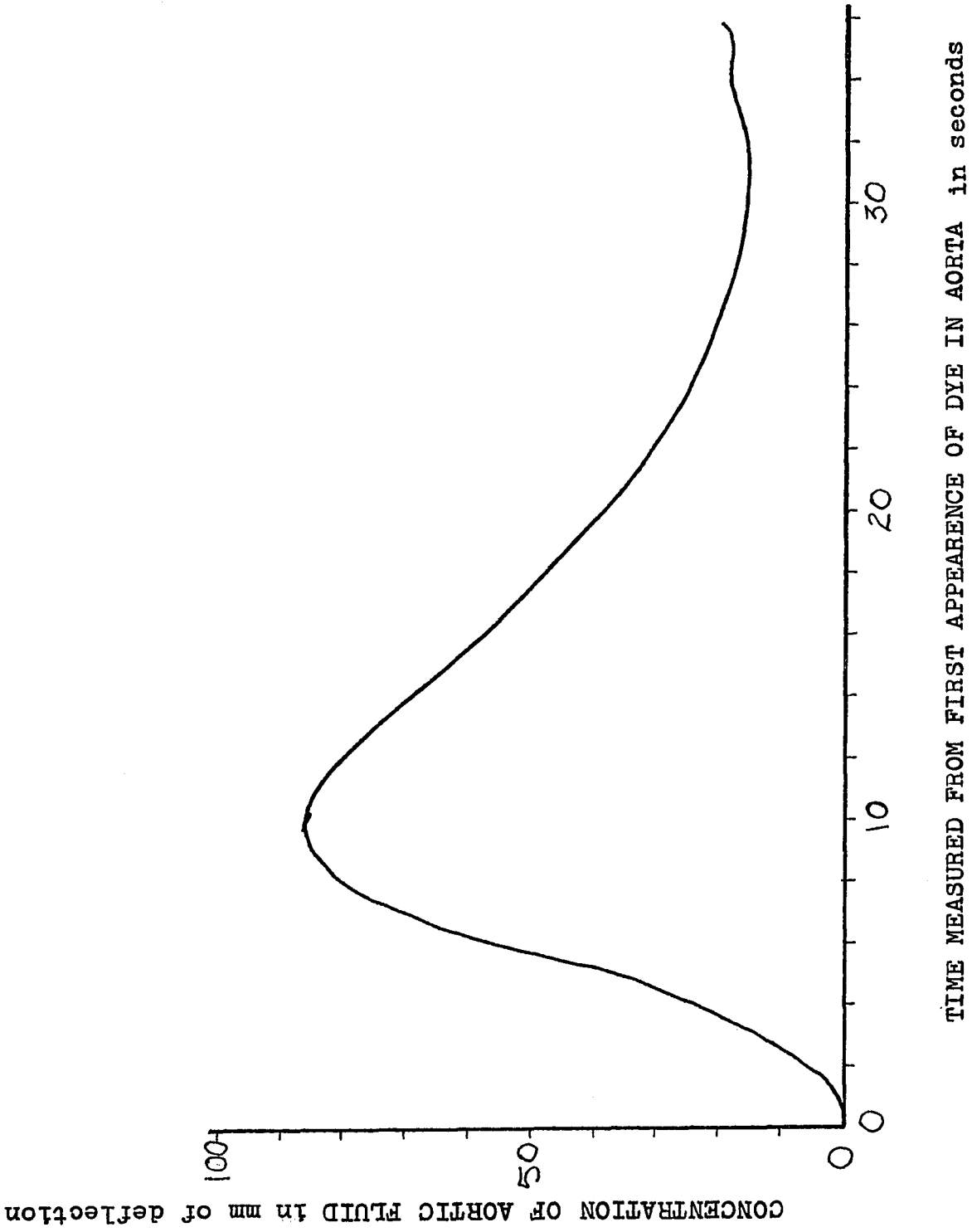


FIGURE 15

## Green Dye Study of a Subject with a Slight Aortic Insufficiency

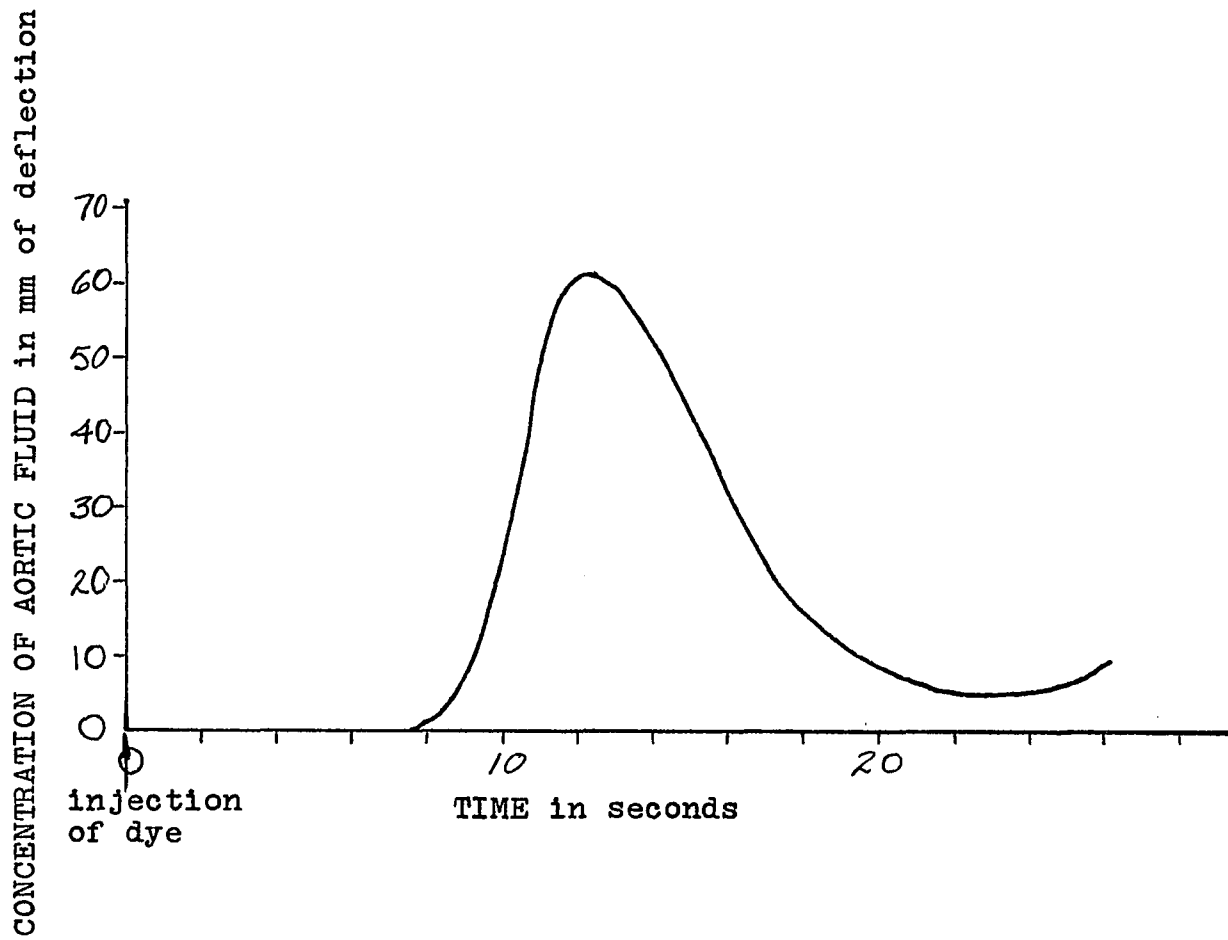


FIGURE 16

Experimental Density Functions for a Normal Heart, Enlarged Heart and a Heart with an Aortic Stenosis

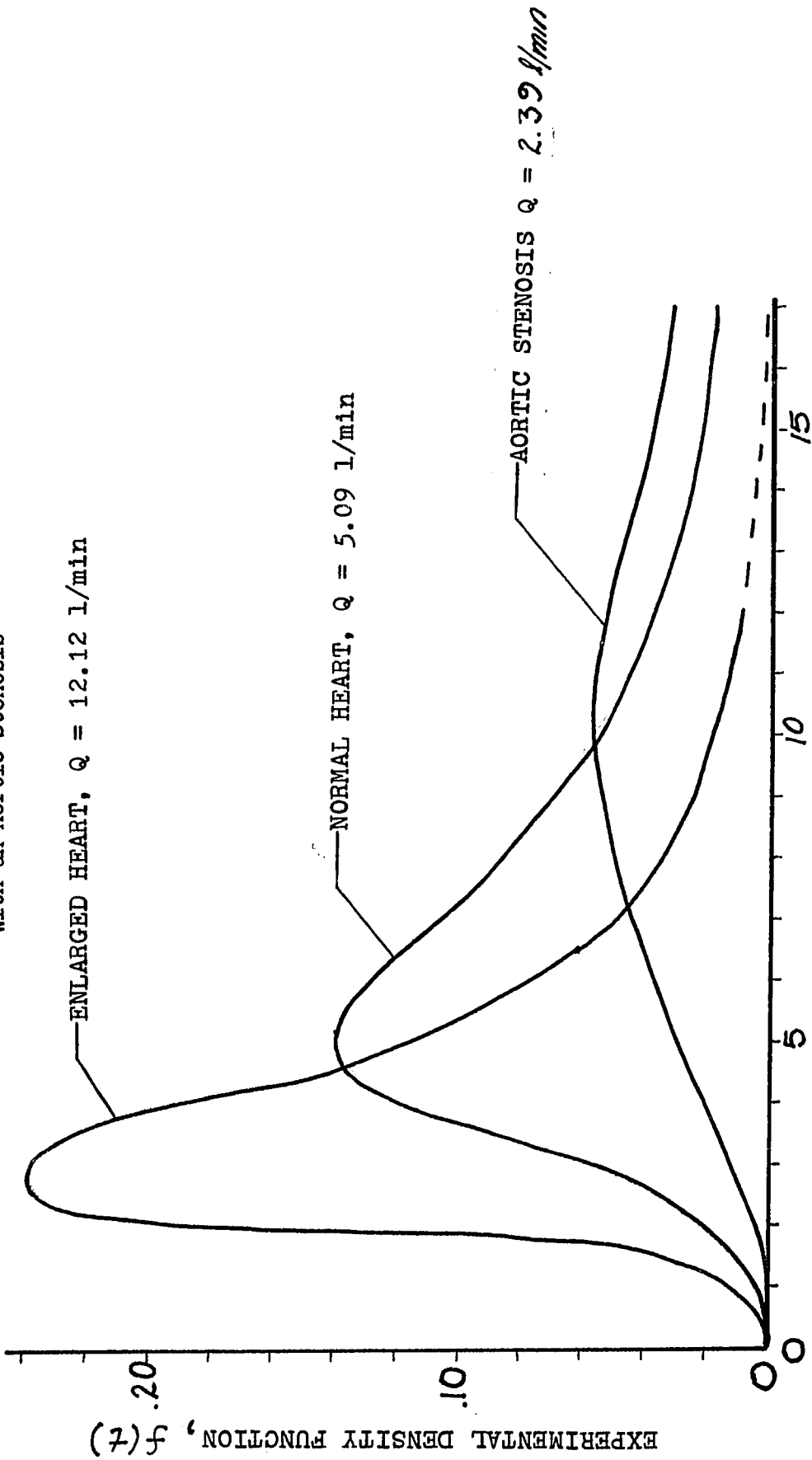


FIGURE 17



Experimental Density Functions for a Normal Heart, a Heart with Aortic Insufficiency  
and a Heart with Mitral Insufficiency

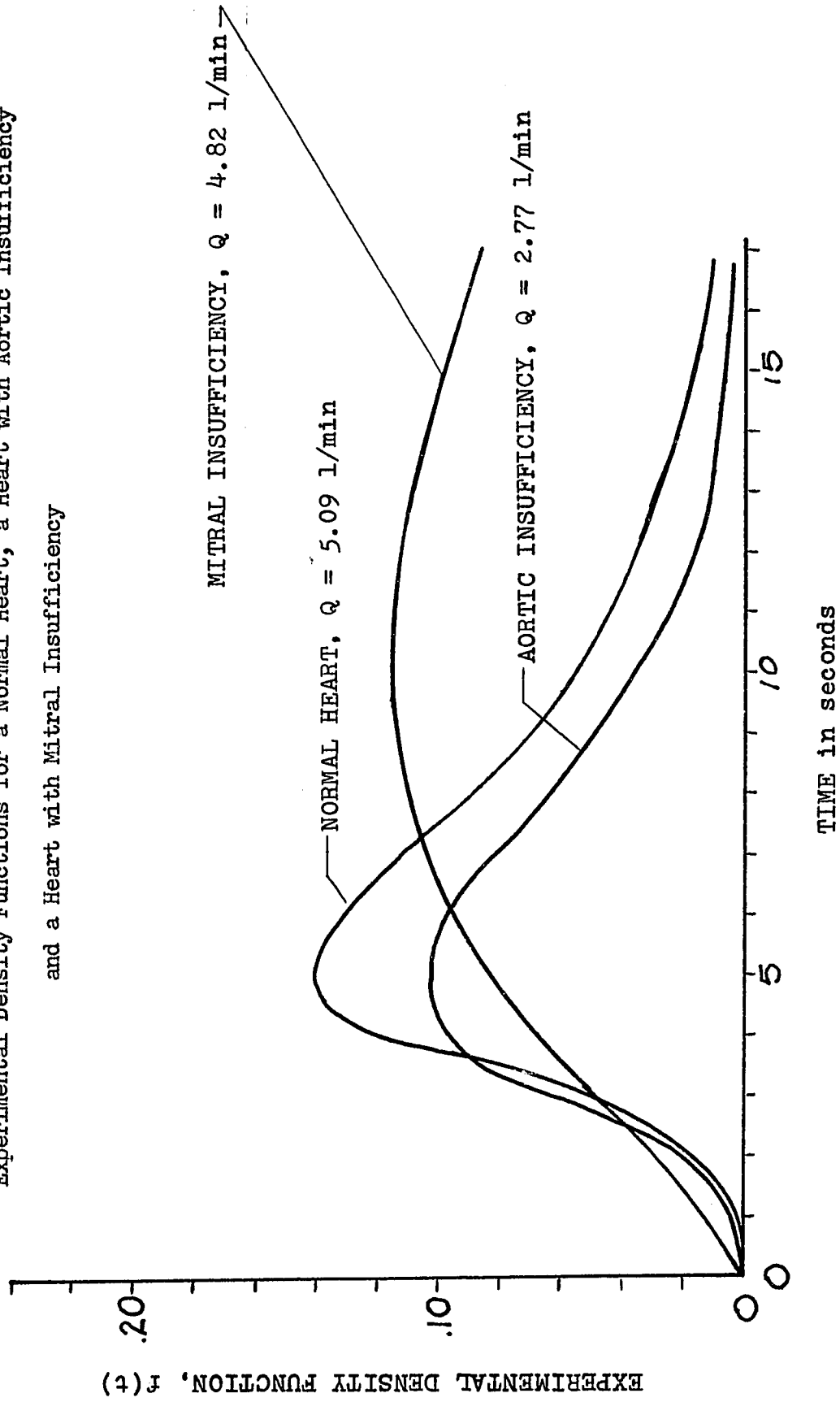


FIGURE 18

Theoretical and Experimental

Density Functions for a

Normal Heart, Enlarged Heart

and a Heart with an Aortic

Stenosis

$N = 9.0, C.V. = 909.0 \text{ cm}^3$

THEORETICAL DENSITY FUNCTION

ENLARGED HEART,  $Q = 12.12 \text{ l/min}$

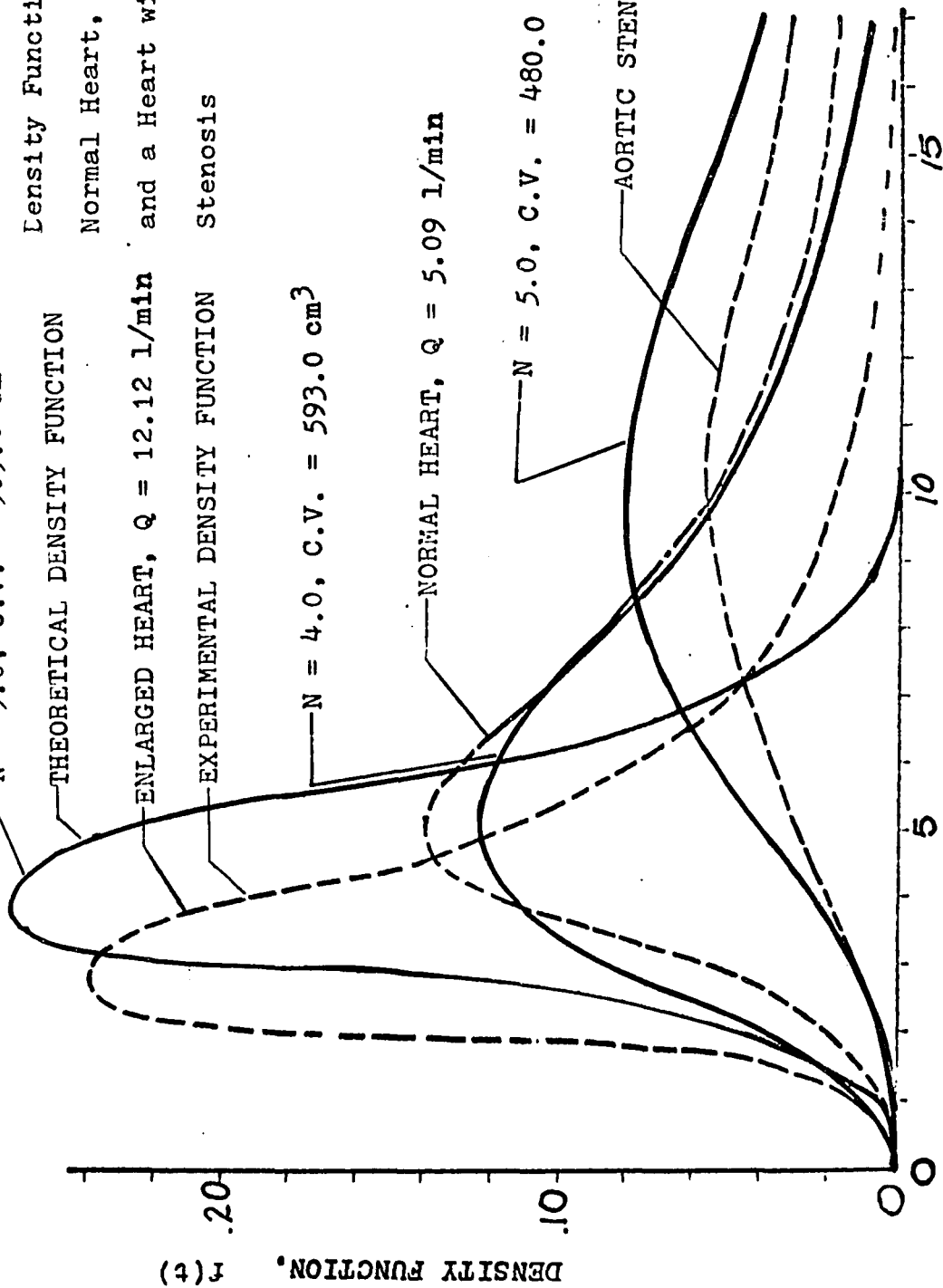
EXPERIMENTAL DENSITY FUNCTION

$N = 4.0, C.V. = 593.0 \text{ cm}^3$

NORMAL HEART,  $Q = 5.09 \text{ l/min}$

$N = 5.0, C.V. = 480.0 \text{ cm}^3$

AORTIC STENOSIS  $Q = 2.39 \text{ l/min}$



TIME MEASURED FROM FIRST APPEARANCE OF DYE IN AORTA in seconds

Fluid Dye Concentration versus Time for Green Dye  
Studies Employing Various Injection Sites

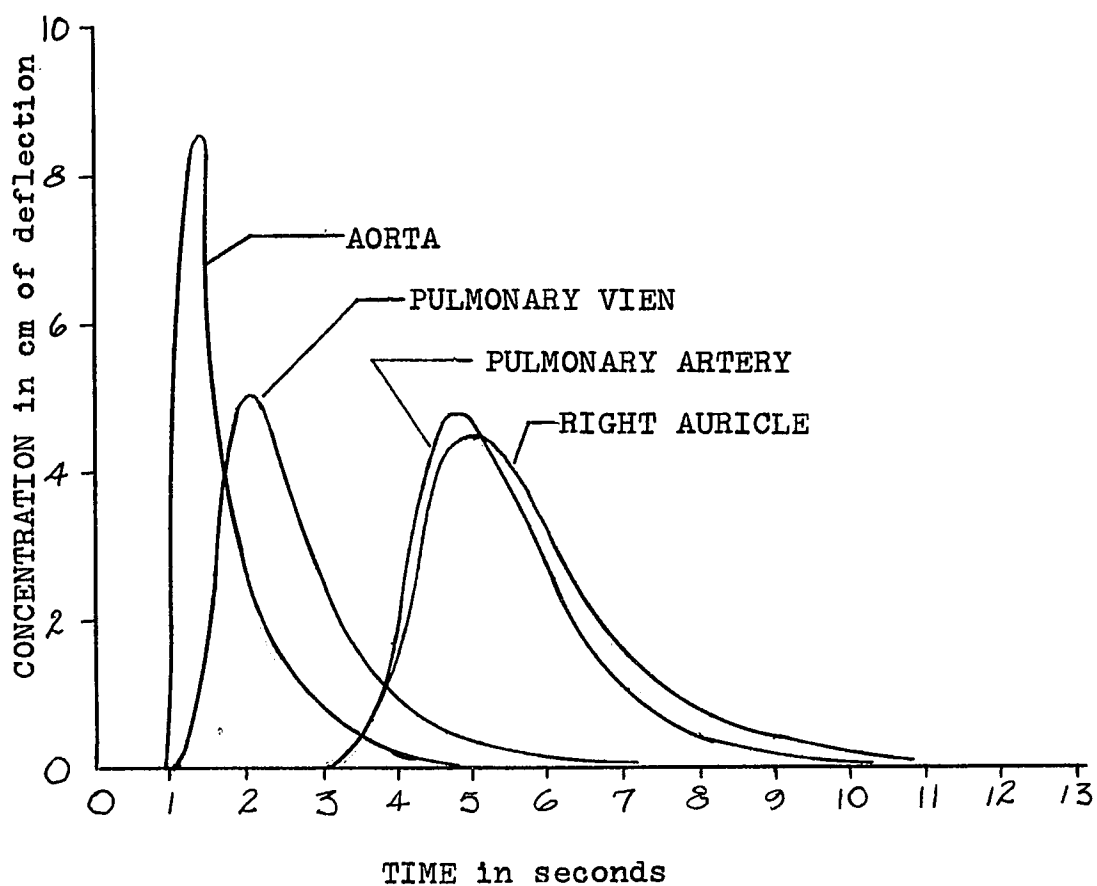


FIGURE 20

Fluid Dye Concentration versus Time Measured from the First Appearance of Dye in the Carotid Artery for Green Dye Studies Employing an Injection of Dye in the Right Auricle, Pulmonary Artery and the Pulmonary Vien

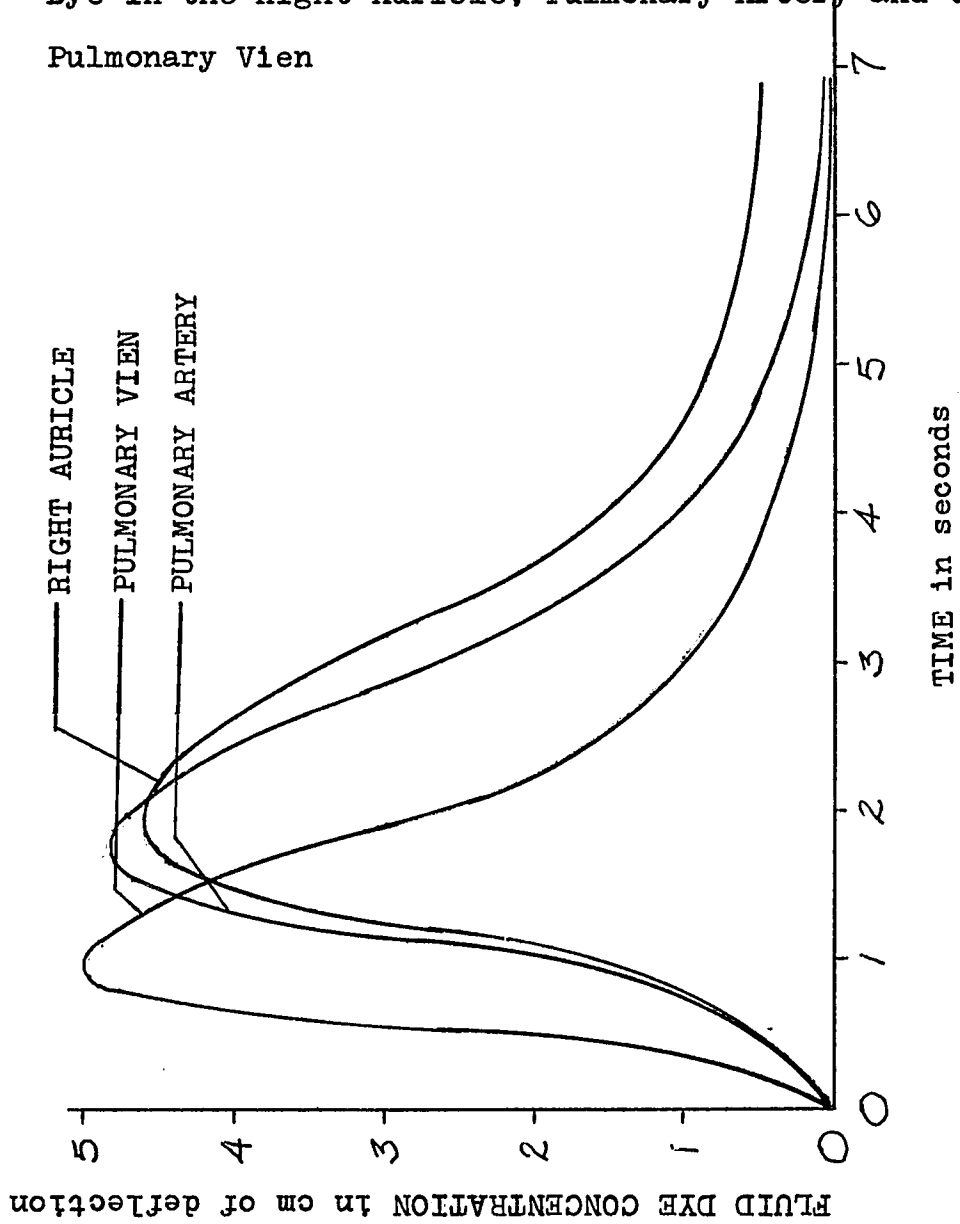
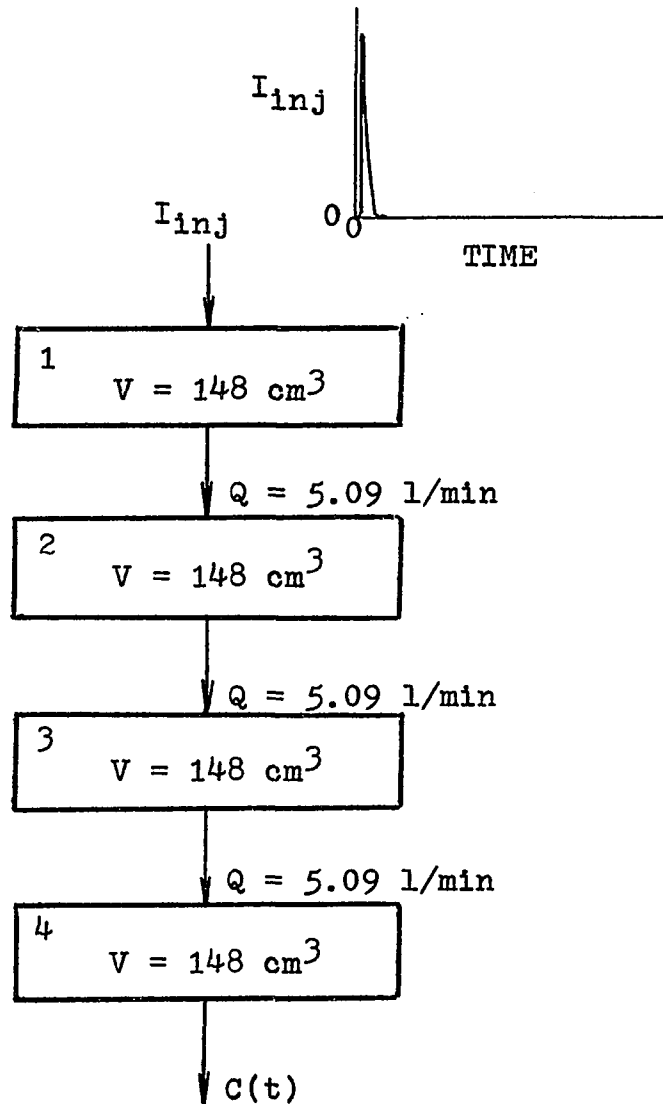


FIGURE 21



Multichamber Model for the Normal Heart Shown in  
Figure 17

FIGURE 22

Density Function versus Time for the Models obtained by adding  
1, 2, and 4 Mixing Chambers to the Model in Figure 22

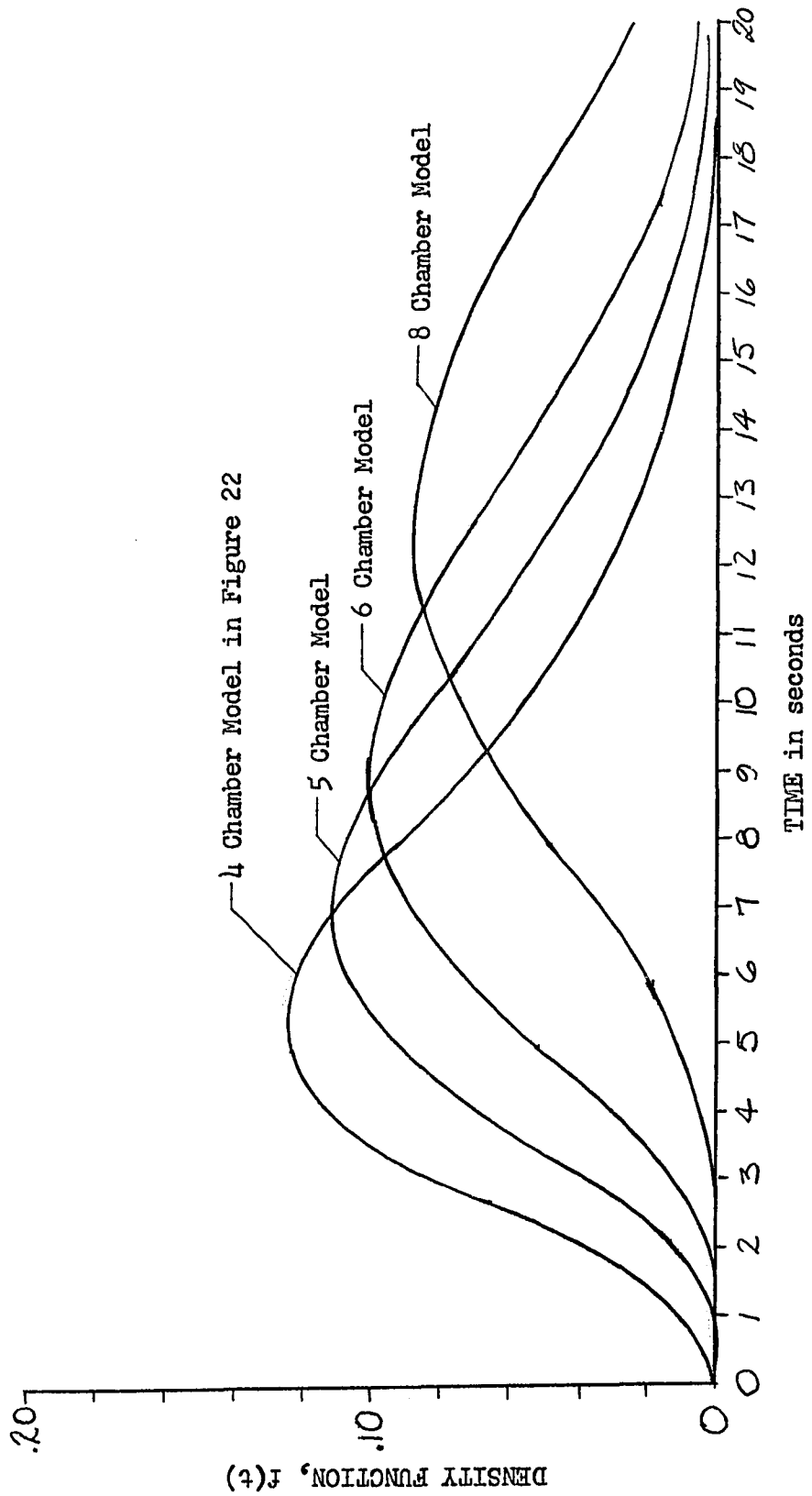
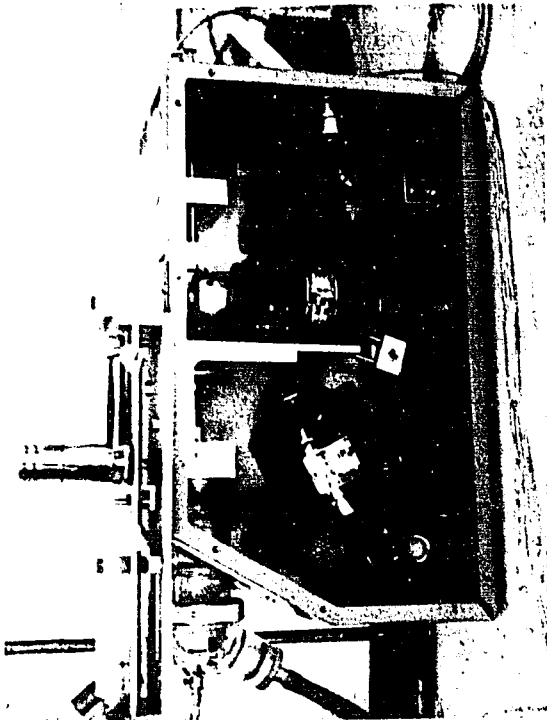
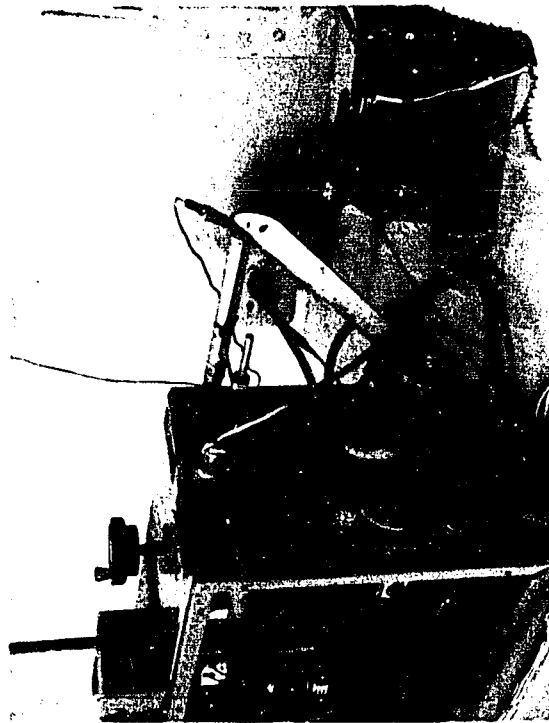


FIGURE 23

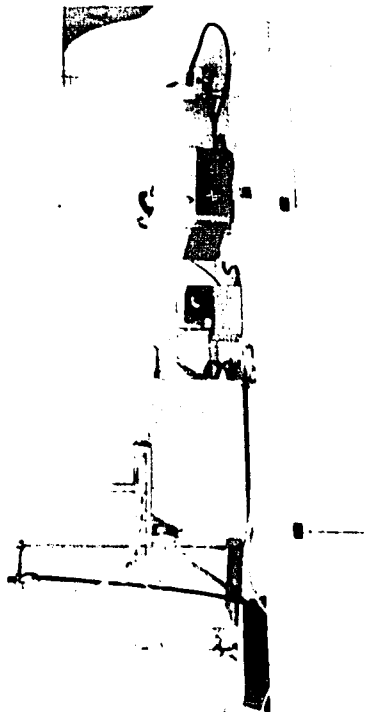
EXPERIMENTAL APPARATUS



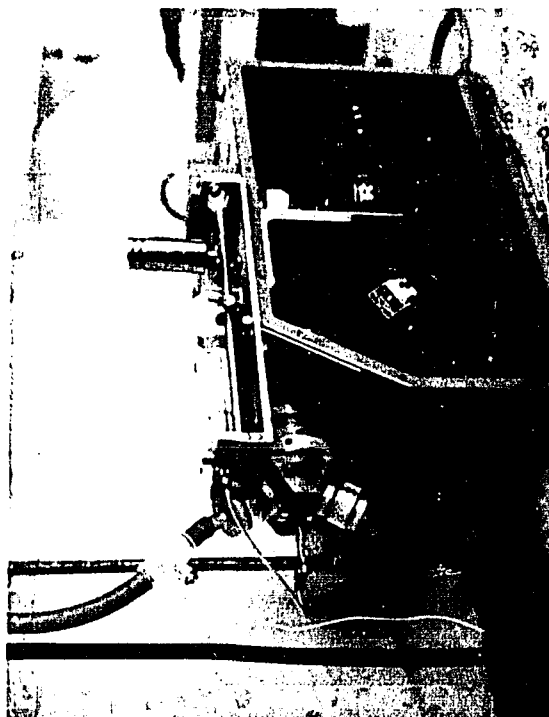
Heart Model



Resistance Potentiometer



Experimental Assembly



Injector Device

FIGURE 24

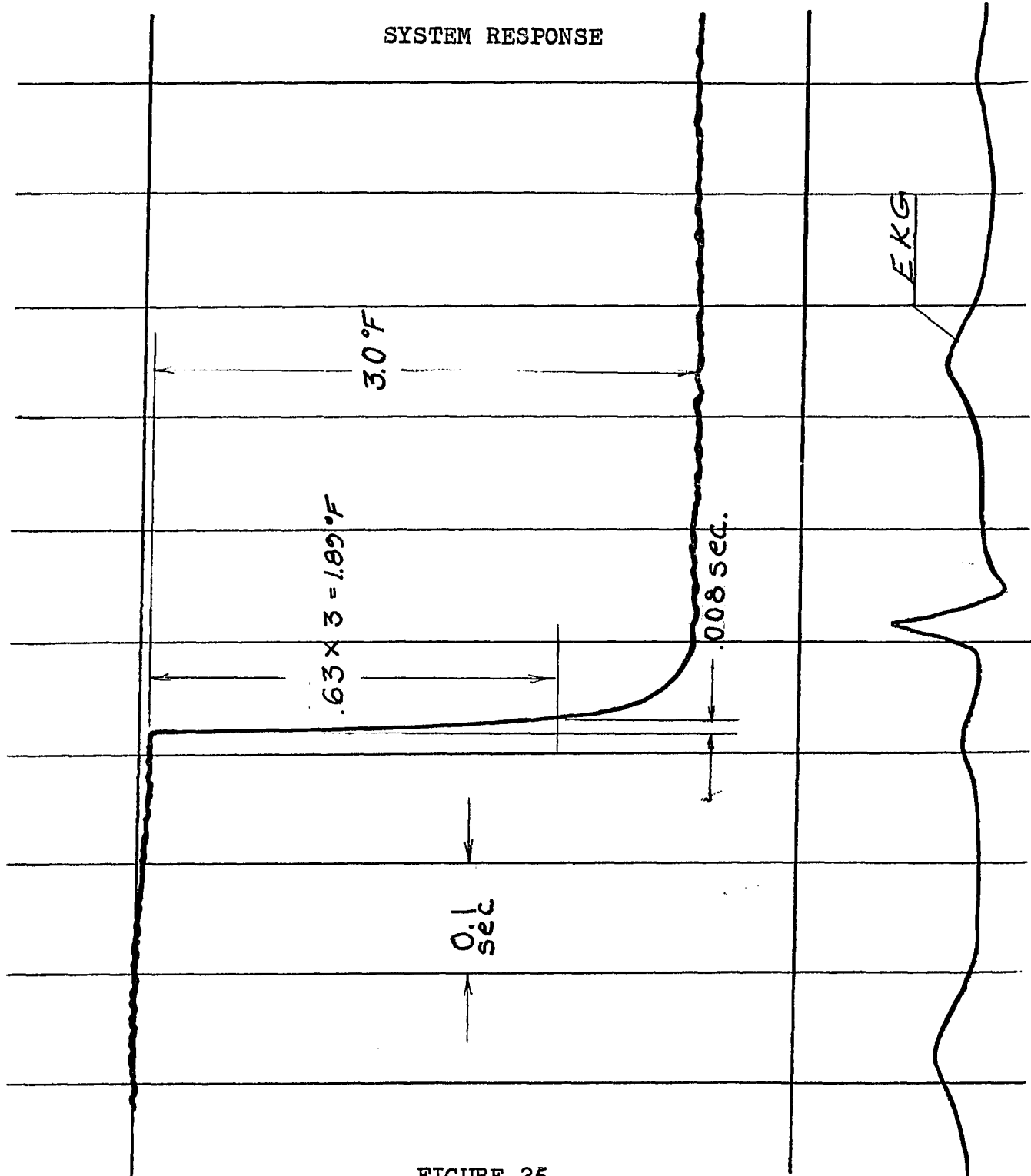


FIGURE 25



## Simultaneous Green Dye and Thermodilution Study in a Dog

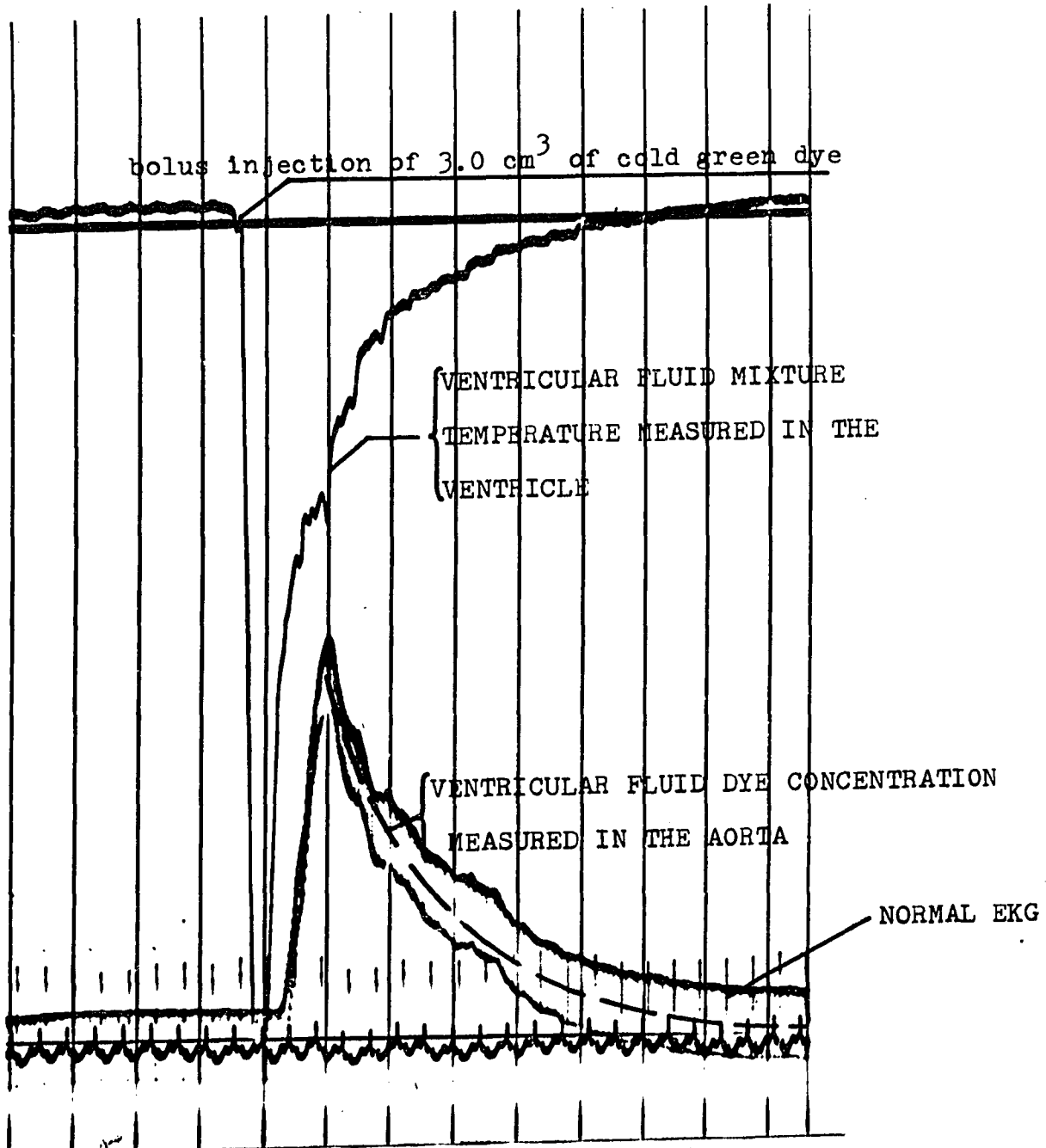
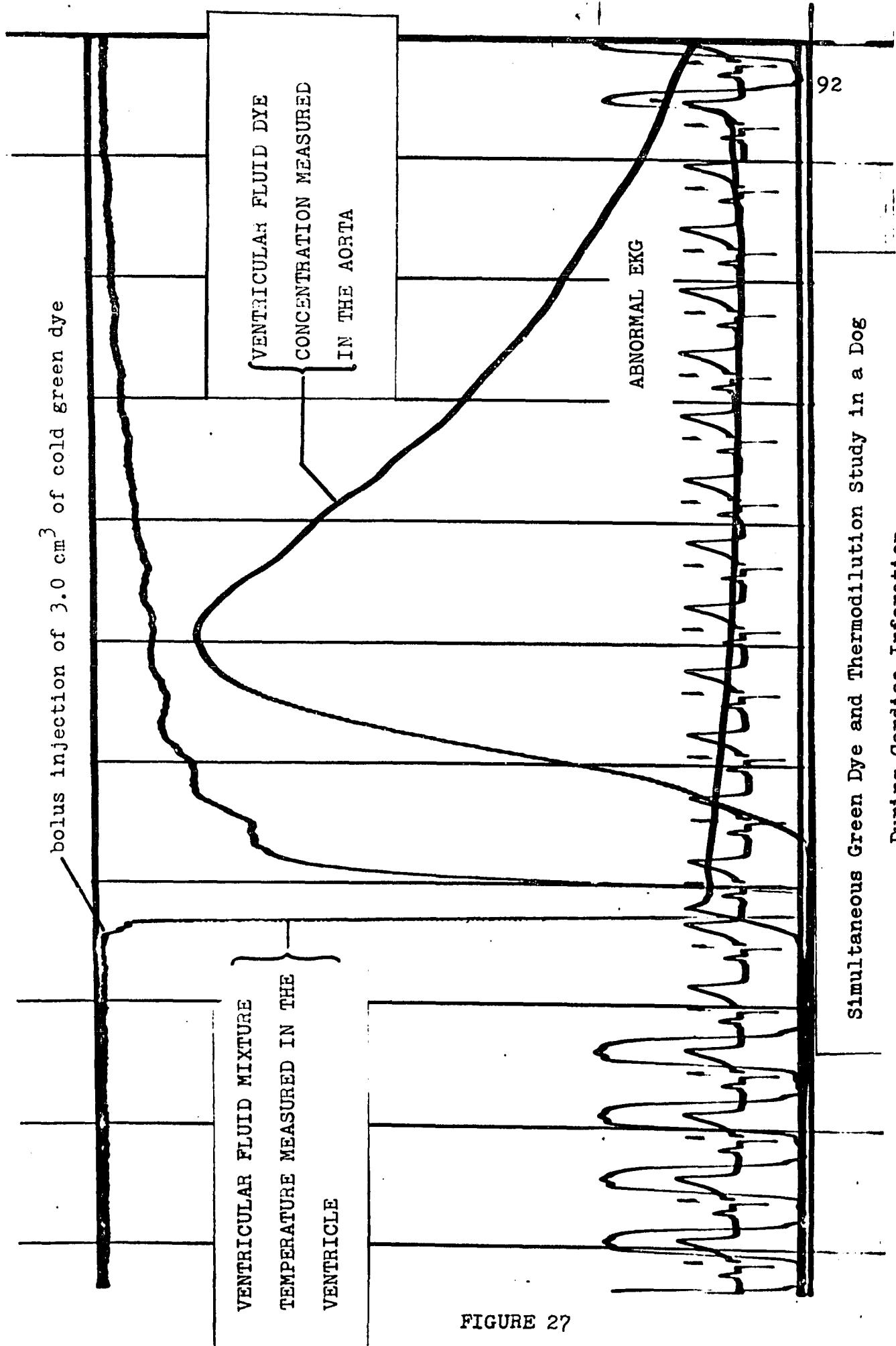


FIGURE 26



Simultaneous Green Dye and Thermodilution Study in a Dog  
During Cardiac Infarction

FIGURE 27

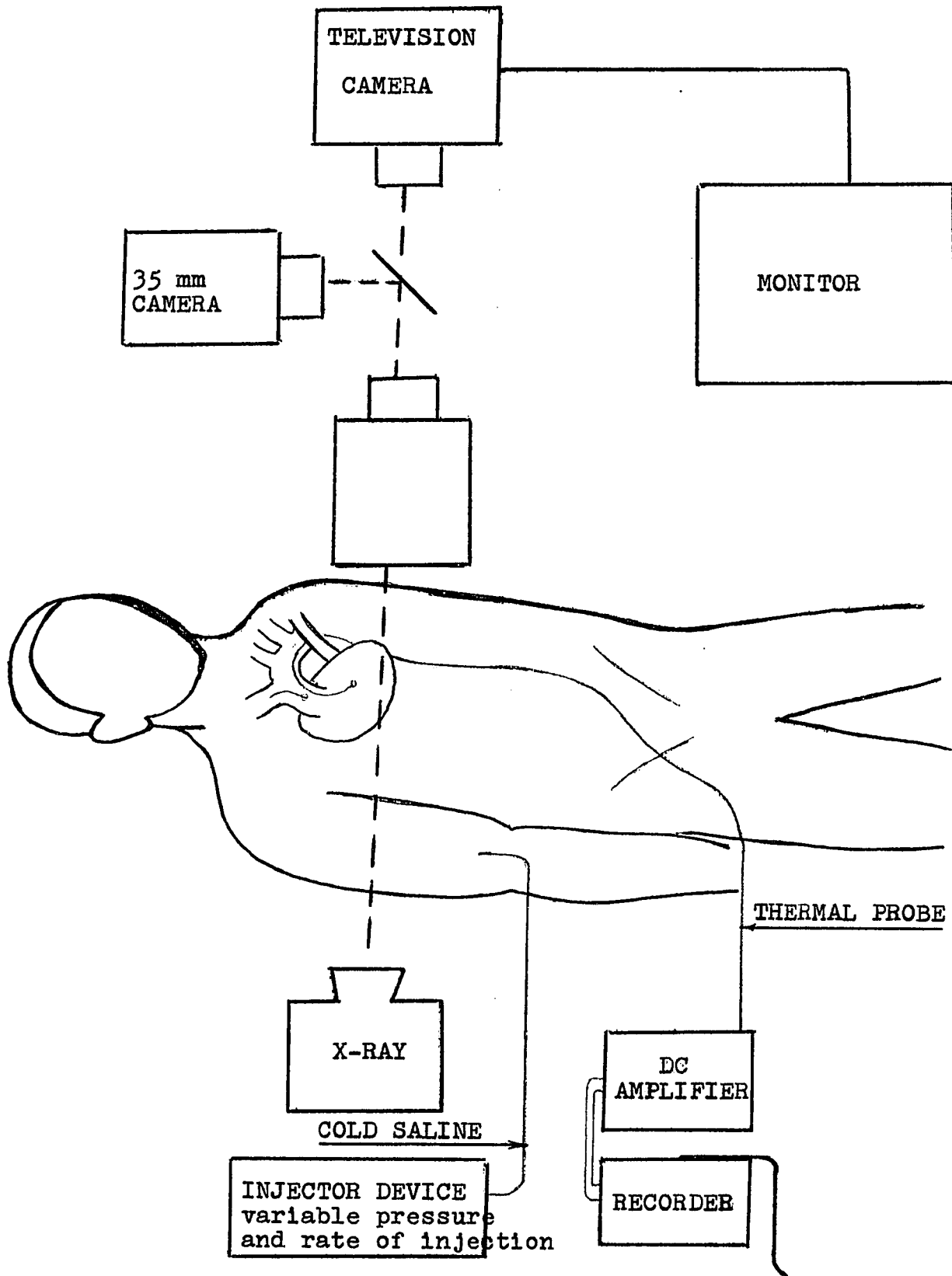


FIGURE 28

The Proper Catheter Configuration in the Left Ventricle

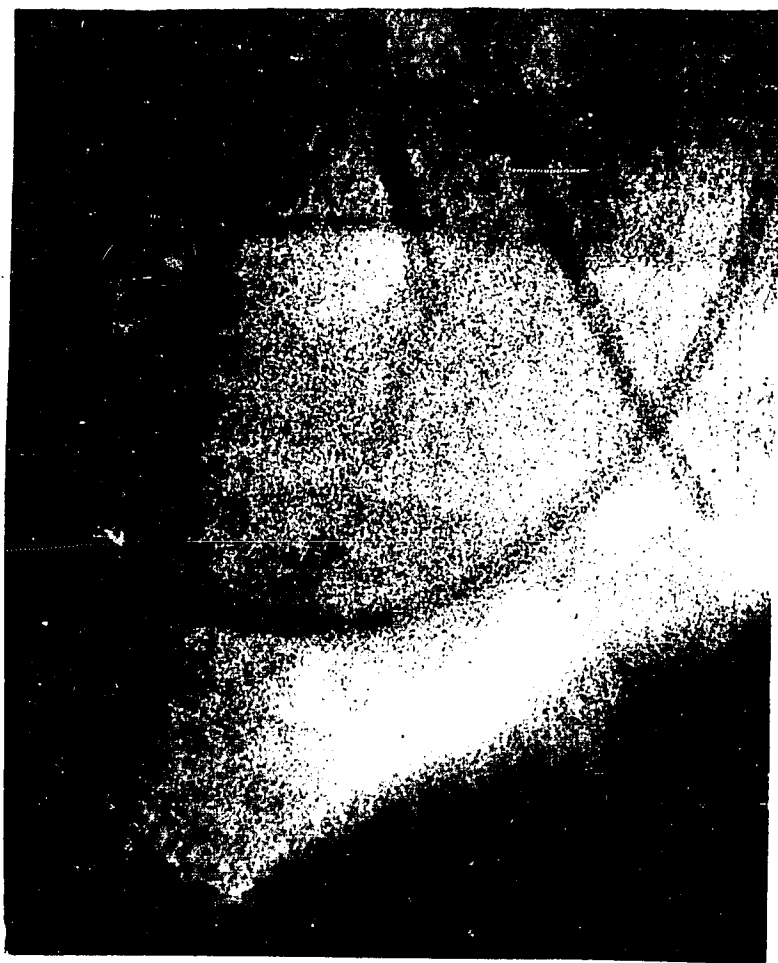
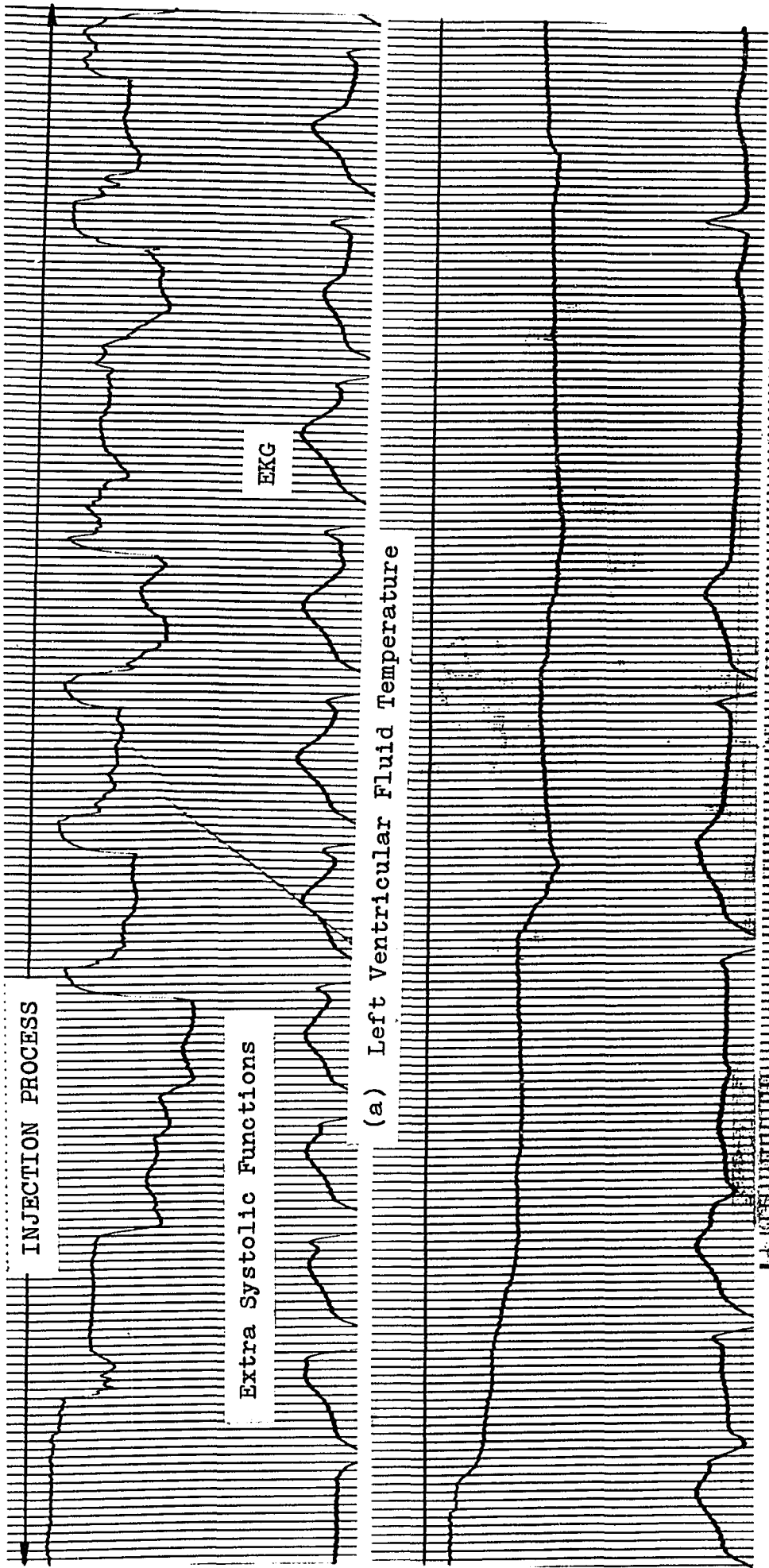


FIGURE 29



THEM-DILUTION STUDY  
 IN MAN IN WHICH THE  
 INJECTION PROCESS  
 PRODUCED PVC'S THUS  
 CONFUSING THE TEM-  
 PERATURE-TIME TRACE

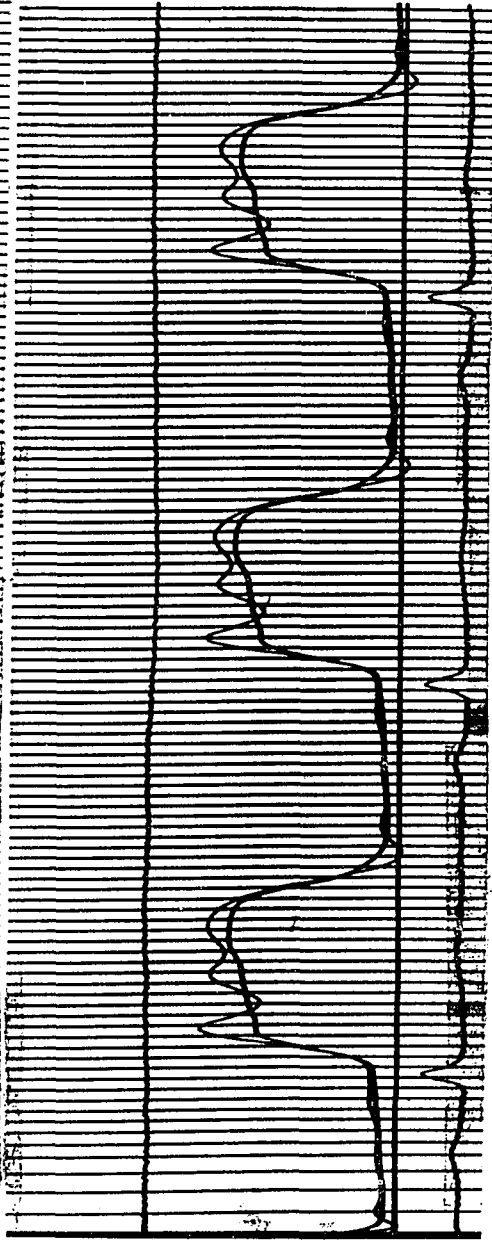


FIGURE 50 95

(b) Left Ventricular Pressure

Catheters in the Left Ventricle during the Injection Process

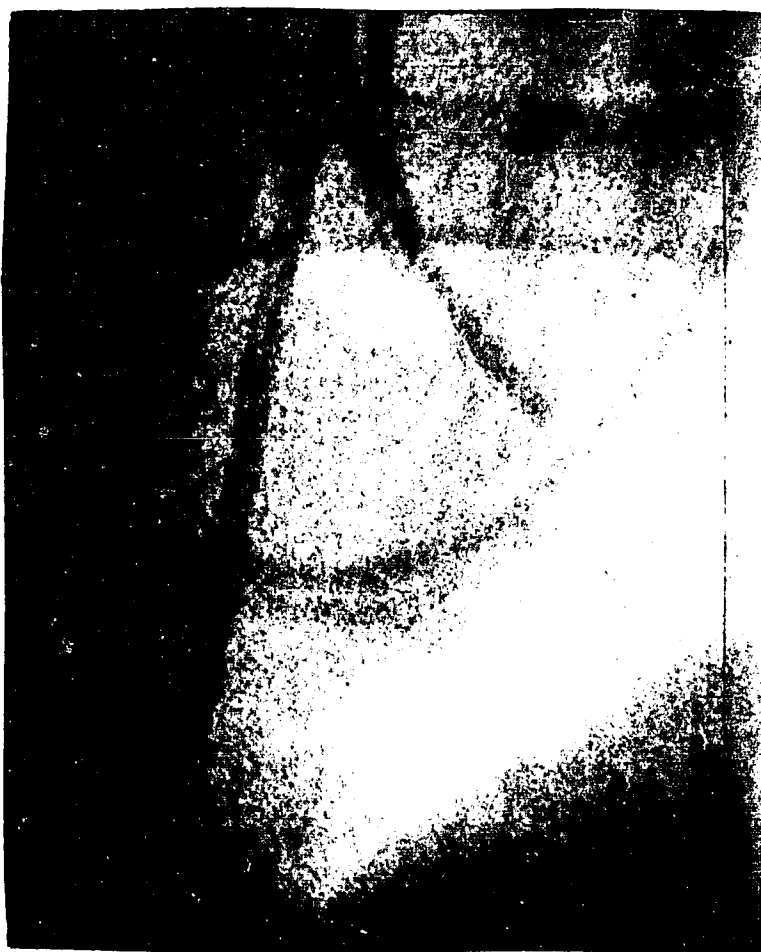


FIGURE 31

Catheters in the Left Ventricle after the Injection Process



FIGURE 32

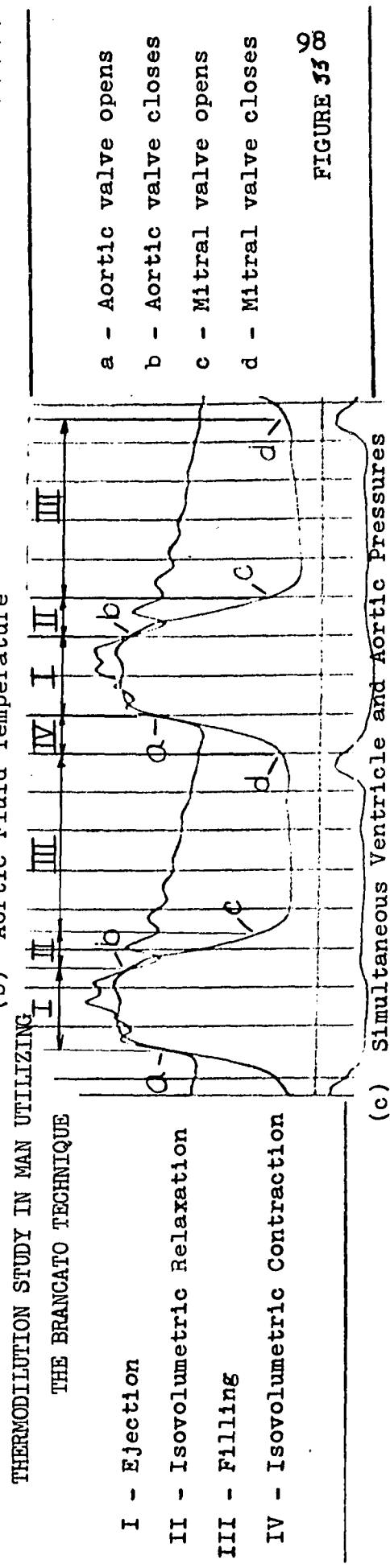
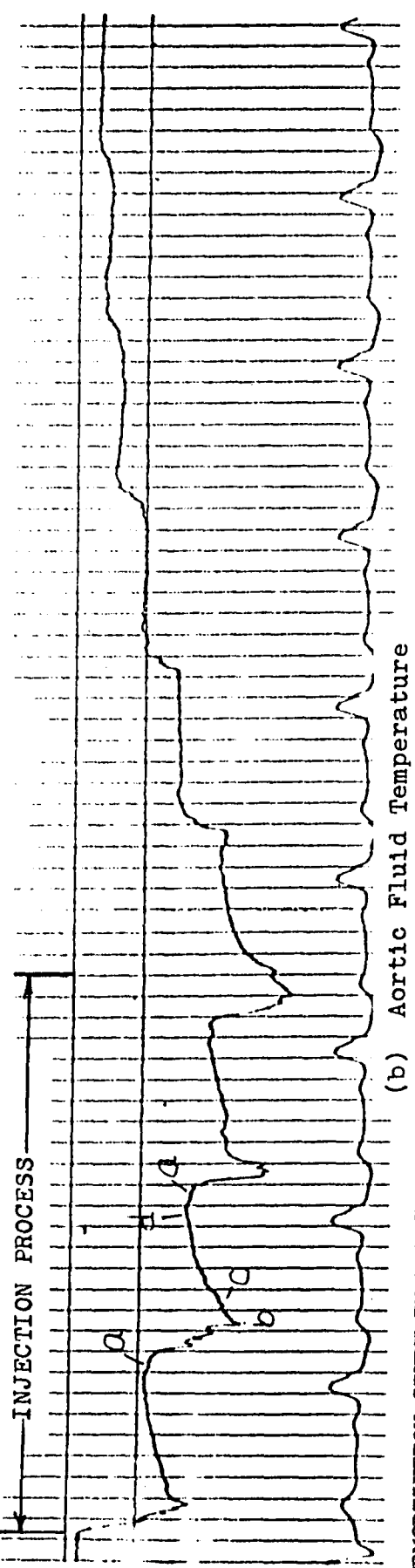
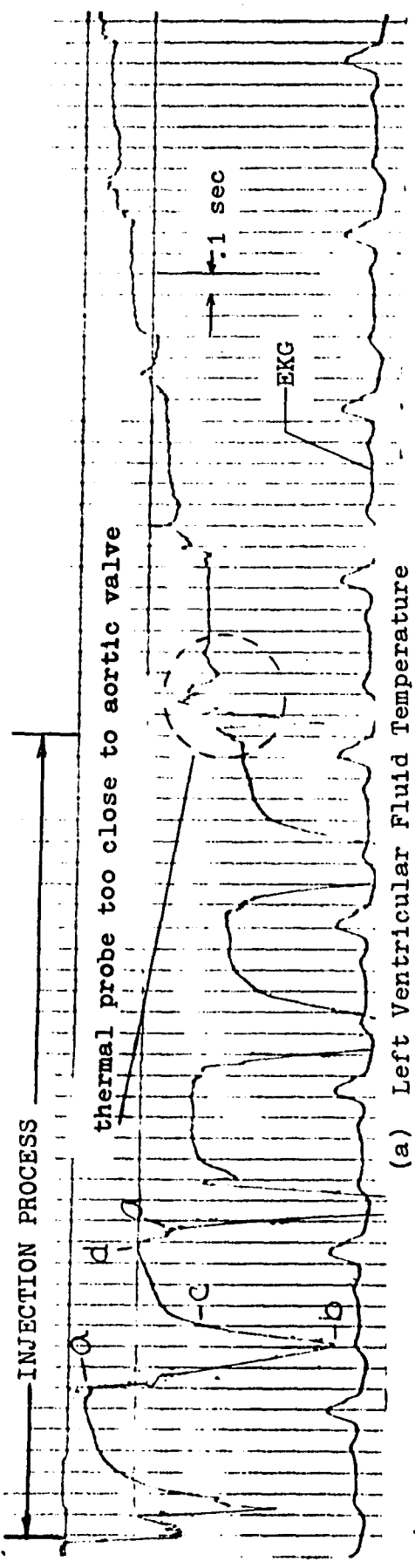


FIGURE 35 00



Calculated Ventricular Volume versus Time  
for the Thermodilution Study in Figure 33

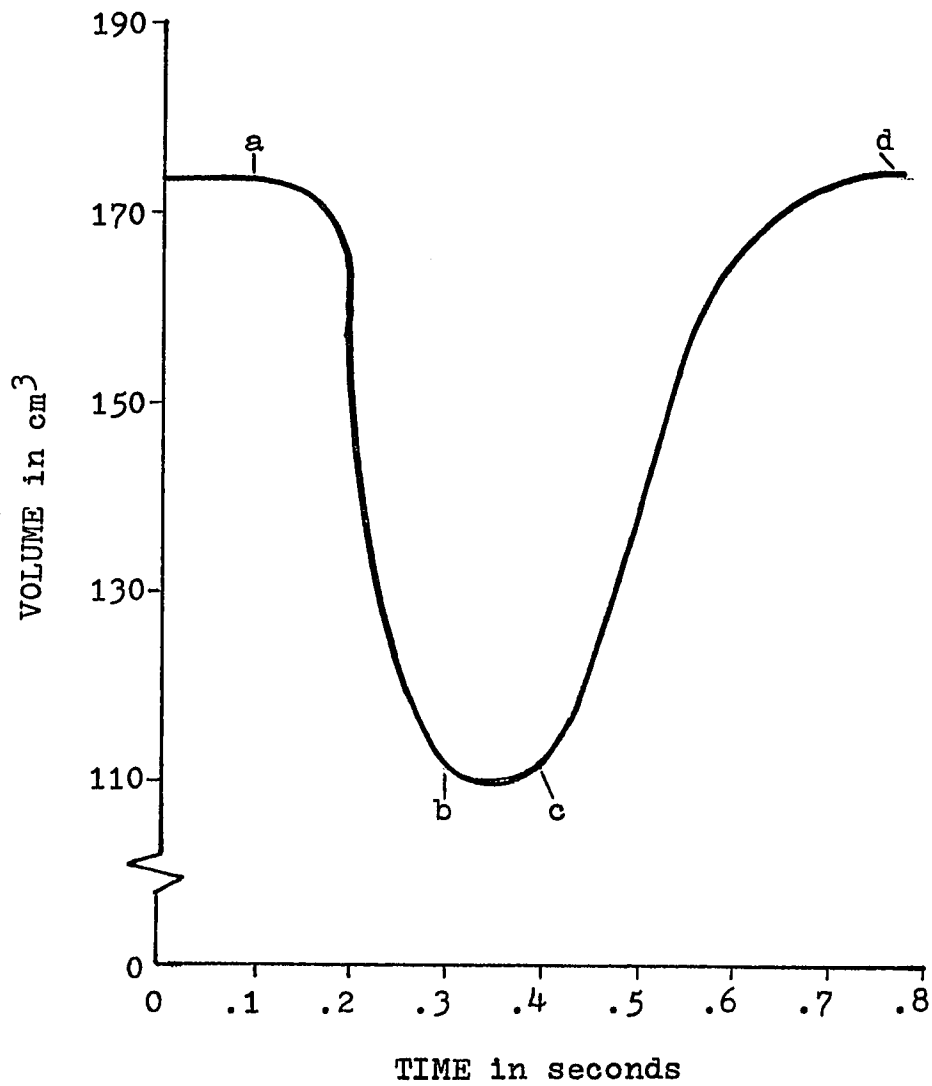


FIGURE 34

## Work Diagram for the Left Ventricle

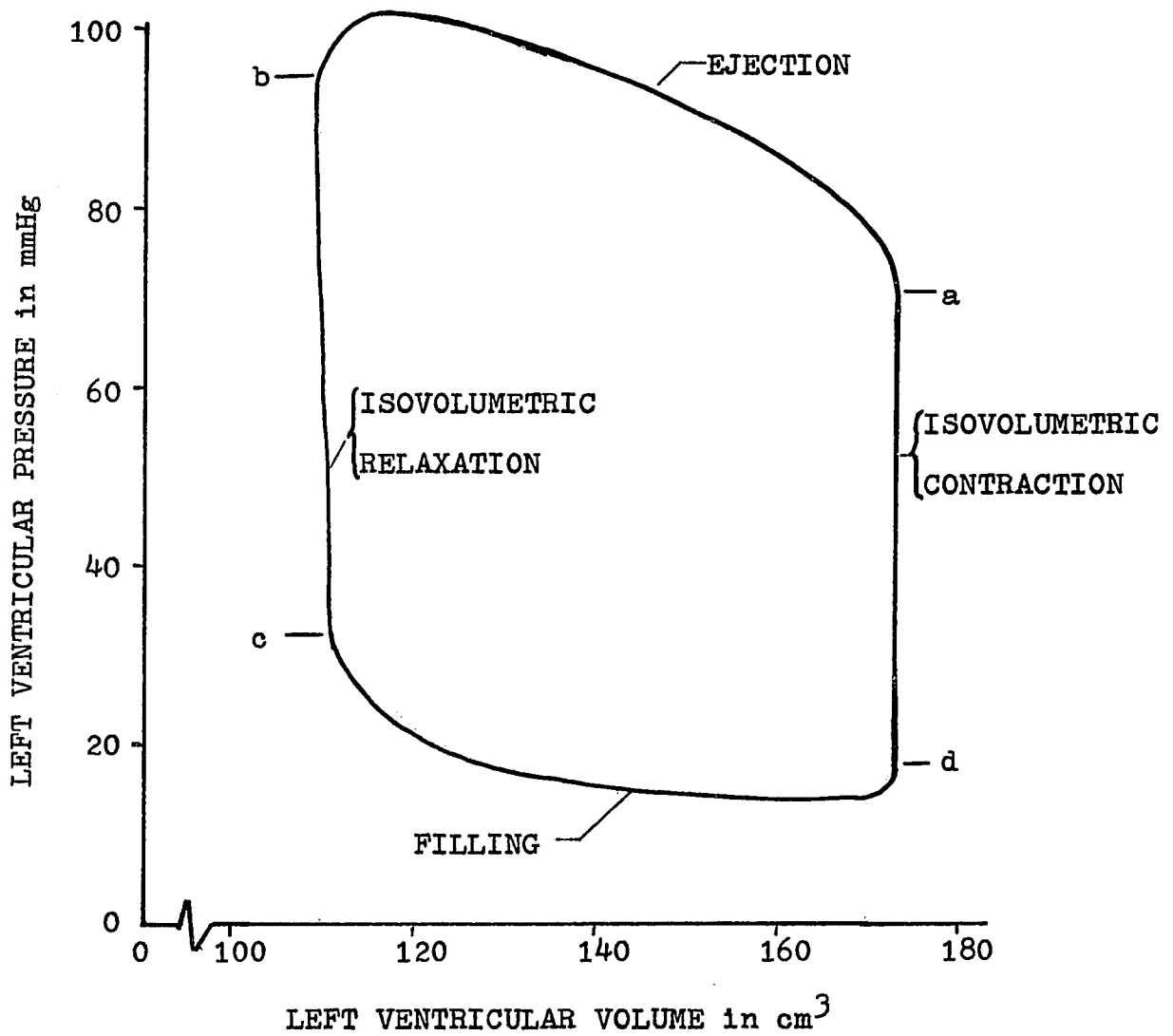
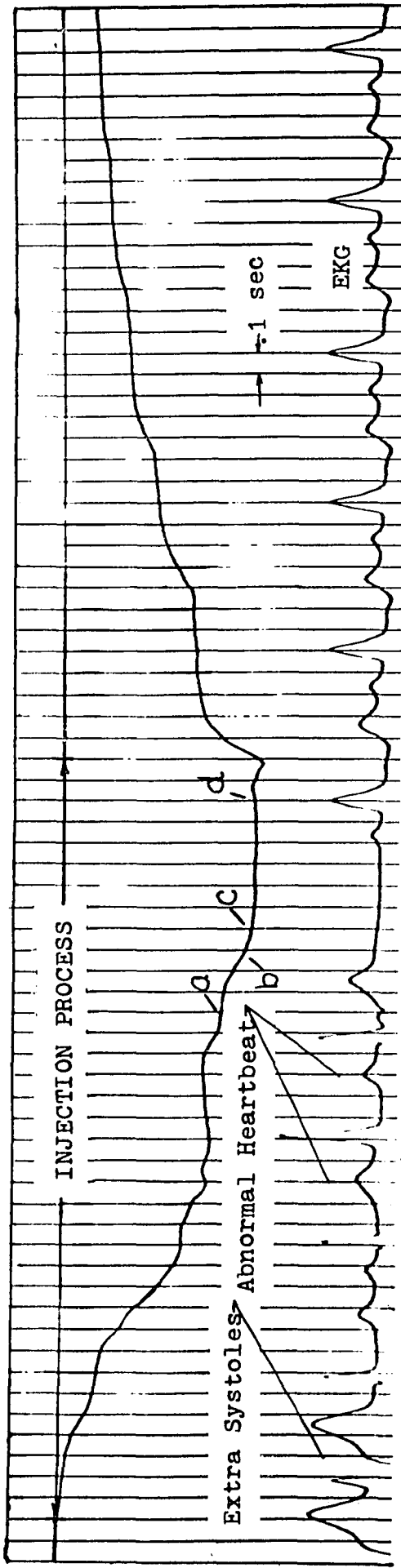


FIGURE 35



(a) Left Ventricular Fluid Temperature

MAN

THERMODILUTION STUDY IN UTILIZING THE BRANCATO TECHNIQUE



(b) Ventricule and Aortic Pull Back Pressures

FIGURE 36

Calculated Ventricular Volume versus Time  
for the Thermodilution Study in Figure 36

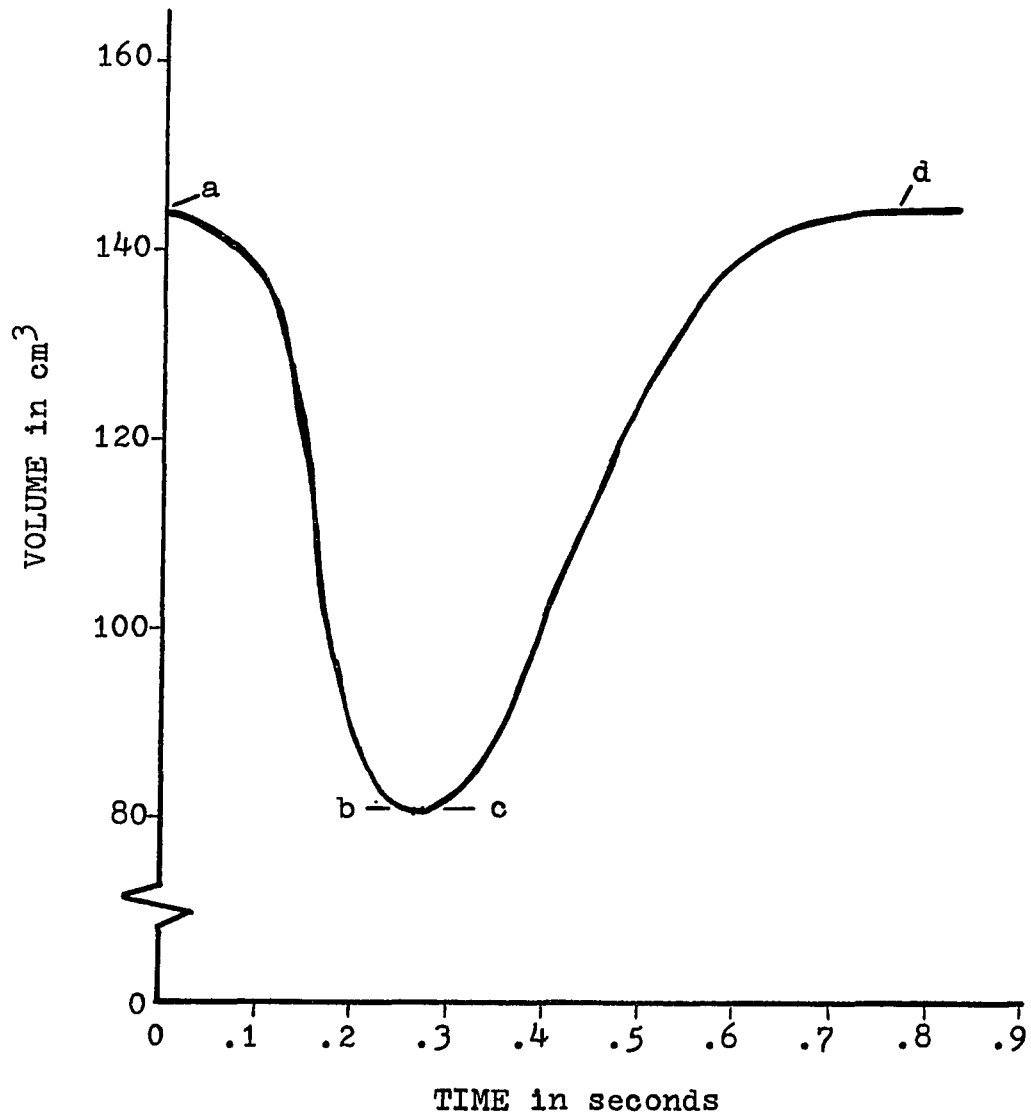


FIGURE 37

Left Ventricular Work Diagram for the Thermodilution  
Study in Figure 36

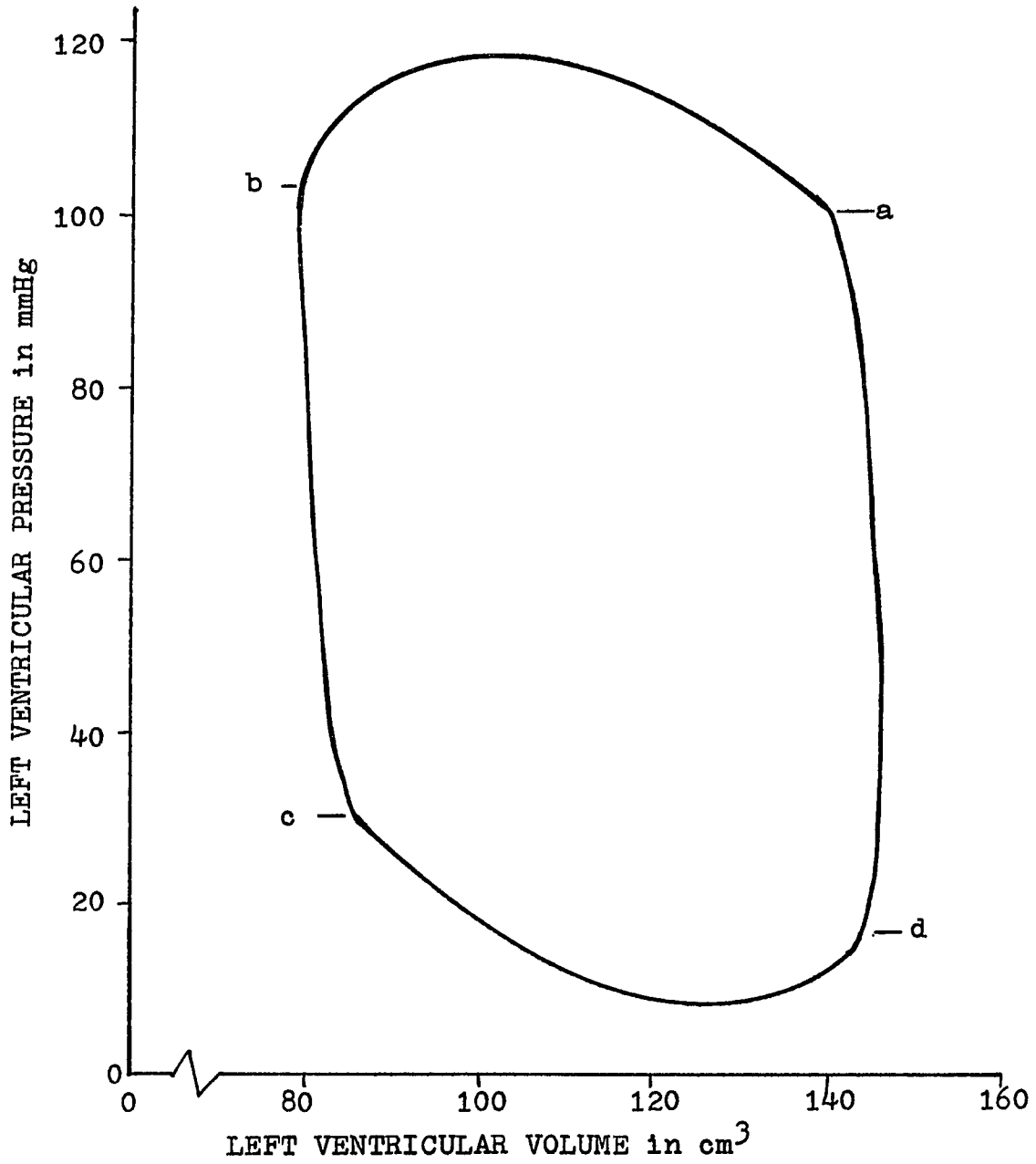
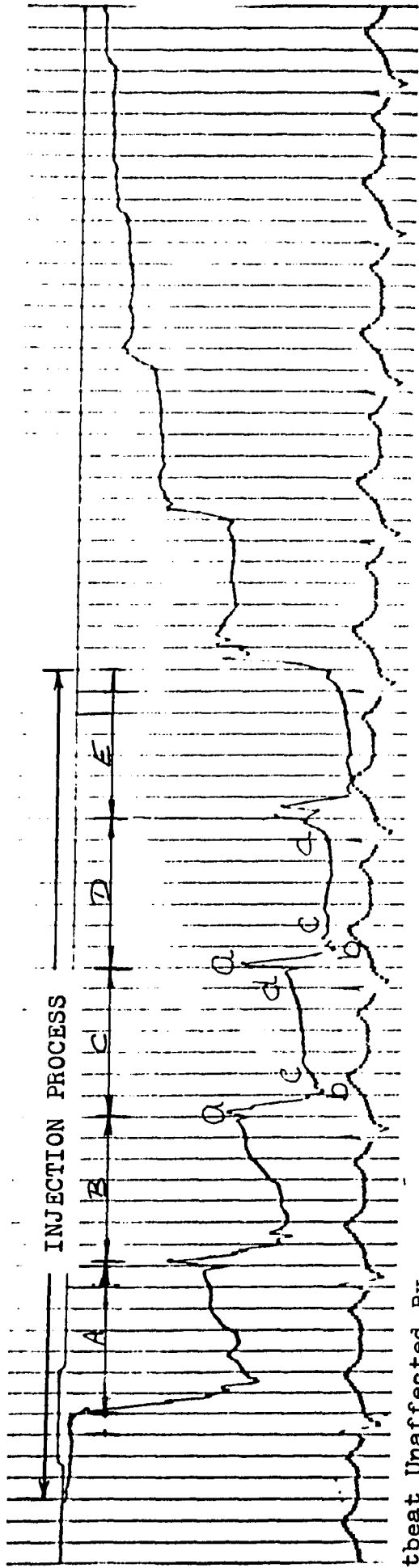


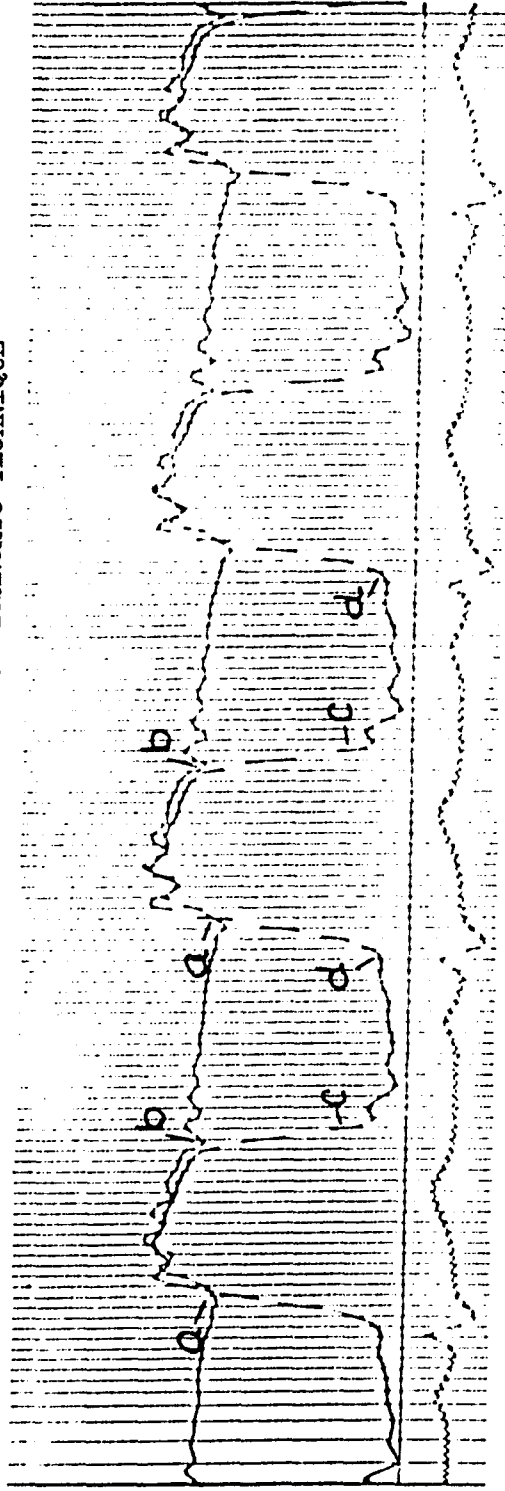
FIGURE 38



(a) Left Ventricular Fluid Temperature

Heartbeat Unaffected By  
Injection Process

THERMODILUTION STUDY IN MAN UTILIZING THE BRANCATO TECHNIQUE



(b) Simultaneous Ventricular and Aortic Pressures

Calculated Left Ventricular Volume  
versus Time  
for the Thermodilution Study in Figure 39, Heartbeat C

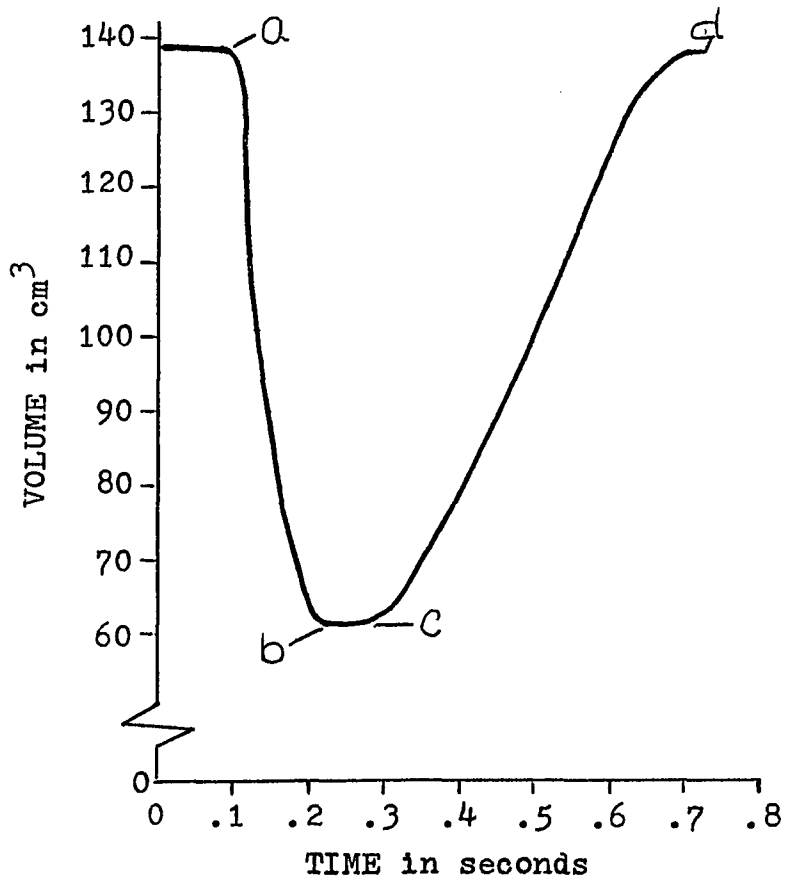


FIGURE 40

Left Ventricular Work Diagram  
for the Thermodilution Study in Figure 39

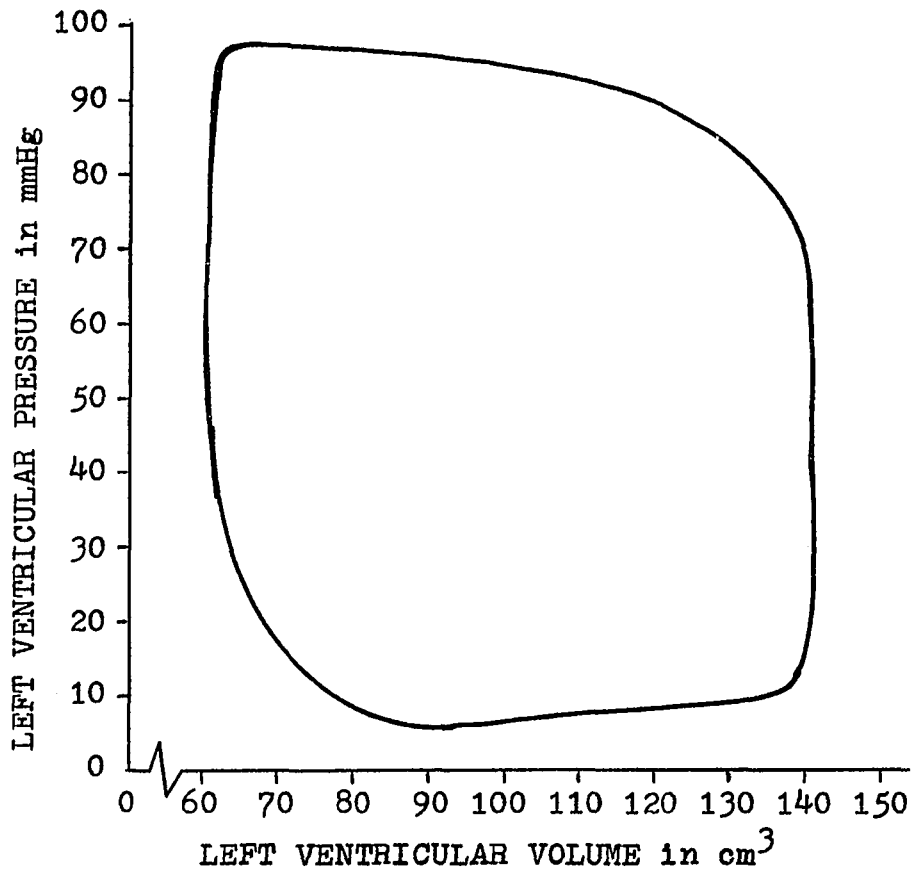


FIGURE 41



Volume versus Time Plots for Heartbeats D, C and E  
in Figure#39

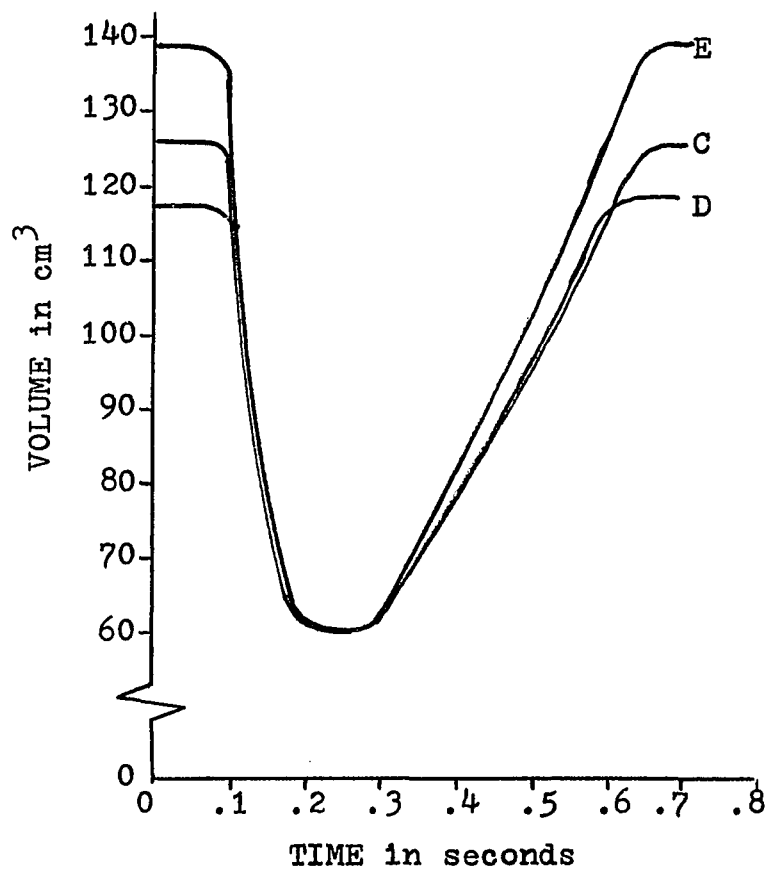
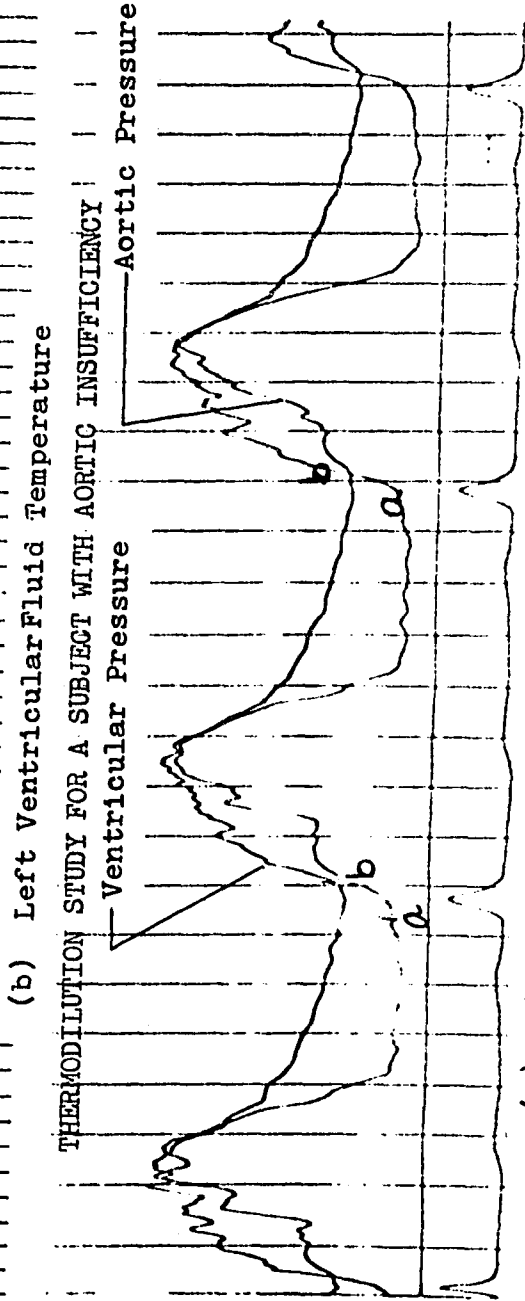
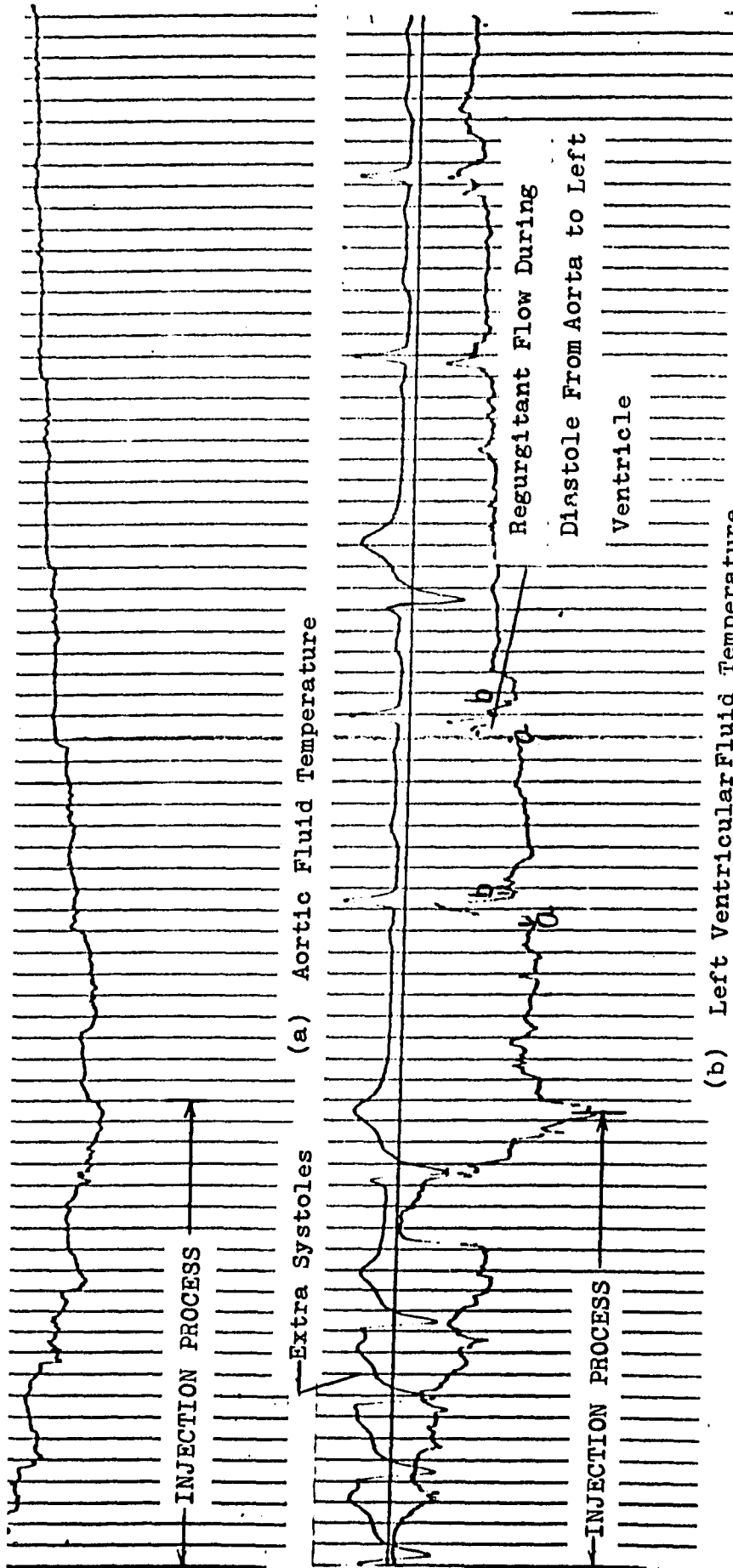


FIGURE 42



(c) Simultaneous Ventricular and Aortic Pressures

FIGURE 43

Thermocatheter Design

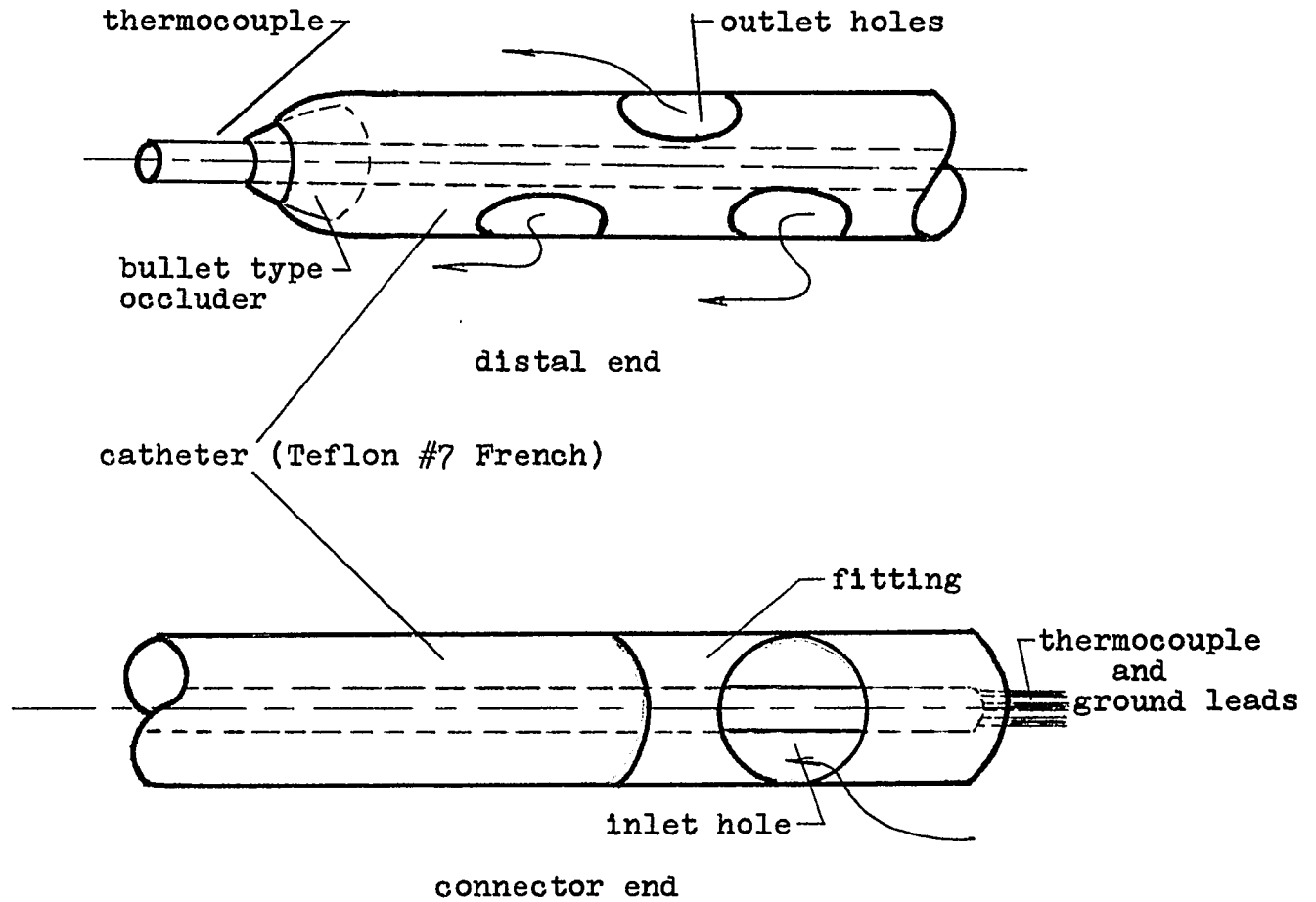


FIGURE 44

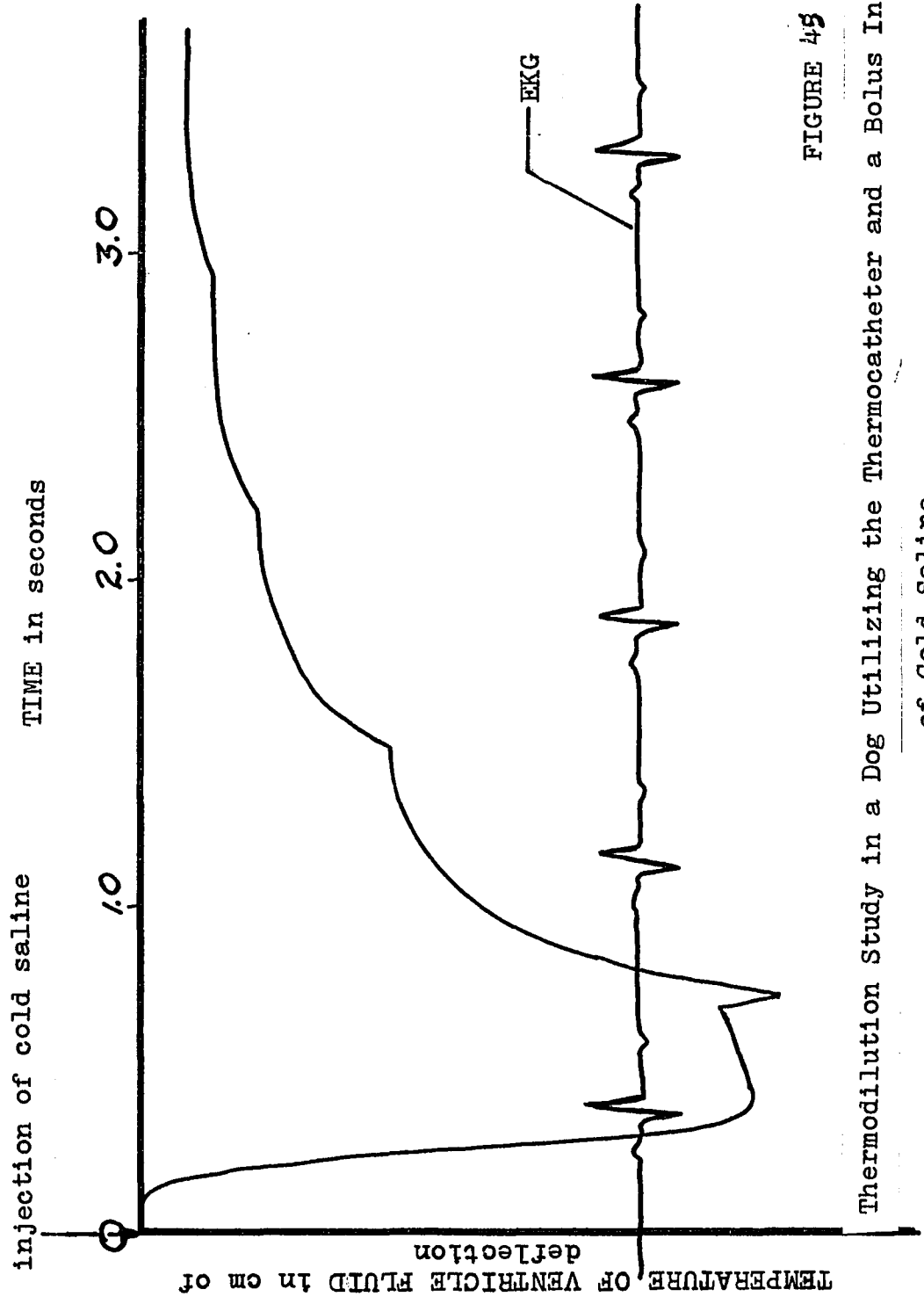
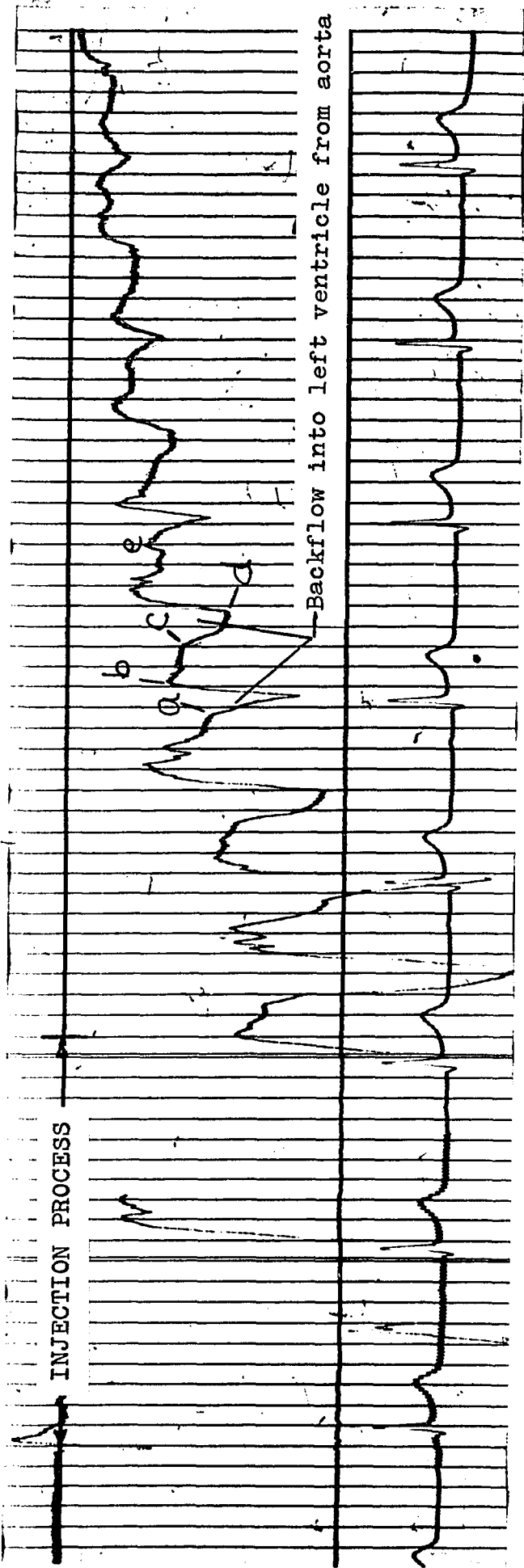


FIGURE 45

Thermodilution Study in a Dog Utilizing the Thermocatheter and a Bolus Injection of Cold Saline



THERMODILUTION STUDY FOR A SUBJECT WITH AORTIC INSUFFICIENCY UTILIZING THE THERMOCATHETER

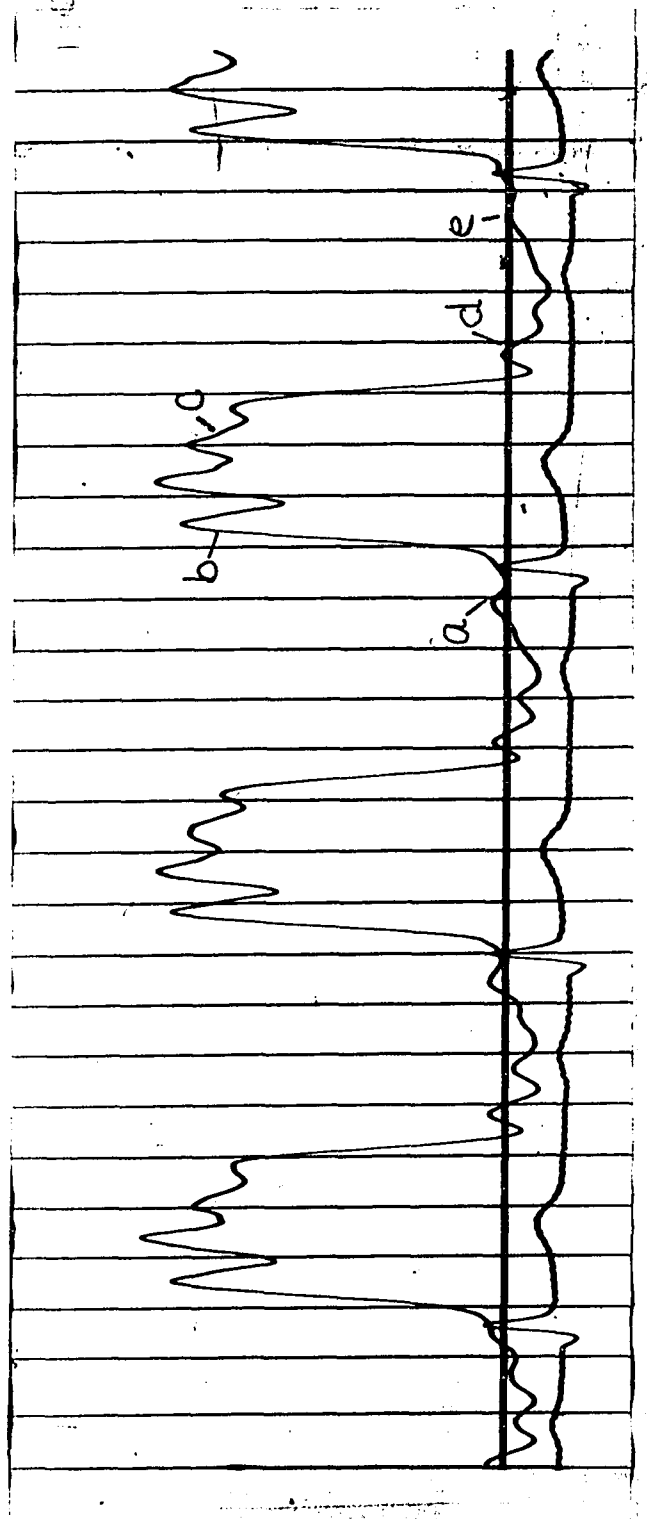


FIGURE 46

Nondimensionalized Left Ventricular Volume  
Plots from the Results of the Thermodilution Studies Employing  
the Brancato Technique and the Thermocatheter

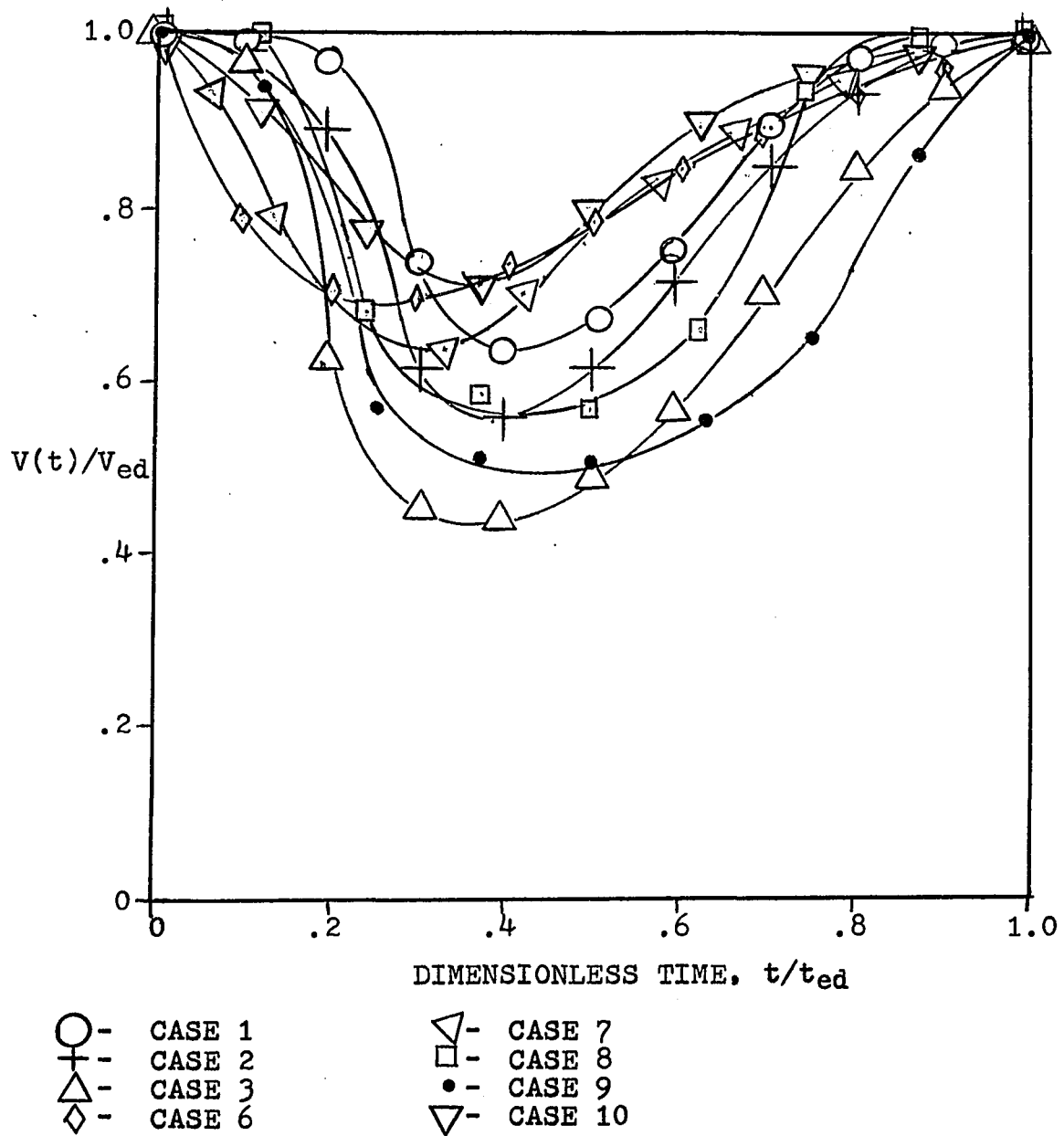


FIGURE 47

## Ventricular Stroke Work versus Ventricular End-Diastolic Volume

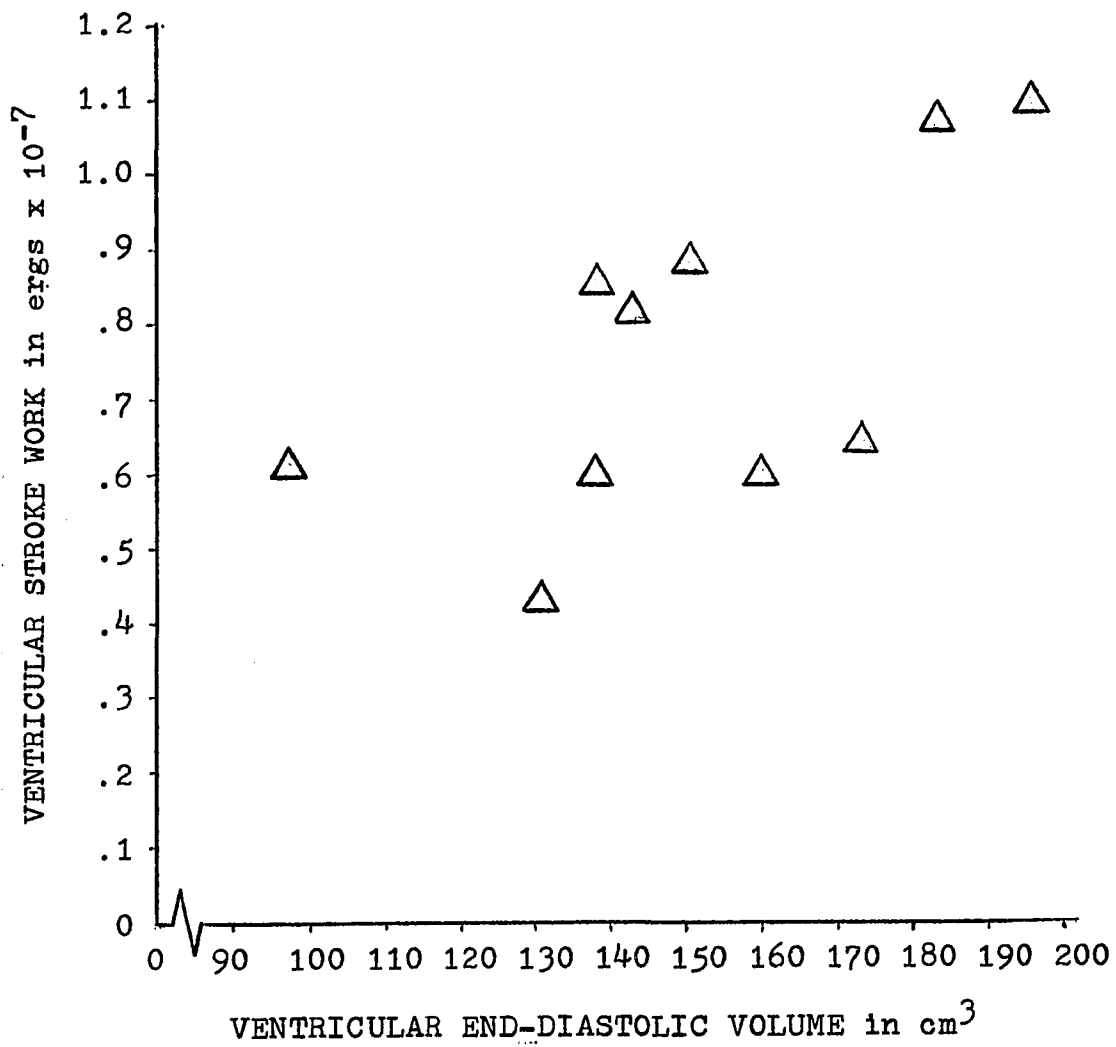


FIGURE 48

## Ventricular Stroke Work versus Ventricular End-Diastolic Pressure

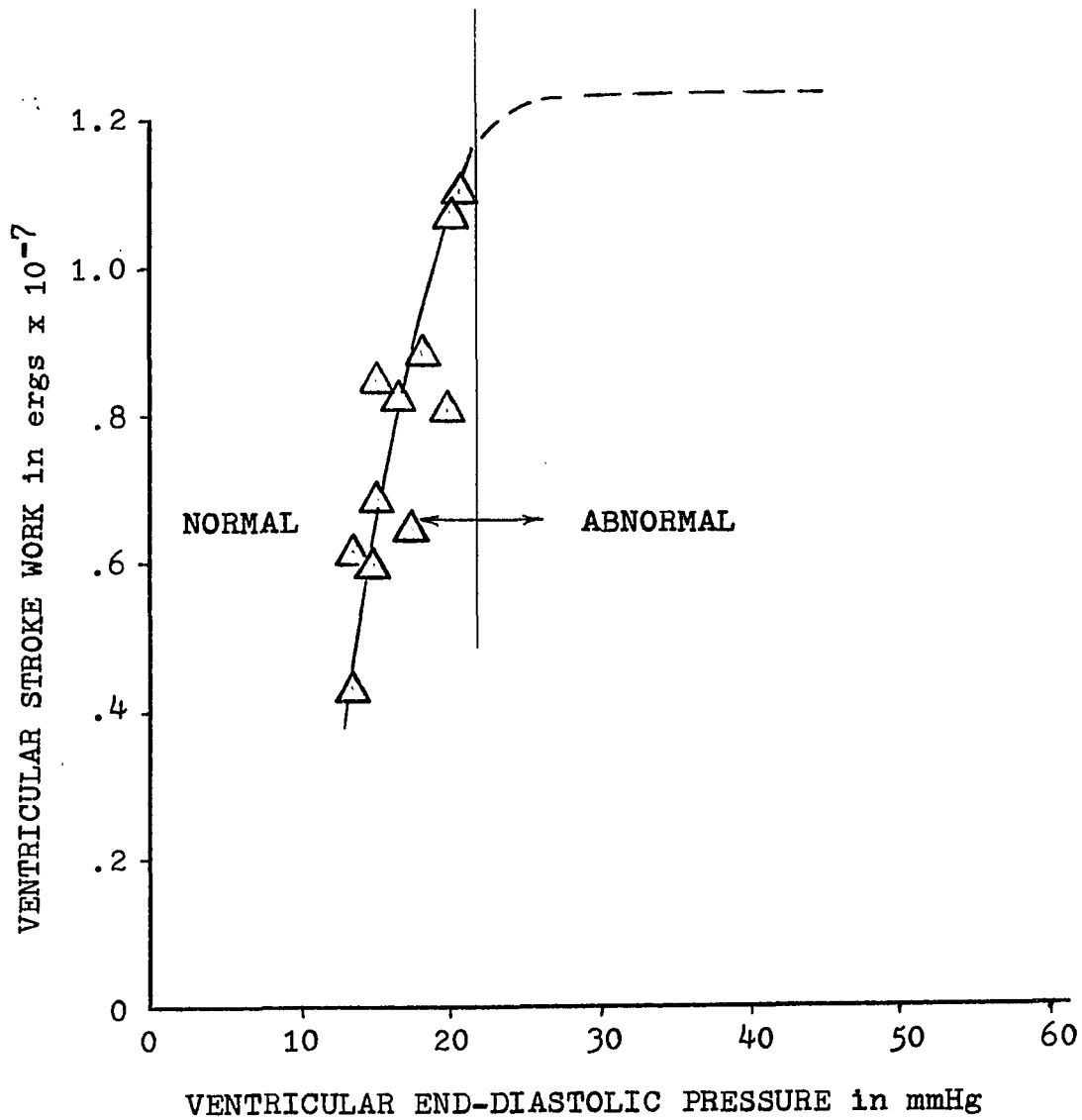


FIGURE 49



Ventricular End-Diastolic Pressure Versus Ventricular End-Diastolic  
Volume

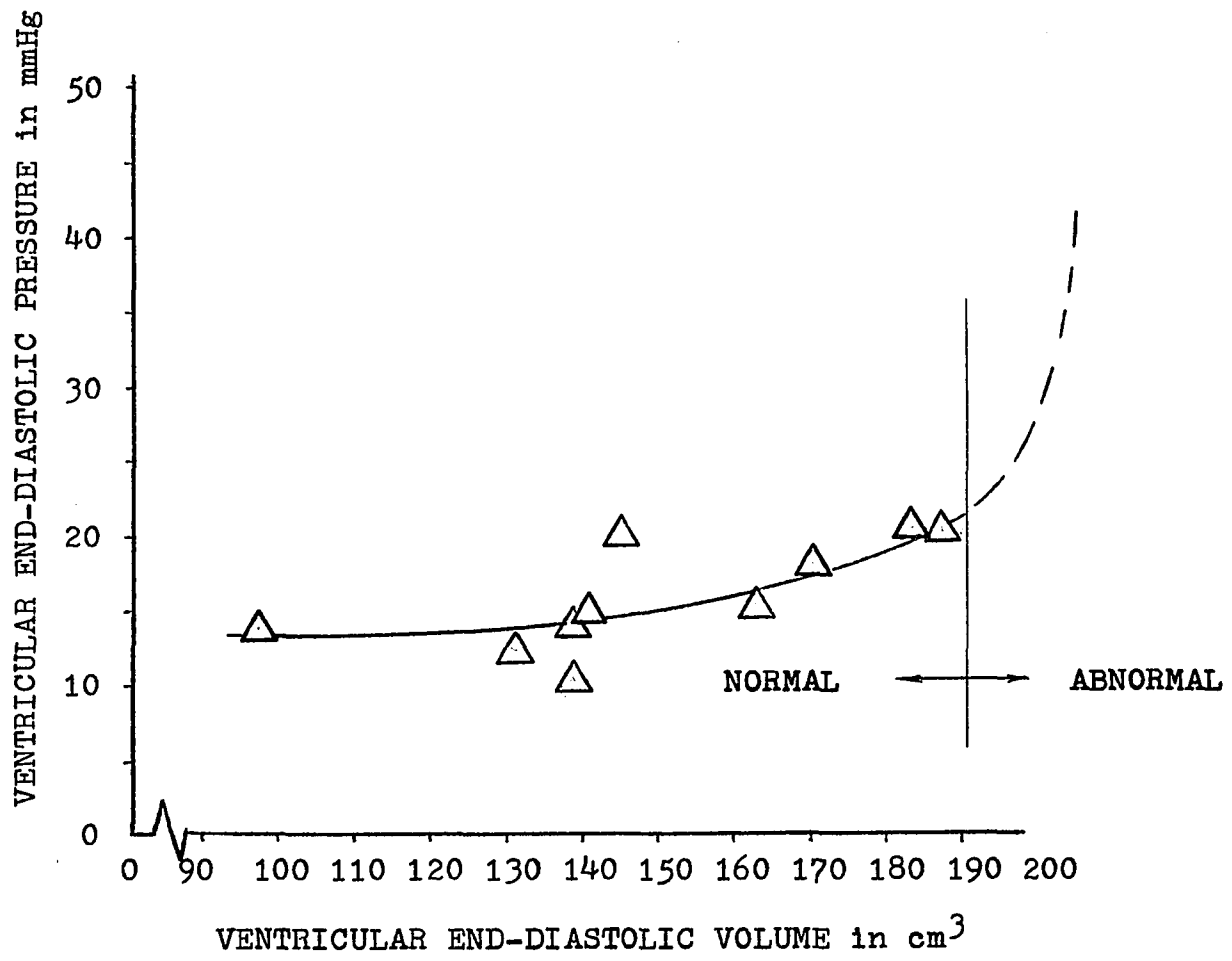
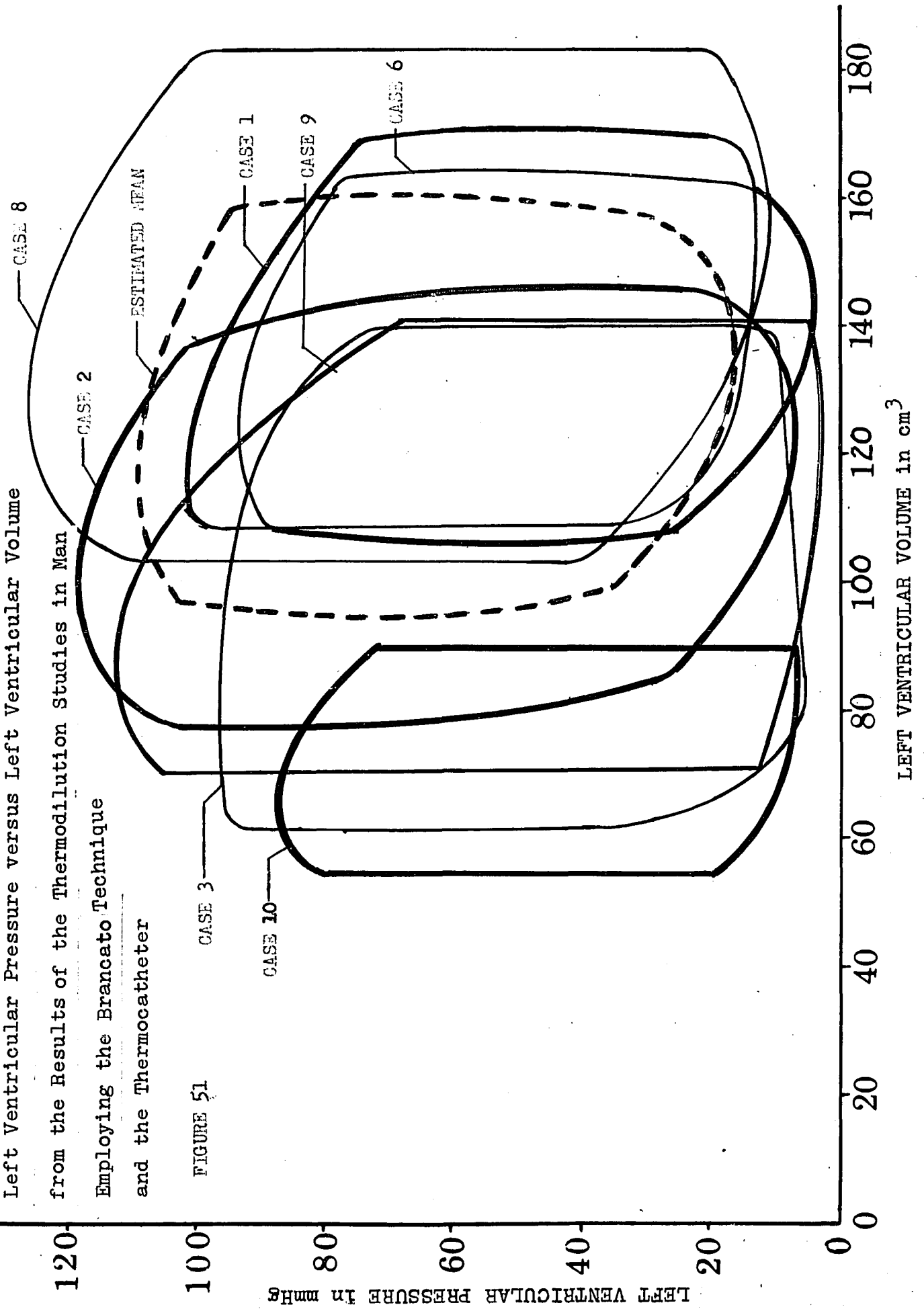


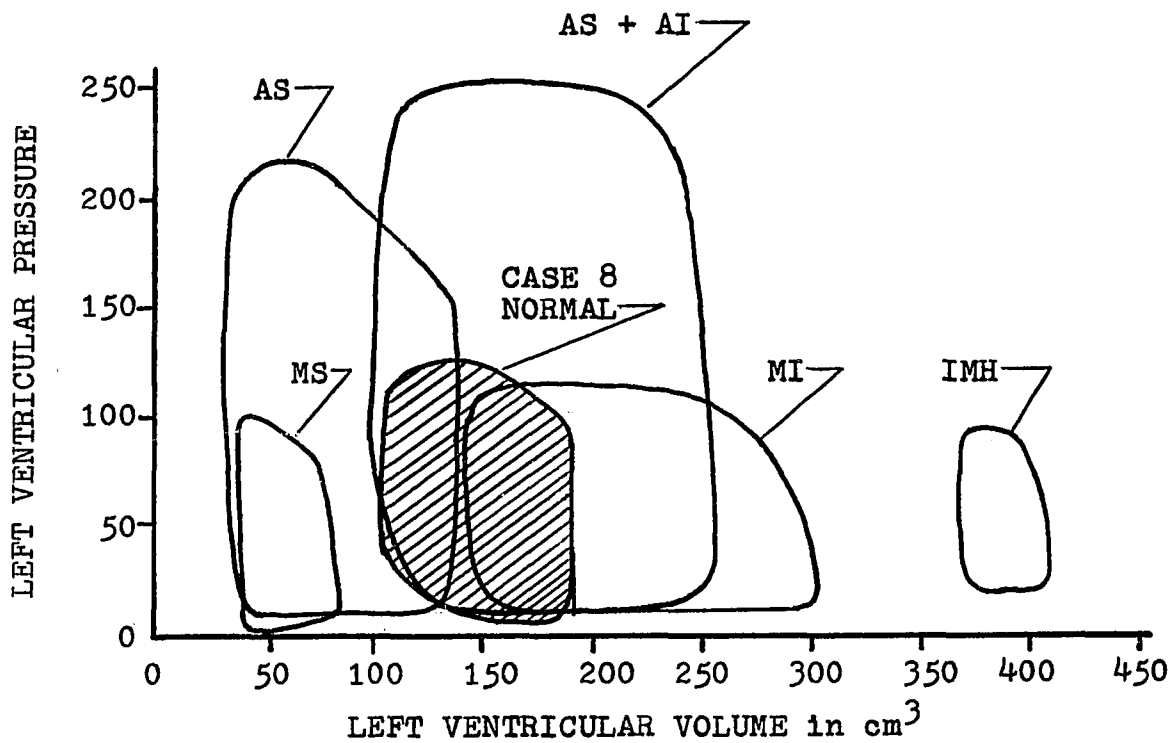
FIGURE 50

Left Ventricular Pressure versus Left Ventricular Volume  
from the Results of the Thermodilution Studies in Man  
Employing the Brancato Technique  
and the Thermocatheter

FIGURE 51



Left Ventricular Pressure versus Volume Plots  
 From Individual Patients with Different Varieties  
 of Heart Disease



AS + AI = aortic valve stenosis and insufficiency  
 IMH = idiopathic myocardial hypertrophy  
 MI = mitral insufficiency  
 MS = mitral stenosis

FIGURE 52

## A. APPENDIX

### A.1 Derivation of the Stewart-Hamilton Relationship

Consider the instantaneous injection of green dye into either the right heart or the left ventricle and the continuous measurement of dye concentration  $C(t)$  in the ascending aorta. Let  $\Delta V$  be the volume of fluid which passes through the cross section of the aorta, where the fluid dye concentration is measured, during the time interval  $t$  to  $t + \Delta t$ . Assuming that the fluid dye concentration is uniform at the cross section of the aorta and  $\Delta t$  is small such that  $C(t) = C(t + \Delta t)$ , the amount of dye in the volume of fluid  $\Delta V$  is given by,

$$\Delta I = \Delta V C(t) \quad (A-1)$$

Taking the limit as  $\Delta t \rightarrow 0$  equation (A-1) becomes,

$$dI = C(t) dV \quad (A-2)$$

Integrating equation (A-2) from time  $t = 0$  to time  $t = \infty$  yields,

$$I_{inj} = \int_{t=0}^{t=\infty} C(t) dV \quad (A-3)$$

Equation (A-3) may be written as,

$$I_{inj} = \int_0^{\infty} C(t) \frac{dV(t)}{dt} dt \quad (A-4)$$

The volumetric flow rate at time  $t$  is given by,

$$Q(t) = dV(t)/dt \quad (A-5)$$

Hence, equation (A-4) becomes,

$$I_{inj} = \int_0^{\infty} C(t) Q(t) dt \quad (A-6)$$

A mean volumetric flow rate  $Q$  may be defined by writing

$$m \int_0^{\infty} C(t) dt \leq \int_0^{\infty} C(t) Q(t) dt \leq M \int_0^{\infty} C(t) dt \quad (A-7)$$

which implies that  $Q$  has a maximum and a minimum value.

Dividing each term in equation (A-7) by  $\int_0^{\infty} C(t) dt$  yields,

$$m \leq \frac{\int_0^{\infty} C(t) Q(t) dt}{\int_0^{\infty} C(t) dt} \leq M \quad (A-8)$$

Therefore the mean volumetric flow rate  $Q$  may be defined as,

$$Q = \frac{\int_0^{\infty} C(t) Q(t) dt}{\int_0^{\infty} C(t) dt} \quad (A-9)$$

as long as  $C(t)$  is non-negative and  $\int_0^{\infty} C(t) dt > 0$ . From equations (A-6) and (A-9) it follows that,

$$Q = I_{inj} / \left[ \int_0^{\infty} C(t) dt \right] \quad (A-10)$$

Equation (A-10) is the Stewart-Hamilton equation used by physiologists to calculate the mean volumetric flow rate, called cardiac output, from dye indicator studies.

## A.2 Use of Stewart-Hamilton Equation in the presence of Valvular Insufficiency or Regurgitation

In the case of aortic insufficiency there is a flow of fluid back into the left ventricle during the diastolic function. This will exaggerate the concentration curve since,

$$\left( \int_0^{\infty} c(t) dt \right)_{\text{aortic insufficiency}} > \left( \int_0^{\infty} c(t) dt \right)_{\text{normal}}$$

Thus, from equation (A-10) the mean cardiac output  $Q$  calculated will be less than it actually is.

For the case of mitral insufficiency and regurgitation similar conclusions can be drawn. The cardiac output calculated by the Stewart-Hamilton equation in the presence of mitral insufficiency will be less than actual. Figure (A-1) is a green dye study of a subject with mitral insufficiency for which  $Q = 1.64$  l/min by equation (A-10). The actual cardiac output was  $Q = 4.82$  l/min, found by the Fick technique which is not affected by the presence of valvular incompetence.

Hence, it was concluded that the Stewart-Hamilton relation cannot be used to calculate cardiac outputs for ventricles with valvular incompetence. Even though the concentration versus time traces for these subjects appear normal in shape.

Green Dye Study of a Subject with Mitral Insufficiency

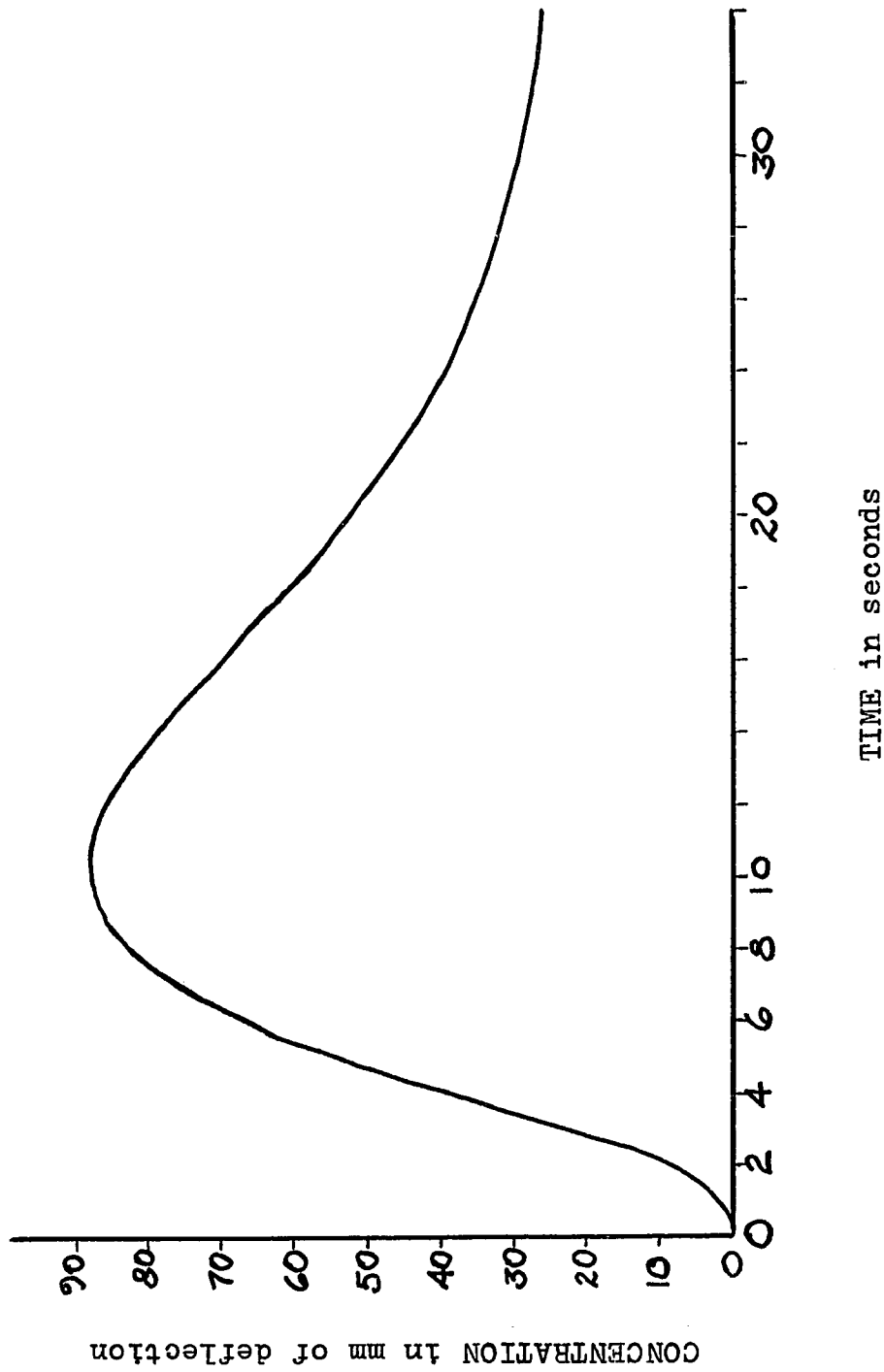


FIGURE A-1

B. APPENDIXB.1 Derivation of the Generalized Thermodilution Equation (41)

The general energy equation for a deformable control volume with mass flowing across the boundaries in several places and boundaries which themselves move is given by,

$$Q - W_{\text{shear}} - W_{\text{boundary}} + \sum_{\substack{\text{mass} \\ \text{entering}}} (pV + E) - \sum_{\substack{\text{mass} \\ \text{leaving}}} (pV + E) = \Delta E_s \quad (\text{B-1})$$

where  $\Delta E_s$  is the total energy change of the system which is given by,

$$\Delta E_s = \Delta(\text{kinetic energy})_s + \Delta(\text{potential energy})_s + \Delta U_s \quad (\text{B-2})$$

If the control volume under study is taken as the volume of the ventricle and equation (B-1) is applied to the diastolic function then,

$$\sum_{\substack{\text{mass} \\ \text{leaving}}} (pV + E) = 0 \quad (\text{B-3})$$

Q represents the total heat transferred, during the diastolic function, from the ventricular wall to the ventricular fluid. Q is not zero but its numerical value in thermal units (Btu) is very small compared to the total energy change of the system, the system being the ventricular fluid. Hence,

$$Q \approx 0 \quad (\text{B-4})$$

Since blood is a viscous non-Newtonian fluid it is safe to assume that the shearing stress  $\overline{\tau}$  is a function of the fluid velocities  $v_1$  and the velocity gradients in the ventricle  $v_{1,j}$ .



$$\overline{\tau} = f( v_1, v_{1,j} ) \quad (\text{B-5})$$

where  $v_1$  is the velocity in the  $i$ th direction and  $v_{1,j}$  is the partial derivative of  $v_1$  with respect to the  $j$ th direction. The general stress tensor  $\overline{\overline{T}}$  is given by the vector sum of the shearing stress  $\overline{\tau}$  and the normal stress  $\overline{\overline{E}}$  which is equal to  $-p$  for a viscous fluid at rest,

$$\overline{\overline{T}} = \overline{\tau} + \overline{\overline{E}} \delta_{ij} \quad (\text{B-6})$$

Thus, the shear work is due to the shear stress  $\tau$  and the boundary work due to normal stress or pressure  $p$ .

The rate of shear work done by the fluid in the control volume on the boundary is given by,

$$\dot{W}_{\text{shear}} = - \int_{S \text{ c.v.}} \overline{\tau} \cdot \overline{v} \, dA \quad (\text{B-7})$$

where the integral is over the surface of the control volume. Since the fluid velocities in the ventricle (and the velocity gradients along the ventricle wall) are small it follows that,

$$W_{\text{shear}} \approx 0 \quad (\text{B-8})$$

It is noted that the viscous shear work cannot be neglected in the aorta during the systolic function.

The rate of work done by the fluid system on the boundary during the diastolic function is given by,

$$\dot{W}_{\text{boundary}} = \int_{S \text{ c.v.}} p \overline{v}_b \cdot \overline{n} \, dA \quad (\text{B-9})$$

which may be approximated by,

$$\dot{W}_{\text{boundary}} = \overline{p} V_{sv} / t, \quad (\text{B-10})$$

where  $\bar{p}$  is the mean diastolic pressure and  $t$  is the time length of the diastolic function. Since the mean diastolic pressure is normally less than 10 mmHg it can be shown that the work on the boundary during filling is negligible compared to the total energy change of the system hence,

$$W_{\text{boundary}} \approx 0 \quad (\text{B-11})$$

Since the system is not in motion and remains at the same potential, equation (B-2) becomes

$$\Delta E_s = \Delta U_s \quad (\text{B-12})$$

and likewise, assuming as negligible, the potential and kinetic energy of the mass inflow

$$\Delta E = \Delta U \quad (\text{B-13})$$

Substituting equations (B-3), (B-4), (B-8), (B-11), (B-12) and (B-13) into equation (B-1) yields,

$$\sum_{\substack{\text{mass} \\ \text{entering}}} (p V + U) = \Delta U_s \quad (\text{B-14})$$

Enthalpy  $H$  is defined as,

$$H = p V + U \quad (\text{B-15})$$

Hence, equation (B-14) becomes,

$$\sum_{\substack{\text{mass} \\ \text{entering}}} H = U_{s,\text{final}} - U_{s,\text{initial}} \quad (\text{B-16})$$

Equation (B-16) is the generalized thermodilution equation which is employed in section 3.2 and is used to derive the fundamental thermodilution equations.

## B.2 Derivation of the Fundamental Thermodilution Equations

Consider a heart in which an injection 8 ml of cold saline at 50 °F is made into the ventricle thus lowering the temperature of the ventricular fluid. If the above injection process is done during the diastolic function, equation (B-16) can be stated as,

$$\left[ \begin{array}{l} \text{energy in:} \\ \text{mass inflow} \\ \text{from atrium} \end{array} \right] + \left[ \begin{array}{l} \text{energy in:} \\ \text{injected} \\ \text{saline} \end{array} \right] = \left[ \begin{array}{l} \text{stored} \\ \text{energy} \\ \text{final} \end{array} \right] - \left[ \begin{array}{l} \text{stored} \\ \text{energy} \\ \text{initial} \end{array} \right] \quad (\text{B-17})$$

Applying the basic caloric equations for a homogeneous incompressible fluid which are given by,

$$H = \rho C_p T V \quad \text{and} \quad U = \rho C_v T V \quad (\text{B-18})$$

equation (B-16) becomes,

$$\rho C_p T_{sv} V_{sv} + \rho_{inj} C_{p,inj} T_{inj} V_{inj} + \rho C_v T_o V_o = U_f \quad (\text{B-19})$$

The final energy of the system  $U_f$  is given by,

$$U_f = \sum_{i=1}^N (\rho_i C_{v,i} T_i V_i)_f \quad (\text{B-20})$$

where the end-diastolic volume has been divided up into  $N$  equal, arbitrarily small, volumes  $V_i$ . It follows that,

$$V_f = \sum_{i=1}^N V_{i,f} \quad (\text{B-21})$$

If complete mixing is assumed there will be no temperature gradient within the ventricle hence,

$$T_{i,f} = T_f \quad \text{for all values of } i.$$

Assuming constant properties ( $\rho$ ,  $C_p$  are constant and not a

function of temperature) and  $C_p = C_v$  for all liquids:

$$C_p = C_{p,inj} = C_{p,f} \quad \text{and} \quad \rho = \rho_{inj} = \rho_f \quad (\text{B-22})$$

Equation (B-19) becomes,

$$T_o V_o + T_{sv} V_{sv} + T_{inj} V_{inj} = T_f V_f \quad (\text{B-23})$$

where  $T_f$  represents the ventricular fluid temperature at the end of diastole, with the assumption of complete mixing in the ventricle. During the systolic function which follows diastole, the ventricle is partially emptied. Assuming no heat transfer from the heart wall to the ventricular fluid, the temperature of the fluid will still equal the  $T_f$  calculated.

Systole ends, the heart rests for a short time (less than .1 second) and the diastolic function begins again. During each diastolic function the warmer body blood enters the ventricle and raises the ventricular fluid temperature. The energy equation for this process, again assuming complete mixing and constant properties, is given by,

$$T_{o,n} V_{o,n} + T_{sv} V_{sv} = T_{f,n+1} V_{f,n+1} \quad (\text{B-24})$$

and from a mass balance,

$$V_{o,n} + V_{sv} = V_{f,n+1} \quad (\text{B-25})$$

where  $n$  equals 2, 3, 4, ..... $n$ .

Since  $T_o$  and  $V_o$  represent the initial temperature and volume respectively they may be denoted as the end-systolic temperature  $T_{es,1}$  and the end-systolic volume  $V_{es,1}$ .  $T_f$  and  $V_f$  represent the end-diastolic conditions and are given by  $T_{ed,2}$  and  $V_{ed,2}$  respectively. Equation (B-23) becomes.

$$T_{es,1} V_{es,1} + T_{sv} V_{sv} + T_{inj} V_{inj} = T_{ed,2} V_{ed,2} \quad (B-26)$$

and from a mass balance,

$$V_{es,1} + V_{inj} + V_{sv} = V_{ed,2} \quad (B-27)$$

Notice that the injection takes place during the second diastole and a heartbeat consists of a diastolic and systolic function. Hence, for the third diastolic function,

$$T_{es,2} V_{es,2} + T_{sv} V_{sv} = T_{ed,3} V_{ed,3} \quad (B-28)$$

and

$$V_{ed,3} = V_{es,2} + V_{sv} \quad (B-29)$$

Solving equations (B-28) and (B-29) simultaneously yields,

$$V_{sv} = V_{es,2} (T_{ed,3} - T_{es,2}) / (T_{sv} - T_{ed,3}) \quad (B-30)$$

and from Figure 4,

$$T_{sv} - T_{ed,3} = \Delta T_2 \quad \text{and} \quad \Delta T_{\max} - \Delta T_2 = T_{ed,3} - T_{es,2} \quad (B-31)$$

Therefore equation (B-30) becomes,

$$V_{sv} = V_{es,2} (\Delta T_{\max} - \Delta T_2) / (\Delta T_2) \quad (B-32)$$

or in general,

$$V_{sv} = V_{es,n+1} (\Delta T_n - \Delta T_{n+1}) / (\Delta T_{n+1}) \quad (B-33)$$

where n equals 1, 2, 3, .....n.

Substituting for  $V_{es,2}$  as given by equation (B-29) into equation (B-28) yields,

$$V_{ed} = V_{sv} / (1-k) \quad (B-34)$$

where

$$k = \Delta T_{n+1} / \Delta T_n \quad (B-35)$$

Solving equations (B-26) and (B-27) simultaneously yields,

$$V_{ed} = V_{inj} ( T_b - T_{inj} ) / \Delta T_{max} \quad (B-36)$$

where  $T_b$  is the body temperature which is equal to  $T_{es,1}$ . The values of temperature appearing in the above equation may be determined experimentally. Thus the value of end-diastolic volume may be calculated with equation (B-36), the stroke volume with equation (B-34), and the end-systolic volume with the general equation given by,

$$V_{es} = V_{ed} - V_{sv} \quad (B-37)$$

The fundamental thermodilution equations allow for the calculation of ventricular end-volumes from the temperature data of a thermodilution study which consists of a single injection of cold saline into the left ventricle during a single diastolic function. In appendix C equations are derived for the instantaneous ventricular volumes during the injection of cold saline over multiple heartbeats. The advantages of the continuous injection over multiple heartbeats are discussed in chapter 4.

C. APPENDIXC.1 Theory of Thermal Tracers in Multicompartment Systems

Consider a system composed of  $n$  compartments which exchange mass and thermal energy with each other. Define  $M_i$  and  $c_i$  as the mass and thermal energy concentration of the  $i$ th compartment such that,

$$C_i = c_i M_i \quad (C-1)$$

where  $C_i$  is the total thermal energy of the  $i$ th compartment measured in Btu. Defining a transport or exchange rate  $b_{ij}$  (gm/sec) from the  $i$ th compartment to the  $j$ th compartment, it follows for the  $i$ th compartment,

$$dC_i/dt = \sum_{\substack{j=1 \\ j \neq i}}^n (c_j b_{ji} - c_i b_{ij}) \quad (C-2)$$

From equation (C-1),

$$dC_i/dt = M_i dc_i/dt + c_i dM_i/dt \quad (C-3)$$

and from a mass balance,  $M_i dc_i/dt = \sum b_{ji} (c_j - c_i)$

$$dM_i/dt = \sum_{\substack{j=1 \\ j \neq i}}^n (b_{ji} - b_{ij}) \quad (C-4)$$

Combining equations (C-2), (C-3) and (C-4) yields,

$$M_i dc_i/dt = \sum_{j \neq i}^n (c_j b_{ji} - c_i b_{ij}) \quad (C-5)$$

or

$$M_i dc_i/dt = \sum_j b_{ji} (c_j - c_i) \quad (C-6)$$

Applying the caloric equations given by,

$$C_i = \rho C_p T_i V_i \quad (C-7)$$

it follows that,

$$c_i = C_p T_i \text{ and } M_i = \rho V_i \quad (C-8)$$

Hence, assuming  $\rho$  and  $C_p$  constant equation (C-6) becomes,

$$\rho V_i dT_i/dt = \sum_j b_{ji} (T_j - T_i) \quad (C-9)$$

Equation (C-9) is a general expression for the instantaneous volume  $V_i$  of the  $i$ th compartment. Thus, the total volume of the system is given by,

$$V(t) = \sum_{i=1}^n V_i(t) \quad (C-10)$$

Combining equations (C-9) and (C-10) yields an expression for the instantaneous volume of an  $n$  compartment system with a nonuniform temperature distribution,

$$\rho \sum_{i=1}^n V_i dT_i/dt = \sum_{i=1}^n \sum_{\substack{j=1 \\ j \neq i}}^n (b_{ji} (T_j - T_i)) \quad (C-11)$$

## C.2 Three Compartment System

Consider a three compartment system ( $n = 3$ ) consisting of the atrium, ventricle and aorta represented by compartments 1, 2, and 3 respectively. In a normal heart there will be only one non-zero exchange rate  $b$  between them at any particular time during the heartbeat. In the presence of valvular regurgitation or insufficiency more than one non-zero exchange rate will exist. Various modes of exchange rates are given below in Table 1.



TABLE 1

CASE	CONDITION	NON-ZERO b's DURING DIASTOLE	DURING SYSTOLE
1	normal heart function	$b_{12}$	$b_{23}$
2	aortic insufficiency	$b_{12}, b_{32}$	$b_{23}$
3	mitral insufficiency	$b_{12}$	$b_{23}, b_{21}$

Other modes are possible such as, mitral insufficiency and aortic regurgitation where the non-zero exchange rates are found be combining cases 2 and 3. For a three compartment system equation (C-9) becomes,

$$V_1 \frac{dT_1}{dt} = \sum_{j=1}^3 b_{j1} (T_j - T_1) \text{ for } i = 1, 2 \text{ and } 3 \quad (\text{C-12})$$

Equation (C-12) represents three differential equations given by,

$$V_1 \frac{dT_1}{dt} = b_{21} (T_2 - T_1) + b_{31} (T_3 - T_1) \quad (\text{C-13})$$

$$V_2 \frac{dT_2}{dt} = b_{12} (T_1 - T_2) + b_{32} (T_3 - T_2) \quad (\text{C-14})$$

$$V_3 \frac{dT_3}{dt} = b_{13} (T_1 - T_3) + b_{23} (T_2 - T_3) \quad (\text{C-15})$$

for the atrium, ventricle and aorta respectively. The above equations may be employed to evaluate abnormal flows between chambers following the injection of cold saline into the left ventricle. This would involve simultaneous temperature measurements in the chambers being studied and the simultaneous solution of equations (C-13), (C-14) and (C-15). An application of these equations to derive an expression for instantaneous

ventricular volumes during diastole and systole is presented below.

### C.3 Derivation of Equations for Instantaneous Ventricular Volumes during the Heartbeat

For the normal functioning heart from Table 1 equations (C-13), (C-14) and (C-15) become,

$$\rho V_1 dT_1/dt = 0 \quad (C-16)$$

$$\rho V_2 dT_2/dt = b_{12} (T_1 - T_2) \quad (C-17)$$

$$\rho V_3 dT_3/dt = b_{23} (T_2 - T_3) \quad (C-18)$$

For the diastolic function the solution of equations (C-16) and (C-18) are,  $T_1 = \text{constant}$  and  $T_3 = \text{constant}$ . Equation (C-17) becomes,

$$V_2 dT_2/dt = dV_2/dt (T_1 - T_2) \quad (C-19)$$

since from a mass balance,

$$b_{12} = \rho dV_2/dt \quad (C-20)$$

Separating the variables in equation (C-19) and integrating yields,

$$V_2(t) = V_2(0) \left[ T_2(0) - T_1 \right] / \left[ T_2(t) - T_1 \right] \quad (C-21)$$

where  $V_2(t)$  is the instantaneous volume of the ventricle. Equation (C-21) is the same equation derived by the author in reference (24) using the generalized thermodilution equation derived in appendix B.

For the systolic function let compartment 1 represent the volume of an injecting syringe containing a volume  $V_{inj}$

of cold saline at temperature  $T_{inj}$ .  $b_{12}$  therefore represents the mass rate of injectate into the left ventricle. Equation (C-17) may be written as,

$$\rho V_2 dT_2/dt = b_{12} (T_{inj} - T_2) \quad (C-22)$$

Since,  $b_{12} = \rho_{inj} \dot{V}_{inj}$  and assuming  $\rho = \rho_{inj}$ ,

$$V_2(t) = \dot{V}_{inj} (T_2 - T_{inj}) / \left| \frac{dT_2}{dt} \right| \quad (C-23)$$

Equation (C-23) allows for the calculation of the ventricular volume during systole and during the continuous injection of cold saline.

An expression for the diastolic volume during the injection of cold saline is derivable in the same manner. Equation (C-14) may be written as,

$$\rho V_2 dT_2/dt = \dot{V}_{inj} \rho_{inj} (T_{inj} - T_2) + b_{12} (T_1 - T_2) \quad (C-24)$$

and a mass balance yields,

$$b_{12} + \rho_{inj} \dot{V}_{inj} = \rho dV_2/dt \quad (C-25)$$

Substituting  $b_{12}$  as given by equation (C-25) into equation (C-24) and defining,

$$\theta_0 = T_{inj} - T_1 \text{ and } \theta = T_2 - T_1$$

yields,

$$d(\theta V_2)/dt = \dot{V}_{inj} \theta_0 \quad (C-26)$$

Solving for the instantaneous volume during diastole yields,

$$V(t) = V_{inj}(t) \frac{T_{inj} - T_{sv}}{T(t) - T_{sv}} + V_{es} \frac{T_{es} - T_{sv}}{T(t) - T_{sv}} \quad (C-27)$$

where  $T_{sv} = T_1$ ,  $V(t) = V_2$ ,  $V_{es} = V_2(0)$  and

$$V_{inj}(t) = \int_0^t \dot{V}_{inj} dt \quad (C-28)$$

Equations (C-27) and (C-28) allows for the calculation of the ventricular volume during diastole and during the continuous injection of cold saline over multiple heartbeats.

#### C.4 Theoretical Thermodilution Study

Figure C-1 is a volume versus time plot for a normal left ventricle. <sup>(33)</sup> This figure and equations (C-23), (C-27) and (C-21) may be employed to construct a theoretical thermodilution study utilizing a continuous injection of cold saline over multiple heartbeats. The temperature versus time plot calculated is for a normal left ventricle. The theoretical temperature trace was compared to the experimental results to verify its general shape and to diagnose abnormal thermodilution studies.

Assuming that the injection process begins at the start of systole equation (C-23) may be written as,

$$\frac{dT(t)}{dt} = \dot{V}_{inj} (T(t) - T_{inj})/V(t) \quad (C-29)$$

where  $T(t)$  is the ventricular fluid temperature and  $V(t)$  is the ventricular volume during the systolic function. Equation

(C-29) may be solved for  $T(t)$ ,

$$\frac{-1.0}{V_{inj}} \ln \left( \frac{T(t) - T_{inj}}{T_{ed} - T_{inj}} \right) = \int_0^t G(\eta) d\eta \quad (C-30)$$

where  $T_{ed} = T(0)$ ,  $G(\eta) = 1/V(\eta)$  and  $\eta$  is a dummy variable. Equation (C-30) was solved numerically for  $T(t)$ .

During the diastolic function which follows systole, equation (C-27) may be employed to evaluate  $T(t)$ ,

$$T(t) = T_{sv} + \frac{V_{inj}(t) (T_{inj} - T_{sv})}{V(t)} + \frac{V_{es} (T_{es} - T_{sv})}{V(t)} \quad (C-31)$$

where  $T(t)$  is the ventricular fluid temperature during the diastolic function and  $V_{inj}(t)$  is given by equation (C-28). After the completion of the injection process there should theoretically be no change in ventricular fluid temperature during the systolic function which follows. Equation (C-21) may be employed to calculate the fluid temperature during the diastolic functions following the completion of the injection of cold saline,

$$T(t) = T_{sv} + \frac{V_{es}}{V(t)} (T_{es} - T_{sv}) \quad (C-32)$$

Figure C-2 is the theoretical thermodilution study for the ventricular volume plot in Figure C-1 and for the injection of saline at a temperature of 60 °F at a rate of 10 cm<sup>3</sup>/sec. This theoretical thermodilution study was verified by the experimental results.

## Volume versus Time Plot for a Normal Left Ventricle

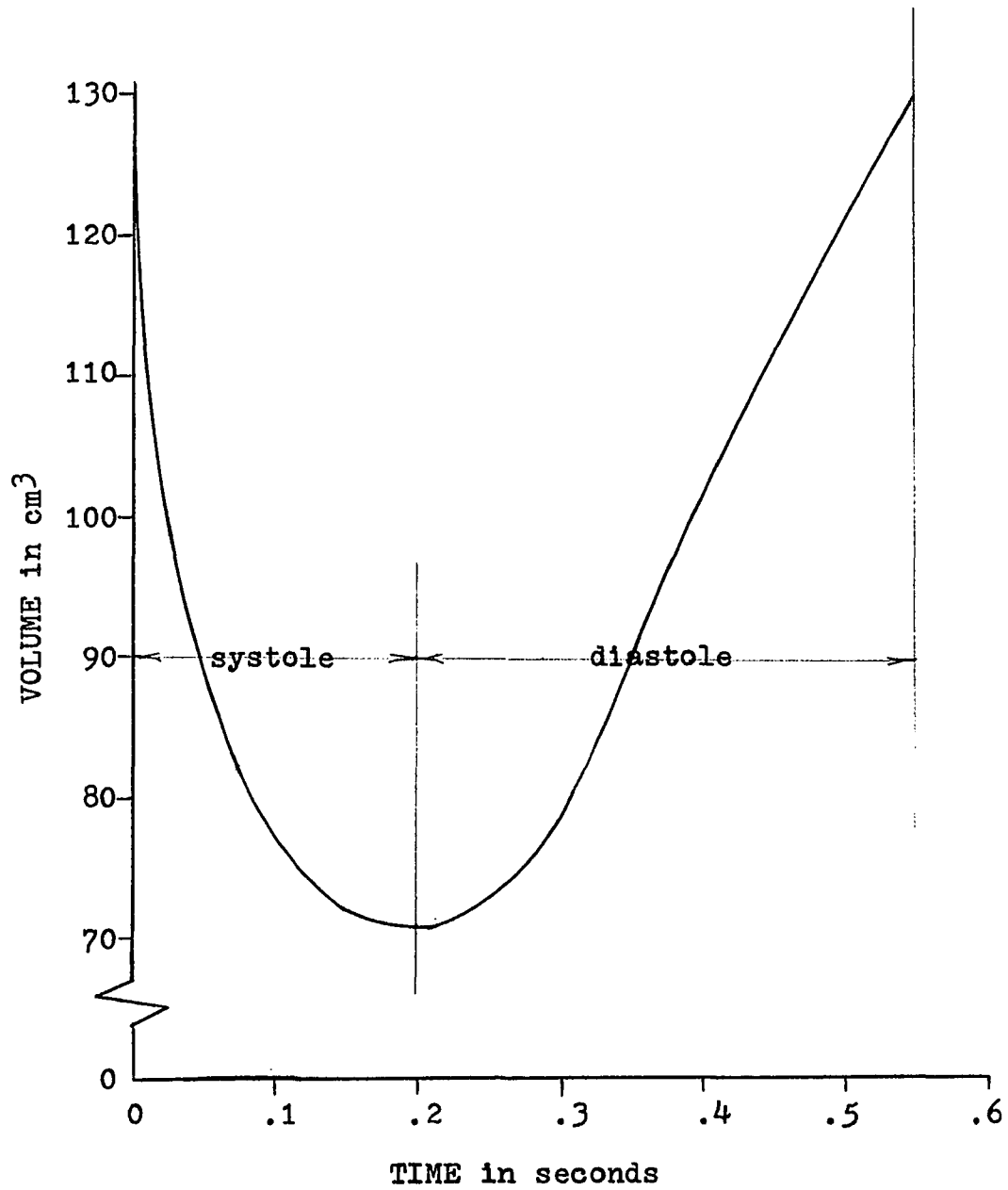


FIGURE C-1

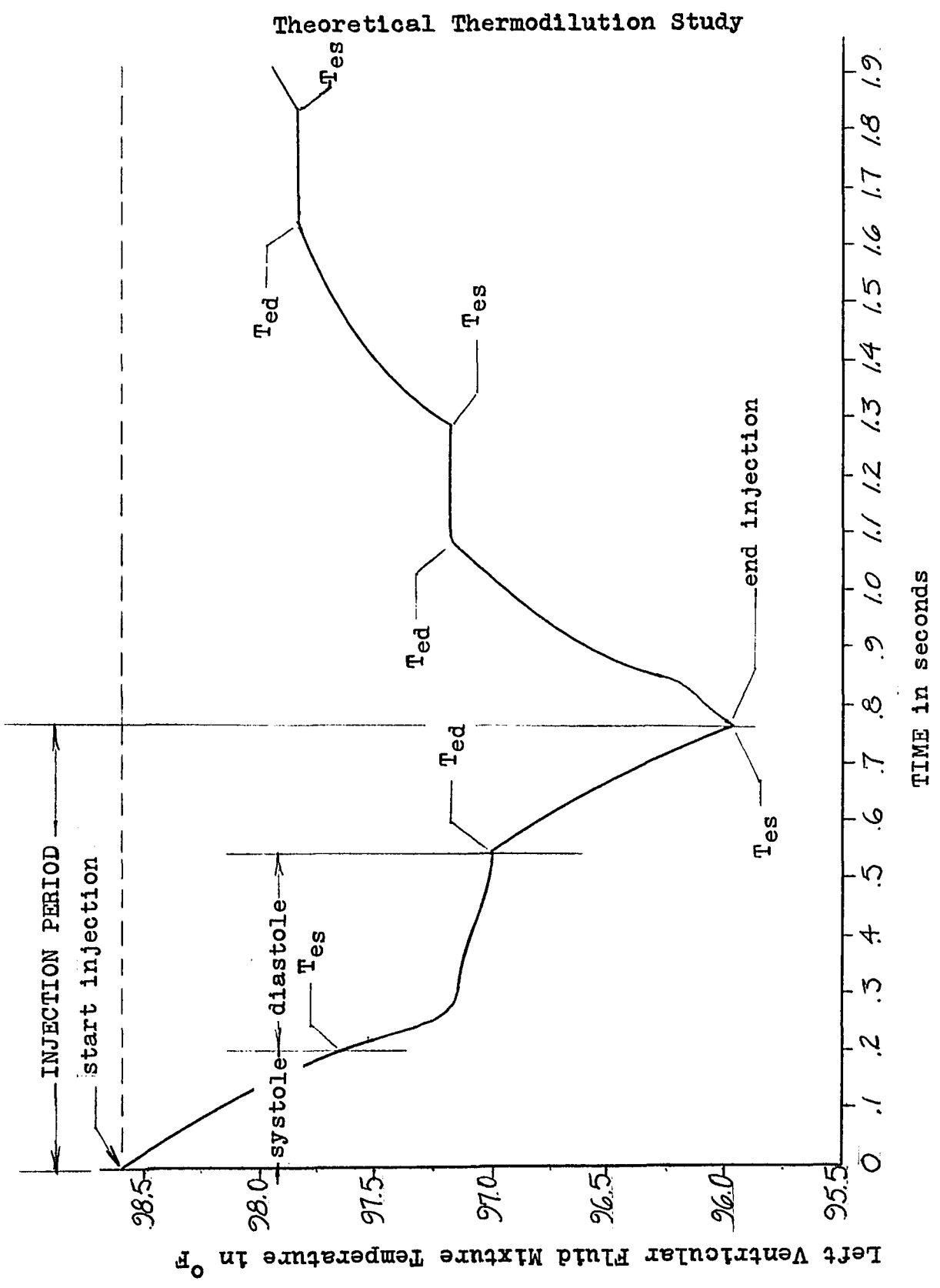


FIGURE C-2

Computer Solution for the Calculation of Ventricular Volume During the Systolic Function

C. CALCULATION OF SYSTOLIC VENTRICULAR VOLUME DURING

C. THE CONTINUOUS INJECTION OF COLD SALINE

1 READ, VINJ, TINJ, DELT

2 READ, TED

3 READ, T

4 IF (T - 100.0) 6, 11, 11

5 DET = TED - T

6 V = (VINJ \* (T - TINJ) \* DELT) / DET

7 PUNCH, V, T

8 VES = V

9 TED = T

10 GO TO 3

11 CONTINUE

12 PUNCH, VES

STOP

END

11.4 45.0 025

98.6

98.429 98.378 98.268 98.158 98.002 97.818 97.606 97.369

110.0

137.33652

98.489000

137.05152

98.378000

138.91254

98.258000

137.72754

98.158000

96.822576

98.002000

81.810489

97.818000

70.722730

97.606000

62.708570

97.368000

52.708570

FIGURE C-3



Computer Solution for the Calculation of Ventricular Volume During the Diastolic Function

```

C  CALCULATION OF SINGLE VENTRICULAR VOLUME
C  DURING THE CONTINUOUS INJECTION OF COLORED FLUID
1  READ, VED, TEND, TSD, VES, VED
C = C + 1
2  READ, C
3  T1 = S / D
4  T = (S * A - T1)
5  IF (T1 - T) 6, 9, C
6  V = (VIND * DELT * C) * ((T1 - T) / (T1 - TSD)) + VES * ((TEND - TSD) / (T1 - TSD))
7  PUNCH, V, T
VED = V
8  C = C + 1.0
GO TO 2
C  CONTINUE
9  STOP
10 PUNCH, VED, VES, SV
STOP
END
11.4 45.0  CE
95.54 95.4  1.5  42.0
1.7 1.7  1.0  1.0  1.0  1.0  1.0  1.0  1.0  1.0
62.057817  65.542333
72.001534  71.045321
82.812256  85.571420
91.247117  91.002715
1.0  1.0  1.0  1.0  1.0  1.0  1.0  1.0  1.0  1.0
117.7  1.0  1.0  1.0  1.0  1.0  1.0  1.0  1.0  1.0
126.74844  95.657142
130.12634  95.7142

```

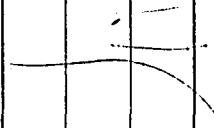


FIGURE C-4

Alternate Computer Solution for the Calculation of Ventricular Volume During the Systolic Function

C		CALCULATION OF SYSTOLIC VENTRICULAR VOLUME DURING	
C		THE CONTINUOUS INJECTION OF COLD SALINE	
1	READ. VINJ. TINJ. DELT. TED		
3	READ. T1		
	IF (T1 - 100.0) 4,4,13		
4	X1 = (T1 - TINJ)/(TED - TINJ)		
5	X = (-1.0/VINJ)*LOGF(X1)		
6	G1 = X/DELT		
7	V = 1.0/G1		
10	PUNCH. T1, V, G1		
11	TED = T1		
12	GO TO 3		
13	CONTINUE		
	STOP		
	END		
11.4	45.0	.025	
98.6			
95.49	98.38	98.27	98.16 98.00 97.92 97.61 97.37
98.490000		138.73022	7.2082248E-02
98.380000		138.44521	7.2230726E-03
98.270000		138.16011	7.2370789E-03
98.160000		137.87478	7.2520576E-03
98.000000		04.548440	1.0576580E-02
97.800000		82.774010	1.1036876E-02
97.610000		71.541500	1.3077862E-02
97.370000		62.331591	1.6043206E-02

FIGURE C-5

D. APPENDIXD.1 Derivation of Probability Density Function for N Volume Chamber Model

Following the injection of a bolus of dye indicator into the first chamber in Figure 13 at time  $t = 0$ , the conservation equation,

(Rate of dye in)-(Rate of dye out)=(Rate Change of Stored Dye) (D-1)  
applied to the first chamber becomes,

$$-C(t) Q = V \frac{dC(t)}{dt} \quad (D-2)$$

The solution of equation (D-2) is given by,

$$C(t) = C(0) \exp(-\lambda t) \quad (D-3)$$

where  $\lambda = Q/V$  and  $C(0) = \lambda I_{inj}/Q$ .

For the second chamber equation (D-1) becomes,

$$C(t) Q - C'(t) Q = V \frac{dC'(t)}{dt} \quad (D-4)$$

or

$$\frac{dC'(t)}{dt} + C'(t) \lambda = C(t) \lambda \quad (D-5)$$

The solution of equation (D-5) is given by,

$$C'(t) = \lambda^2 (I_{inj}/Q) t \exp(-\lambda t) \quad (D-6)$$

From equation (2-22),

$$f(t) = \lambda^2 t \exp(-\lambda t) \quad (D-7)$$

For the third chamber equation (D-1) becomes,

$$\frac{dC''(t)}{dt} = \lambda^2 t (I_{inj}/Q) \exp(-\lambda t) - C''(t) \lambda \quad (D-8)$$

which yields,

$$f(t) = \lambda/2 (\lambda t)^2 \exp(-\lambda t) \quad (\text{D-9})$$

For the fourth chamber,

$$f(t) = ((t\lambda)^3/3!) \lambda \exp(-\lambda t) \quad (\text{D-10})$$

Hence for the Nth chamber,

$$f(t) = (\lambda^N/(N-1)!) t^{N-1} \exp(-\lambda t). \quad (\text{D-11})$$

E. APPENDIXE.1 Temperature Correction for Warming of Injected Fluid  
in Catheter during the Injection Process

An energy balance between the inlet and outlet of the catheter during the steady flow injection of cold saline yields,

$$\dot{q} = \dot{M}_{inj} C_{p,inj} \Delta T_{outlet-inlet} \quad (E-1)$$

where  $\dot{q}$  is the rate of heat transfer to the injected fluid and  $\Delta T_{outlet-inlet} = T_{outlet} - T_{inlet}$  is the difference in the bulk fluid temperature between the outlet and the inlet sections of the catheter. The rate of heat transfer by convection, at any location along the catheter, between the surface of the catheter and the injected fluid is given by,

$$d\dot{q} = h_c(x) ( T_{wall} - T(x) ) dA \quad (E-2)$$

where  $dA$  is the heat transfer area and  $( T_{wall} - T(x) )$  is the difference between the surface temperature of the catheter lumen, which is assumed to be uniform along the length of the catheter, and the bulk fluid temperature of the injected fluid at the location in question.  $h_c(x)$  is the local convective heat transfer coefficient defined by equation (E-2).

Assuming that,

$$h_c(x) [ T_{wall} - T(x) ] = \bar{h}_c [ T_{wall} - ( T_{outlet} + T_{inlet} ) / 2 ] \quad (E-3)$$

where  $\bar{h}_c$  is the average convective heat transfer coefficient. Equation (E-2) becomes,

$$\dot{q} = \bar{h}_c \left[ T_{\text{wall}} - (T_{\text{outlet}} + T_{\text{inlet}}) / 2 \right] A \quad (\text{E-4})$$

and combining equations (E-1) and (E-4) yields,

$$\bar{h}_c = \dot{M}_{\text{inj}} C_{p,\text{inj}} \Delta T_{\text{outlet-inlet}} / \left[ A \left( T_{\text{wall}} - \frac{T_{\text{outlet}} + T_{\text{inlet}}}{2} \right) \right] \quad (\text{E-5})$$

Equation (E-5) was employed to calculate the average convective heat transfer coefficient  $\bar{h}_c$  for the experimental studies described below.

## E.2 Experimental Evaluation of $\bar{h}_c$

The warming of the injected fluid in the catheter was studied experimentally by placing a #7 French catheter in a water bath at a temperature of 95 °F to simulate the catheter in the artery. Injections of 40.0 cm<sup>3</sup> of cold saline at various temperatures ranging from 40 °F to 60 °F at 14.3 cm<sup>3</sup>/sec were made at the inlet of the catheter and the injected fluid temperature fluid temperature was measured at the outlet tip of the catheter by a thermocouple.

Figure E-1 is the temperature of the injected cold saline measured at the tip of the catheter during the injection of saline at 55 °F at 14.3 cm<sup>3</sup>/sec. Applying equation (E-5) the average convective heat transfer coefficient  $\bar{h}_c$  was found to equal 770 B / hr °F ft<sup>2</sup>. Assuming that the heat transfer

coefficient  $\bar{h}_c$  varies directly with the mass flow rate  $\dot{M}_{inj}$  and inversely with the inside diameter of the catheter, the average convective heat transfer coefficient was found to equal,

$$\bar{h}_c = 660 \text{ B/hr } ^\circ\text{F ft}^2 \quad (\text{E-6})$$

for a #6 French catheter and an injection rate of  $11.4 \text{ cm}^3/\text{sec}$ .

Equations (E-5) and (E-6) were used to calculate the  $\Delta T_{\text{outlet-inlet}}$  for the thermodilution studies presented in this paper. The average calculated  $\Delta T_{\text{outlet-inlet}}$  was approximately  $10^\circ\text{F}$ , with a range from  $8^\circ\text{F}$  to  $12^\circ\text{F}$ . This  $10^\circ\text{F}$  temperature rise was also experimentally verified. Hence,  $10^\circ\text{F}$  was added to the injected fluid temperature at the inlet of the catheter to correct for the warming of the fluid in the catheter during the injection process for the thermodilution studies presented in this paper.

### E.3 Analytical Considerations

The injection rate employed in the thermodilution studies presented in this paper was usually  $11.4 \text{ cm}^3/\text{sec}$ . For a #6 French catheter, assuming the viscosity and density of saline is similar to that of water at the same temperature, the Reynolds number corresponding to the above injection rate is 8000. Hence, the flow in the catheter is in transitional flow. The mechanisms of heat transfer and fluid flow in the transition region (Re between 2100 and 10,000) vary considerably from system to system. Kreith<sup>(42)</sup> presents curves which

may be used to estimate the Nusselt number for fluids flowing in tubes in the transition regime for different L/D ratios. However the author states that the actual value of the Nusselt number may deviate considerably from that predicted by these curves. This was the case experienced by this author. Hence, it is concluded that the average convective heat transfer coefficient  $\bar{h}_c$  for the injection of cold saline in a catheter should be determined experimentally when  $2100 < Re < 10,000$ .



Temperature Correction for Warming of Injected Fluid in Catheter

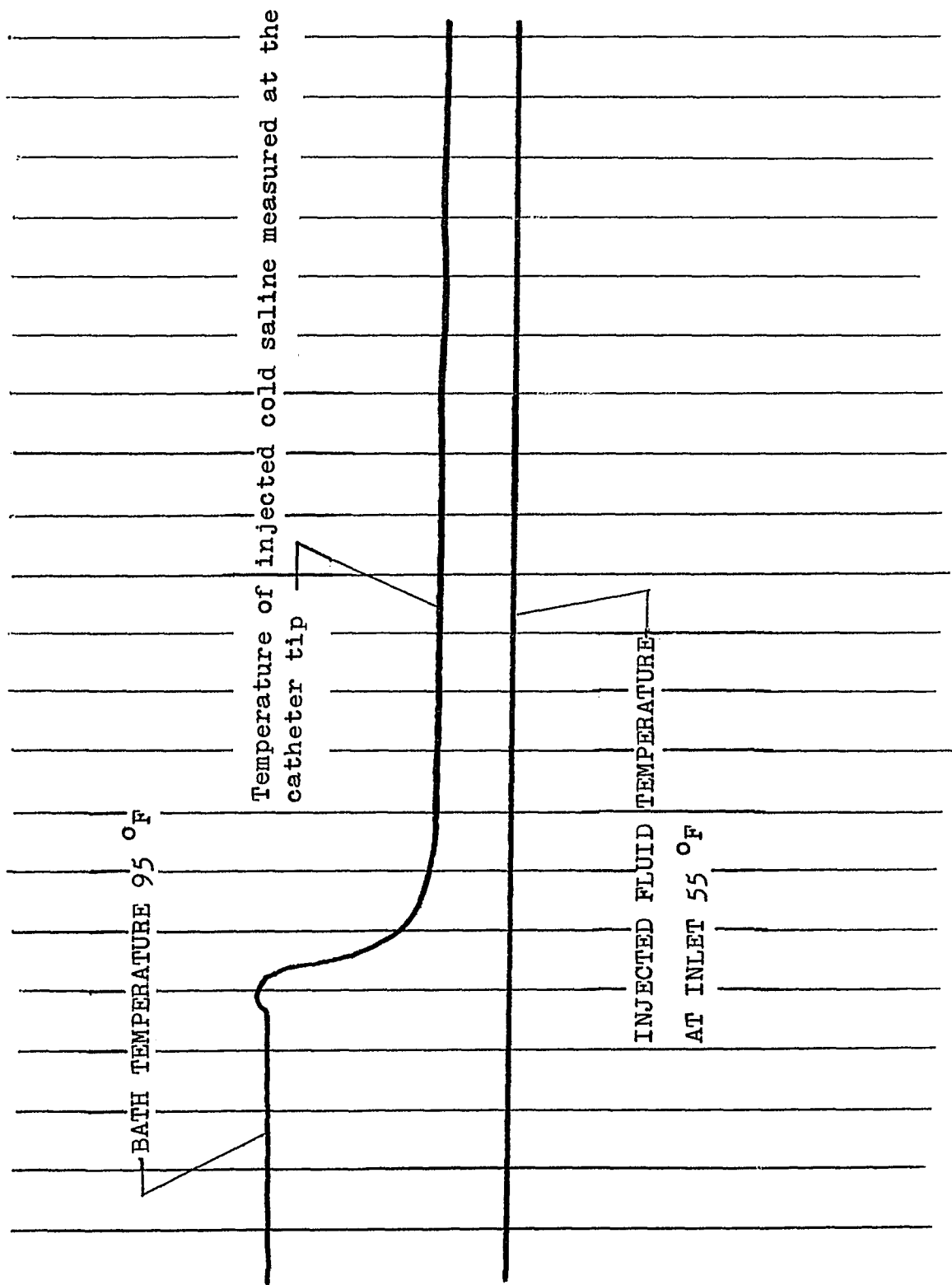


FIGURE E-1

REFERENCES

- 1 Stewart, G. N., "Researches on the circulation time in organs and on the influences which affect it", *Journal of Physiology*, 15:1, 1894.
- 2 Hamilton et al, "Studies on the circulation", *American Journal of Physiology*, 99:534, 1932.
- 3 Newman, E. V. et al, "The dye dilution method for describing the central circulation", *Circulation*, 4:735, 1951.
- 4 Bing, R. J. et al, "An estimation of the residual volume of blood in the right ventricle of normal and diseased human hearts in vivo", *American Heart Journal*, 42:483, 1951.
- 5 Holt, J. P., "Estimation of left ventricular end-diastolic volume and end-systolic volume in the dog", *American Journal of Physiology*, 179:645, 1954.
- 6 Swan, H. J. C. and Beck, W., "Ventricular non mixing as a source of error in the estimation of ventricular volume by the indicator-dilution technique", *Circulation Research*, 8:989, 1960.
- 7 Folse, R. and Braunwald, E., "Determination of fraction of left ventricular volume fraction ejected per beat and

- of ventricular end-diastolic and residual volumes",  
Circulation, 25:674, 1962.
- 8 Fegler, G., "Measurement of cardiac output in anaesthetized animals by a thermodilution method", Quarterly Journal of Experimental Physiology, 39:153, 1954.
- 9 Holt, J. P., "Estimation of the residual volume of the ventricle of the dog's heart by two indicator dilution techniques", Circulation Research, 4:187, 1956.
- 10 Rolett, E. L., Sherman, H., and Gorlin, R., "Appraisal of the thermodilution method for left ventricle volume measurement", Journal of Applied Physiology, 19:1167, 1964.
- 11 Hosie, K. F., "Thermal-Dilution Techniques", Circulation Research, 10:491, 1962.
- 12 Armelin, E., Donald, D. E., Wood, E. H., "Comparison of dilution techniques using aortic injection with upstream sampling for assessment of aortic regurgitation", Circulation Research, 15:287, 1964.
- 13 Bristow, J. D., Crislip, R. L., Farrehi, C., Harris, W. E., Lewis, R. P., Sutherland, D. W. and Griswold, H. E., "Left ventricular volume measurements in man by thermodilution", Journal of Clinical Investigation, 43:1015, 1964.
- 14 James, G. W., Paul, M. H., and Wessel, H. U., "Thermal dilution: instrumentation with thermistors", Journal of

- Applied Physiology, 20:547, 1965.
- 15 Rapaport, E., "Usefulness and limitations of thermal wash-out technics in ventricular volume measurement", American Journal of Cardiology, 18:226, 1966.
- 16 Holt, J. P., "Symposium on measurement of left ventricular volume. Indicator-dilution methods", American Journal of Cardiology, 18:208, 1966.
- 17 Khalil, H. H., Richardson, T. Q., and Guyton, A. C., "Measurement of cardiac output by thermal-dilution and direct Fick methods in dogs", Journal of Applied Physiology, 21:1131, 1966.
- 18 Cropp, G. J. A., "Measurements of variable ventricular output by thermodilution; model experiments", Journal of Applied Physiology, 21:1624, 1966.
- 19 Khalil, H. H., "Repeated or continual measurements of cardiac output in the squirrel monkey by thermodilution", Naval Aerospace Medical Institute, report NAMI-1032, March, 1968.
- 20 Branthwaite, M. A. and Bradley, R. D., "Measurement of cardiac output by thermal dilution in man", Journal of Applied Physiology, 24:434, 1968.
- 21 Khalil, H. H., "A refined thermodilution cardiac output catheter", Naval Aerospace Medical Institute, report NAMI-048, August, 1968.

- 22 Fleming, J., "Left ventricular volume in aortic stenosis measured by an angiocardiographic and a thermodilution method", *British Heart Journal*, 30:475, 1968.
- 23 Krayenbuhl, H. P. and Luthy, E., "The Thermodilution Method", *Medilamunci*, 1968.
- 24 Welland, S. M., A New Approach to Evaluation of Cardiac Work by Means of the Thermal Dilution Technique, Master of Science Thesis, Newark College of Engineering, 1968.
- 25 Levinson, G. and Frank, M., "Studies of cardiopulmonary blood volume measurement of left ventricle by dye dilution", *Circulation*, 35:1038, 1967.
- 26 Irisawa, H., Wilson, M. F. and Rushmer, R. F., "Left ventricle as a mixing chamber", *Circulation Research*, 8:183, 1960.
- 27 Shillingford, J., "Simple method for estimating mitral regurgitation by dye dilution curves", *Clinical Science*, 17:229, 1958.
- 28 Lange, R. L., and Hecht, H. H., "Quantitation of valvular regurgitation from multiple indicator-dilution curves", *Circulation*, 18:623, 1958.
- 29 Lukas, D. S., Arditi, L. I., Winston, A. L. and Pearce, C. W., "Effects of quantitatively controlled left ventricular-atrial regurgitation on indicator-dilution curves in the dog",

- Circulation Research, 9:375, 1961.
- 30 Armelin, E., Donald, D. E., and Wood, E. H., "Comparison of dilution techniques using aortic injection with upstream sampling for assessment of aortic regurgitation", Circulation Research, 15:287, 1964.
- 31 Malcoly, D. A., Verosky, J. M., Crossett, E. S., Hancock, J. A. and Iwen, G. W., "The assessment of cardiac defects by dye-dilution technics", Southwestern Medicine, Volume 46, 1965.
- 32 Rahimtoola, S. H. and Swan, H. J. C., "Calculation of cardiac output from indicator-dilution curves in the presence of mitral regurgitation", Circulation, 31:711, 1965.
- 33 Ackerman, E., Biophysical Science, Prentice Hall, Inc., 1962, pages 157-178.
- 34 Pearce, M. L., McKeever, W. P., Dow, P. and Newman, E. V., "The influence of injection site upon the form of dye dilution curves", Circulation Research, 1:112, 1953.
- 35 Sheppard, C. W., Basic Principles of the Tracer Method, John Wiley & Sons, Inc., 1962, page 180.
- 36 Fegler, G., "The reliability of the thermodilution method for determination of the cardiac output and the blood flow in central veins", Quarterly Journal of Experimental Physiology, 42:254, 1957.

- 37 Jacobs, R. M., Levy, M. J., Brancato, R. W. and Welland, S. M., "A new approach to evaluation of cardiac work by means of the thermal dilution technique", presented to the 21st Annual Conference on Engineering in Medicine and Biology, November 18-21, 1968 by Professor R. M. Jacobs, Newark College of Engineering.
- 38 Liao, C. K., An Application of a New Approach to Evaluation of Cardiac Work by Means of the Thermal Dilution Technique, Master of Science Thesis, Newark College of Engineering, 1969.
- 39 Burton, A. C., Physiology and Biophysics of the Circulation, Year Book Medical Publishers Inc., 1965, pages 106-112.
- 40 Dodge, H. T. et al, "Usefulness and limitation of radiographic methods for determining left ventricular volume", American Journal of Cardiology, 18:10, 1966.
- 41 Welland, S. M., Brancato, R. W., Levy, M. J. and Jacobs, R. M., "Thermodynamic development of the thermodilution equations for the estimation of the ventricular volume in man", Medical and Biological Engineering, submitted for publication.

VITA

Name: Stanley M. Welland

Elementary and Secondary Education:

Maple Avenue Grammar School, Newark, New Jersey

Weequahic High School, Newark, New Jersey

Colleges and Universities: Years attended and Degrees

Newark College of Engineering, 1960-1964, B.S.M.E.

Newark College of Engineering, 1966-1968, M.S.M.E.

Newark College of Engineering, 1968-Present

Professional Experience:

1964-1966 - Design Engineer, General Electric Co.,  
Schenectady, New York

Time Devoted to Research:

This dissertation is the result of more than two years full-time research at Newark College of Engineering. The author's graduate education was sponsored for three years by a National Defense Education Act Fellowship and for one year by an Esso Education Foundation Fellowship.